MINISTRY OF EDUCATION AND SCIENCE OF UKRAINE
DNIPRO UNIVERSITY OF TECHNOLOGY

DNIPRO UNIVERSITY of TECHNOLOGY 1899

Oleksii Ivanov
Dmytro Tsyplenkov

DESIGNING OF THREE-PHASE INDUCTION MOTORS

Textbook

MINISTRY OF EDUCATION AND SCIENCE OF UKRAINE
DNIPRO UNIVERSITY OF TECHNOLOGY

Oleksii Ivanov, Dmytro Tsyplenkov

DESIGNING OF THREE-PHASE INDUCTION MOTORS

Textbook

Dnipro
DniproTech

2023

УДК 621.313
І 98

Рекомендовано вченою радою Національного технічного університету "Дніпровська політехніка" як навчальний посібник для студентів спеціальності 141 Електроенергетика, електротехніка та електромеханіка (протокол № 9 від 21 .09.2023).

Рецензенти:

Андрій Муха, д-р техн. наук, професор, завідувач кафедри електротехніки та електромеханіки Українського державного університету науки і технологій;

Юрій Васьковський, д-р техн. наук, професор, професор кафедри електромеханіки Національного технічного університету України "Київський політехнічний інститут ім. І. Сікорського";

Андрій Некрасов, канд. техн. наук, доцент, доцент кафедри електричних машин Кременчуцького національного університету імені М. Остроградського.

Ivanov O.
І 98 Designing of three-phase induction motors: textbook / Oleksii Ivanov, Dmytro Tsyplenkov; Ministry of education and science of Ukraine Dnipro university of technology. – Dnipro: DniproTech, 2023. – 144 p.

ISBN

The method of designing three-phase asynchronous motors during their development is considered. Additional data on windings, materials used in motors, and sizes of wires with different classes of insulation are given.

Recommended for students of specialty 141 - Electric power engineering, electrical engineering and electromechanics.

ISBN УДК 621.313

Contents

DESIGNING OF THREE-PHASE INDUCTION MOTORS

1. SELECTION OF MOTOR BASIC CONSTRUCTION AND PRINCIPAL DIMENSIONS

1.1. Motor basic construction

Technical specification for induction motor design includes the designed machine ratings, requirements defined by it working conditions, the machine embodiment, degree of protection of enclosure, cooling system. Besides, additional requirements to the designed motor may be assigned, such as the least admissible ratio of maximum and minimum torques. For motors with squirrel cage rotors extreme values of maximum starting current ratio and the least starting torque ratio may be specified. As regards to requirements not indicated in the motor technical specification, they should meet the existing standards.

In most cases, designing a new machine is oriented to a basic model. As such a model one of modern commercially produced machines series can be taken. At designing, decisions in relation of the machine dimensions, its construction and parameters are accepted by designer with orientation toward the machine series adopted as a design model.

The bachelor's curriculum of the specialty 141 "Electric Power, Electrical Engineering, and Electromechanics" envisages a project on electric machines.

In most cases, a project on designing a three-phase induction motor is carried out. In the project, it is recommended to use as the model the induction motors series 4A. The design assignment includes such initial data as the motor rated power P_2, line-to-line voltage U_{1l}, mains frequency f_1, number of poles $2p$, rotor type (wounded or squirrel cage), motor mounting, degree of enclosure protection, duty type. Some other requirements may be also included into the design assignment.

1.2. Determination of motor principal dimensions

The principal dimensions of the induction motor are the stator inner diameter D and the calculated the air gap length l_δ.

1.2.1. To determine the principal dimensions, approximate value of the motor shaft height h above the supporting surface is found using the plots $h = f(P_2)$ given in Fig. 1.1, where P_2 is the motor rated output power on shaft. The curves are given for different number of poles $2p$ separately for motors having degree of enclosure protection IP44 and IP23. The shaft height is standardized (see Table 1.1). Finding the shaft height approximate value from Fig. 1.1 it is necessary to accept the next lower standard shaft height value given in Table 1.1.

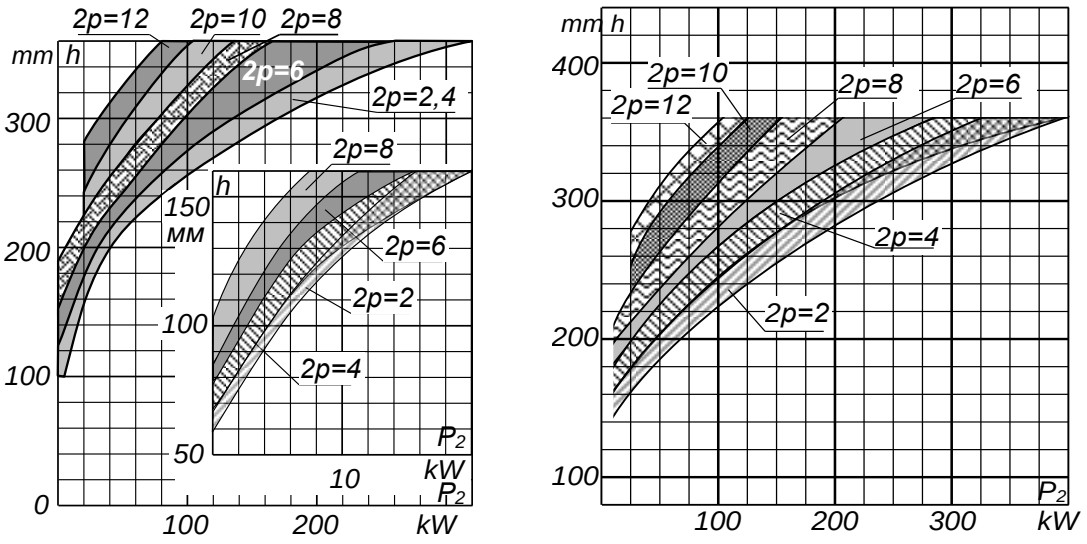

Figure 1.1 Curves for an approximate value of the shaft height determination for induction motors 4A series at degree of enclosure protection IP44 (a) and IP23 (b)

1.2.2. It is recommended to accept the stator outside diameter D_a value given in the same Table 1.1 corresponding to the accepted standard value of the shaft height. After that, one of the principal dimensions - the inner stator diameter value is found as

$$D = k_D D_a \tag{1.1}$$

where k_D is a coefficient which value is accepted based on number of poles $2p$ by the data of Table 1.2.

Table 1.1 Standard values of the shaft height and corresponding values of the stator outside diameter

h, mm	56	63	71	80	90	100	112	132
D_a, m	0.089	0.10	0.116	0.131	0.149	0.168	0.191	0.225

h, mm	160	180	200	225	250	280	315	355
D_a, m	0.272	0.313	0.349	0.392	0.437	0.530	0.590	0.660

Table 1.2 – Coefficient k_D for induction motors 4A series

$2p$	2	4	6	8 - 12
k_D	0.52 – 0.57	0.64 – 0.68	0.70 – 0.72	0.74 – 0.77

1.2.3. The value of pole pitch τ that will be required for further calculations is

$$\tau = \pi D/(2p). \tag{1.2}$$

1.2.4. The estimated apparent power consumed by the motor at full load in V · A is found as

$$P' = P_2 \frac{k_E}{\eta \cos\varphi} \tag{1.3}$$

where k_E is the ratio of the voltage induced in the stator winding to the rated voltage across the stator terminals,

η and $\cos\varphi$ are approximate values of the motor efficiency and power factor respectively.

The value of k_E is defined with curves in Fig. 1.2. Approximate values of η and $\cos\varphi$ are found with the help of curves in Fig. 1.3 and 1.4 depending on the degree of enclosure protection (IP44 or IP23).

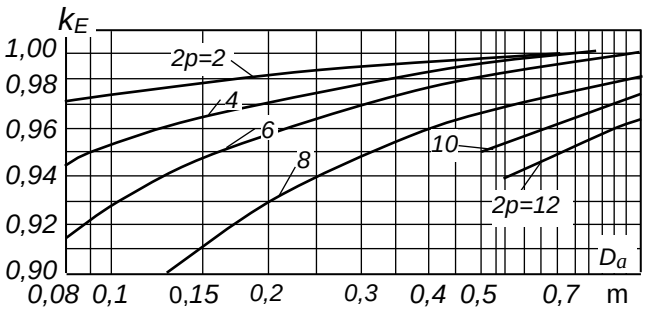

Figure 1.2 Dependence of k_E on stator outside diameter at different poles number

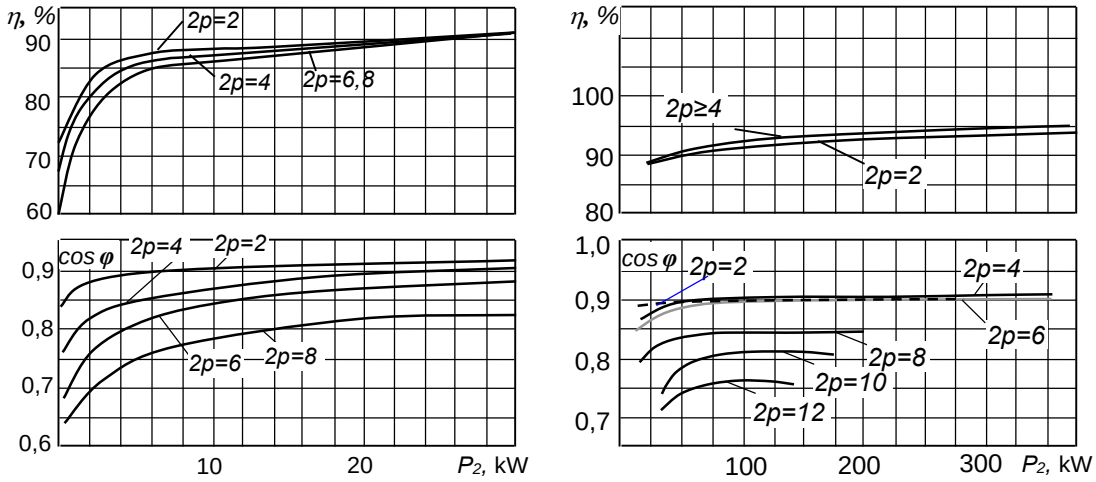

Figure 1.3 Dependence of the efficiency and power factor on the rated power for 4A series induction motors with enclosure protection IP44

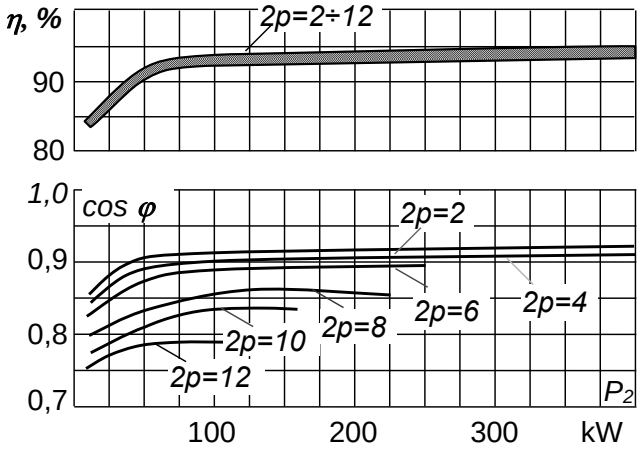

Figure 1.4 Dependence of the efficiency and power factor on rated power for 4A series induction motors with enclosure protection IP23

1.2.5. The axial length of the motor air gap l_δ is equal to

$$l_\delta = \frac{P'}{\mathrm{D}^2 \Omega_1 k_B k_{w1} A B_\delta} \qquad (1.4)$$

where Ω_1 is the synchronous angular speed equal $\Omega_1 = 2\,\pi f_1/p$,

k_B is the machine magnetic flux form factor, its approximate value is accepted equal $k_B = 1.11$, neglecting the flux harmonics,

k_{w1} is the stator winding factor. At this stage of calculation its approximate value is preliminarily accepted based on the winding type. For machines with the shaft height $h \leq 160$ mm single layer windings are applied; for them the value $k_{w1} = 0.95 \ldots 0.96$ is accepted. For machines with $h > 160$ mm two-layer windings are used; for them the winding factor is accepted equal to $k_{w1} = 0.90 \ldots 0.91$ at $2p = 2$, and at greater poles number – to $k_{w1} = 0.91 \ldots 0.92$,

A is tentative value of the electric loading of the machine in A/m,

B_δ is tentative value of amplitude of the magnetic flux density in the air gap. These values may be found with the help of curves that are given in Fig. 1.5 or 1.6.

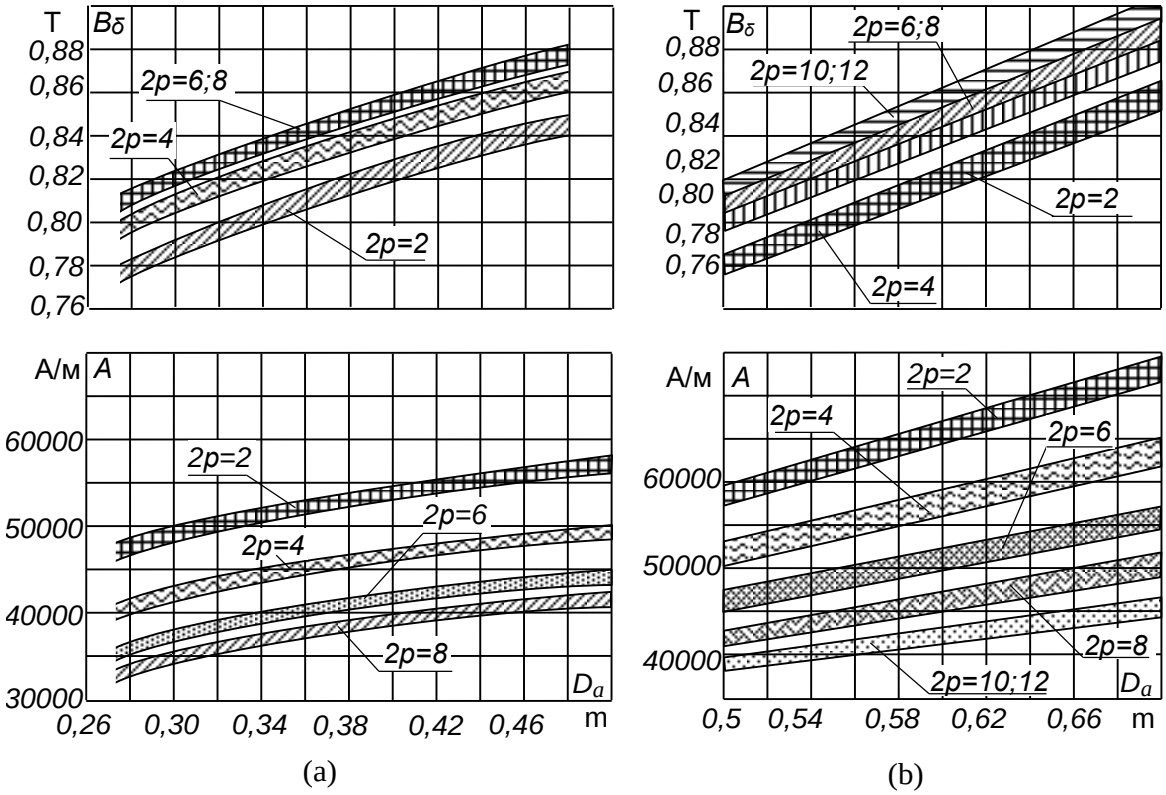

Figure 1.5 Electromagnetic loads of 4A series induction motors with enclosure protection IP23 at $h = 160 \ldots 250$ mm (a), at $h \geq 280$ mm (b)

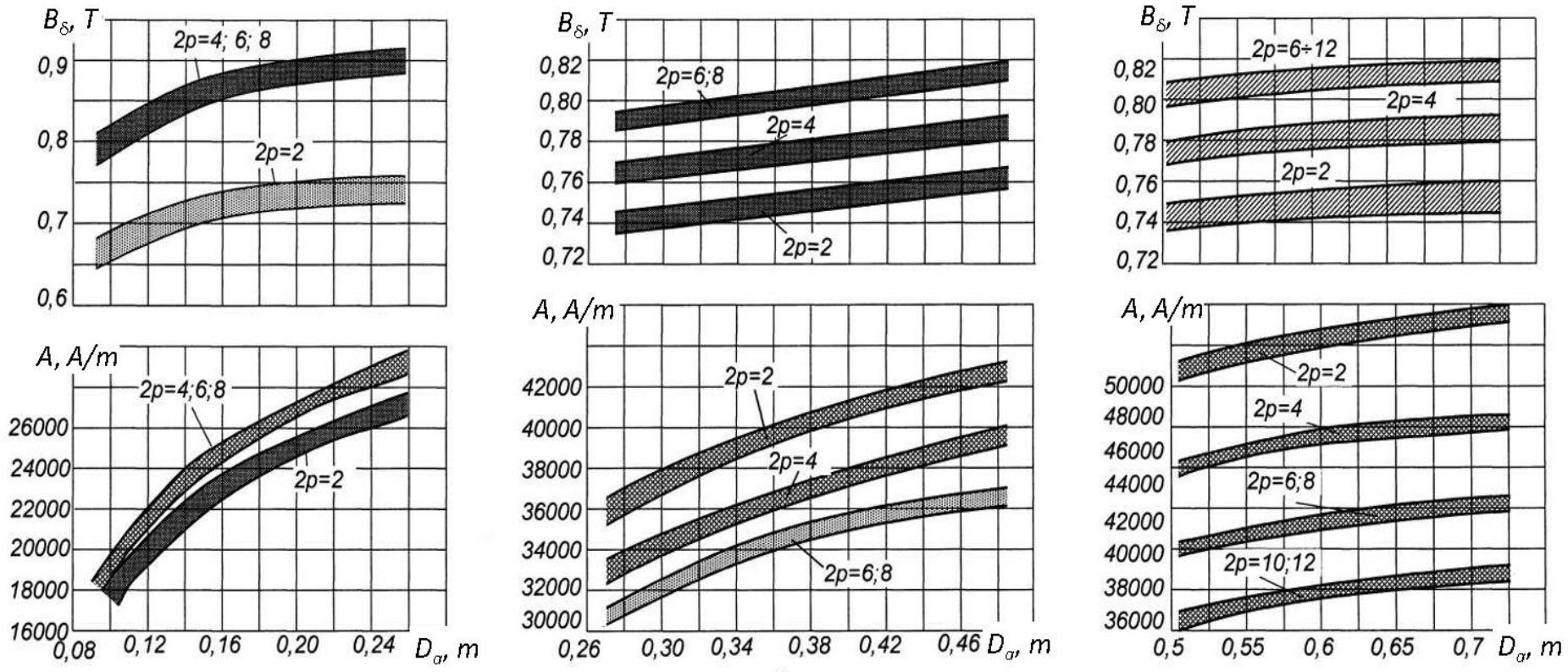

(a) (b) (c)

Figure 1.6 Electromagnetic loads of 4A series induction motors with enclosure protection IP44 at $h < 160$ mm (a), at $h = 160 - 250$ mm (b), at $h > 250$ mm and a blown through rotor construction (c)

1.2.6. The economic performance, characteristics, and cooling conditions of the motor are affected by the ratio of the length of the motor air gap to the pole pitch $\lambda = l_\delta/\tau$. Acceptable value of λ depends on the number of poles and the shaft height and can be found using the curves shown in Fig. 1.7.

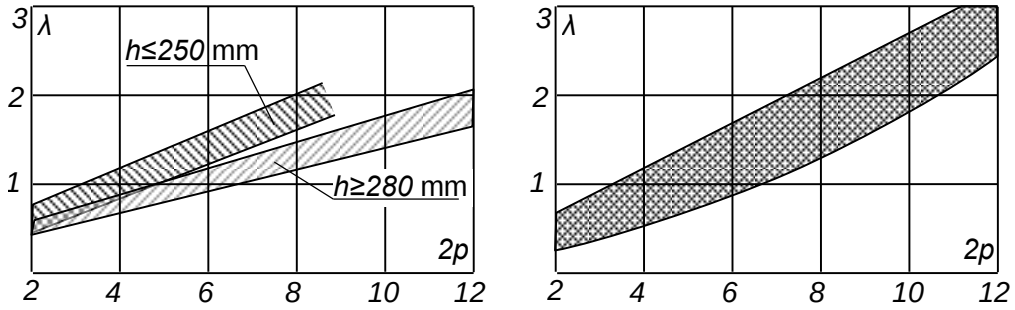

Figure 1.7 Acceptable values of λ for 4A series induction motors with enclosure protection IP44 (a) and IP23 (b)

If λ exceeds the acceptable value, it is necessary to repeat calculations taking the next higher motor shaft standard value. At a value of λ less than the acceptable, the calculations must be repeated for the next lower shaft height standard value.

1.2.7. If radial ventilation ducts are available, full stator core design length l_1 and total core steel lamination packs length l_{cp1} are defined.

In the case of $l_\delta \leq 250 \ldots 300$ mm the radial ducts are not arranged, and the above indicated lengths are accepted equal $l_1 = l_{cp1} = l_\delta$. The rotor core length l_2 and the core steel laminations pack length l_{cs2} are accepted in this case equal $l_2 = l_{cp2} = l_\delta$.

If the axial length of the motor air gap is $l_\delta > 300$ mm , the stator and rotor cores are divided into several longitudinal packs between which radial air ducts are arranged. In motors with slip rings or welded squirrel-cage, each the core pack length l_{cp} is taken equal to 40…60 mm. In motors with

casted aluminum squirrel cage, the length of each separate pack may be increased to 60…80 *mm*.

Number of the steel lamination packs must be integer and defined as

$$n_{cp} = {l_\delta}\Big/{l_{cp}}. \tag{1.5}$$

The number of radial ducts is

$$n_{rd} = n_{pl} - 1. \tag{1.6}$$

The radial duct width is usually accepted equal $b_{rd} = 10$ mm.

For a stator with radial ventilation ducts, total longitudinal length of the core lamination packs, and the stator length are determined as

$$l_{cp1} = l_{cp} n_{cp} \tag{1.7}$$

$$l_1 = l_{cp1} + l_{cp} n_{cp}. \tag{1.8}$$

If radial air ducts are available, the estimated length of the air gap l_δ needs to be clarified considering the magnetic lines in the gap distortion. For this, it is necessary to select the radial size of the air gap δ using Table 1.3.

Table 1.3 Air gap of induction motors

h, mm	Air gap δ, mm, at number of poles equal				h, mm	Air gap δ, mm, at number of poles equal			
	2	4	6 and 8	10 and 12		2	4	6 and 8	10 and 12
50	0.25	0.25	0.25	-	180	1.0	0.60	0.45	-
56	0.30	0.25	0.25	-	200	1.0	0.70	0.50	-
63	0.35	0.25	0.25	-	225	1.0	0.85	0.60	-
71; 80	0.35	0.25	0.25	-	250	1.2	1.0	0.70	-
90	0.40	0.25	0.25	-	280	1.3	1.0	0.80	0.70
100	0.45	0.30	0.30	-	315	1.5	1.0	0.90	0.80
112	0.50	0.30	0.30	-	355	1.8	1.2	1.0	0.90
132	0.60	0.35	0.35	-	400	2.0	1.4	1.2	1.0
160	0.80	0.50	0.50	-	450	2.0	1.4	1.2	1.0

At $\delta < 1.5$ mm the lengthof the air gap is accepted equal to $l_\delta = n_{cp} l_{cp}$.

At $\delta \geq 1.5$ mm the length of the air gap is accepted equal

$$l_\delta = l_1 - b'_{rd} n_{rd}, \tag{1.9}$$

where b'_{rd} = design width of the radial air duct that is found by expressions:

$$b'_{rd} = \gamma' \delta, \qquad \gamma' = \frac{2(b_{rd}/\delta)^2}{5+2(b_{rd}/\delta)}. \tag{1.10}$$

To get the length of the air gap value obtained by expression (1.9) closer to the value previously found by expression (1.4), correction of the core pack length l_{cp} and the number of the packs n_{cp} is made if necessary.

When the radial air ducts are available and $h < 300$ mm, the rotor length l_2 is accepted equal to the stator length l_1 The total longitudinal length of the rotor core lamination packs are found as

$$l_{cp2} = l_2 - b_{rd} n_{rd}. \tag{1.11}$$

At $h \geq 300$ mm the rotor is made longer than the stator by 5 mm, and in large high voltage machines by 10 mm by means of increase the length of its end packs.

2. DESIGN OF THE STATOR AND ROTOR TEETH AREAS AND WINDINGS

2.1. Basic parameters of stator windings and machine electromagnetic loads

2.1.1. Selection of the stator winding construction is made based on the following. At rated voltage less or equal 660 V if the motor rated power on shaft is $P_2 \leq 100$ kW , and at $2p \geq 10$ if h equals 280 or 315 mm, the stator fed-in winding is selected. At the rated power $P_2 > 100$ kW and voltage till 660 V, the partly form-wound windings are used. At a voltage of 3kV and more, the form-wound windings are applied.

2.1.2. For selection of the number of stator slots, define the limits of acceptable value of stator tooth pitch t_{1min} and t_{1max}. For machines with fed-in winding, it is made using the plot in Fig. 2.1. For machines with partly form-wound and form-wound windings, the limits of tooth pitch are taken from Table 2.1.

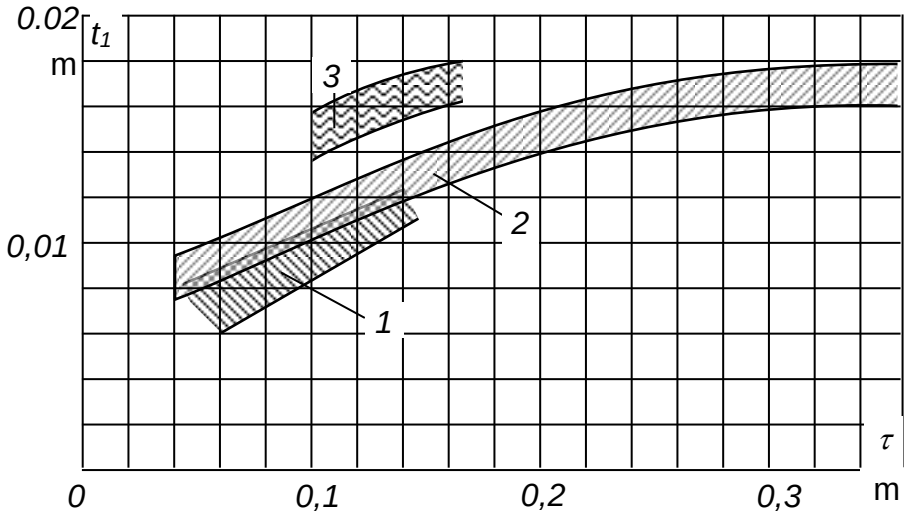

Figure 2.1 The stator tooth pitch of induction motors with fed-in windings: area 1 – at $h \leq 90$ mm , area 2 – at 90 mm $< h \leq 250$ mm, area 3 – at $h \geq 280$ mm

Table 2.1 Stator tooth pitch of induction motors with open and semi-open slots (in m)

Pole pitch τ, m	Tooth pitch of motors with rated voltage (V)		
	till 660	3000	6000
< 0.15	0.016…0.020	0.022…0.025	0.024…0.030
0.15…0.40	0.017…0.022	0.024…0.027	0.026…0.034
>0.40	0.020…0.028	0.026…0.032	0.028…0.038

Acceptable number of stator slots is in the bounds of z_{1min} and z_{1max}:

$$z_{1min} \dots z_{1max} = \frac{\pi D}{t_{1max}} \dots \frac{\pi D}{t_{1min}} . \qquad (2.1)$$

Finally, the number of stator slots z_1 is selected in the above limits so as it would be multiple of the number of machine phases m_1 and the number poles. In such a case the number of slots per pole and per phase

$$q = \frac{z_1}{2pm_1} \tag{2.2}$$

is integer. Fractional slot windings are sometimes applied in machines having number of poles $2p \geq 10$. In such cases, the fractional part of q has as a rule denominator equal 2.

2.1.3. The tooth pitch of the stator is found by the expression:

$$t_1 = \frac{\pi D}{2pmq}. \tag{2.3}$$

It should not go beyond the limits more than for 10 % and, and at $h \geq 56$ mm , should not be less than 6…7 mm.

2.1.4. The number of turn sides embedded into a slot is found as

$$u_{sl} = a u'_{sl} \tag{2.4}$$

where a is the number of parallel circuits in a phase winding and

u'_{sl} is the number of turn sides in a slot at $a = 1$ which is calculated without rounding by the following expression:

$$u'_{sl} = \frac{\pi DA}{I_{1r} z_1}. \tag{2.5}$$

Here, A is the tentative value of the electric loading accepted at determination of l_δ by (1.4),

I_{1r} is the stator phase rated current in Amperes which is found by the formula

$$I_{1r} = \frac{P_{2r}}{mU_{1r}\,\eta\cos\varphi} \tag{2.6}$$

where P_{2r} and U_{1r} are the d moto rater power and phase voltage respectively, m is the number of phases.

Values of the efficiency η and power factor $\cos\varphi$ are taken as it was accepted at determination of P' (1.3).

2.1.5. The number of parallel circuits of a phase winding is accepted out of possible numbers for the selected winding type and given number of poles so that u_{sl} was integer number and, in the case of two-layer winding – an even number. If the required value of turn sides into a slot can't be obtained in this way, the number of parallel circuits is accepted so that getting integer or even value of u_{sl}will require minimal rounding the value obtained from (2.5).

2.1.6. The number of turns of a phase winding is equal to

$$w_1 = \frac{u_{sl} z_1}{2am}. \qquad (2.7)$$

2.1.7. The final value of the machine electric loading is found by the expression:

$$A = 2I_{1r} w_1 m/(\pi D). \qquad (2.8)$$

It is permitted that the obtained value of A would differ only slightly from those previously found tentative value and must be in the limits defined by plots in Fig. 1.5 or 1.6 depending on the degree of the motor enclosure protection.

2.1.8. The coil span is accepted equal:

- $y = \tau$ for single layer windings. For them the pitch factor equals $k_p = 1$ and the winding factor equals the distribution factor, i.e., $k_w = k_d$.
- $y = (0.79 \ldots 0.83)\tau$ for two layer windings. For them the winding factor equals to product of the pitch factor k_p and the distribution factor k_d, i.e., $k_w = k_p k_d$. In the integal slot windings, the coil span (pitch) y is always multiple of the tooth pitch t_1.

The pitch and tooth factors for fundamental harmonic are found by expressions:

$$k_p = \sin(\beta\frac{\pi}{2}),\ k_d = \frac{\sin\frac{\pi}{2m}}{q\sin\frac{\pi}{2mq}} \tag{2.9}$$

where $\beta = \frac{y}{\tau}$ is the relative coil span.

For a fractional winding having $q = b + \frac{c}{d} = \frac{bd+c}{d} = \frac{N}{d}$, the distribution factor is found as

$$k_d = \frac{\sin\frac{\pi}{2m}}{N\sin\frac{\pi}{2mN}}.$$

2.1.9. Refined value of the magnetic flux density fundamental amplitude in the air gap is determined as

$$B_\delta = \frac{\Phi}{\alpha_\delta \tau l_\delta} \cong \frac{p\Phi}{Dl_\delta} \tag{2.10}$$

where

$$\Phi = \frac{k_E U_{1r}}{4k_B w_1 k_{w1} f_1} \tag{2.11}$$

is the magnetic flux passing through a pole pitch. Values of k_E and k_B were accepted at calculations by expressions (1.3) and (1.4) respectively. The coefficient of a pole arc $\alpha_\delta = 2/\pi \cong 0.64$.

If the obtained value of B_δ differs from the value defined by curves given in Fig. 1.5 or 1.6 respectively by more than 5 %, it is necessary to change the value of u_{sl} at the same or other number of parallel circuits (2.4), to find a new number of the phase turns w_1 (2.7), to check a new value of the machine electric loading A (2.8) and to find a new value of the flux density B_δ (2.10), repeating this procedure till obtaining the sufficient value of B_δ.

2.1.10. Allowable stator current density in A/m^2 equals:

$$J_1 = (AJ)/A \tag{2.12}$$

where (AJ) is the recommended value of product of the electric loading and the current density in A^2/m^3 found from Fig. 2.2,

A is electric loading in A/m.

2.1.11. The coil turns side cross-section area, m^2:

$$q_{ef1} = \frac{I_{1r}}{aJ_1}, \tag{2.13}$$

where I_{1r} is taken according (2.6), a is the number of parallel circuits of a phase winding accepted above.

2.2 Selection of stator winding wire and design of teeth area

2.2.1. To select the wire type, it is necessary to choose the insulation thermal class. For three-phase induction motors of 4A series it is chosen depending on the motor shaft height as follows. For motors up to 1000 V with shaft height of 50…132 mm, the insulation thermal class B is accepted. For motors having the shaft height greater than 132 mm, class F should be accepted.

In the case of fed-in winding round copper wires with enamel insulation are used. At the thermal class B are used wires ПЭТВ, at the thermal class F are used wires ПЭТ-155, ПЭТ-155М or ПЭТ-200. The wire ПЭТ-155М is used at mechanized wounding.

For fed-in coils, the round insulated conductor diameter must be not greater than 1.4 mm at mechanized wounding (motors with $h \leq 160$ mm), and not greater than 1.7 mm at hand wounding (motors with $h > 160$ mm).

2.2.2. If the obtained value of the turn side (i.e., of effective conductor) cross-section area (2.13) may be provided only at greater values of the conductor diameter, it is necessary to divide the conductor into several elementary conductors which are wound in parallel. The number of

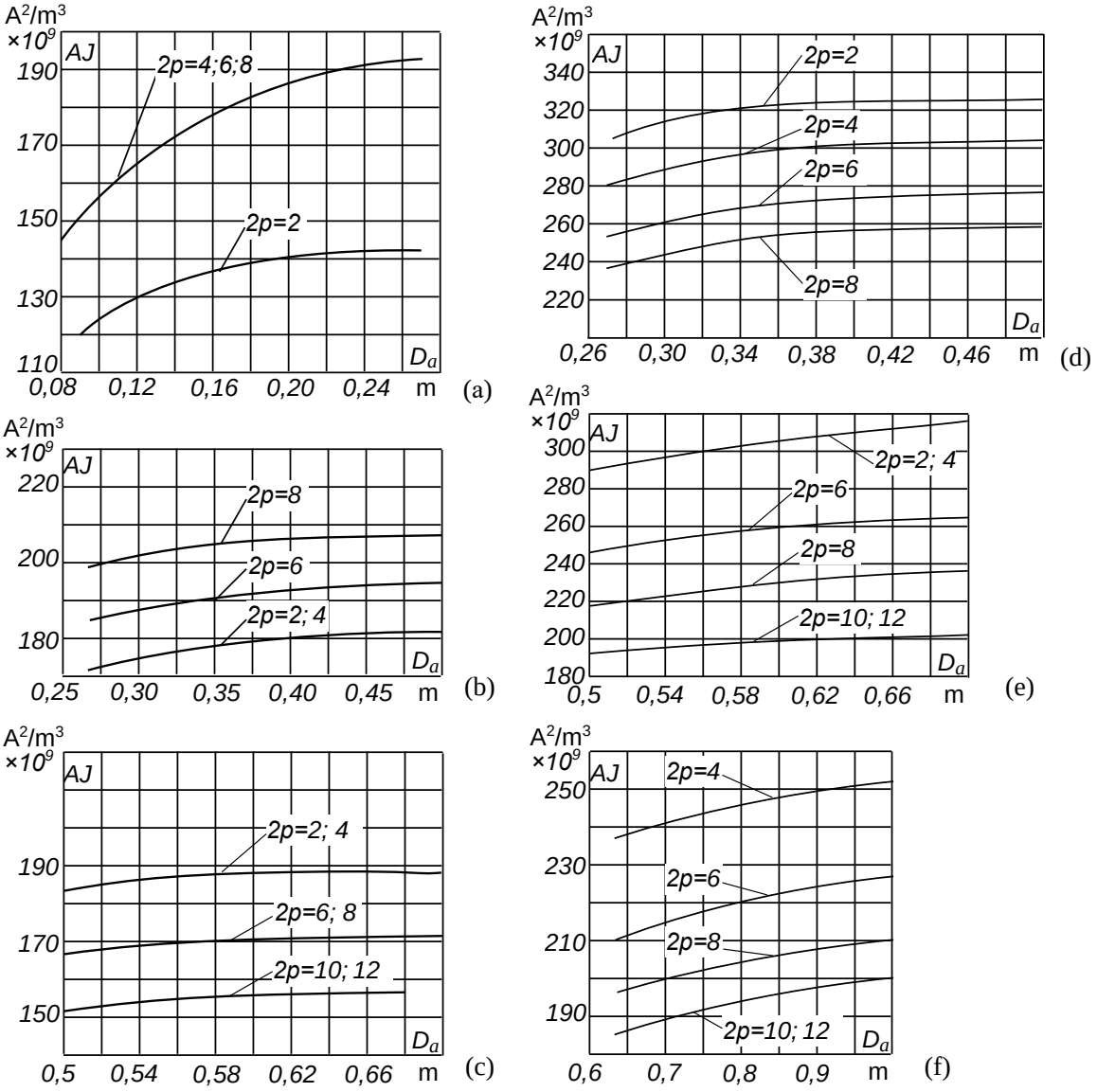

Figure 2.2 Average value of the product (AJ) for motors of 4A series with enclosure protection IP44: $h \leq 132$ mm (a), $h = 160 \ldots 250$ mm (b), $h = 280 \ldots 355$ mm for motors with blown through rotors (c), and IP23: $h = 160 \ldots 250$ mm (d), $h = 280 \ldots 355$ mm at $U < 6000$ V (e), $h = 280 \ldots 355$ mm at $U = 6000$ V (f)

elementary conductors must be such that, with an acceptable diameter of the insulated wire, would be

$$q_{el1} \cdot n_{el1} = q_{ef1}. \tag{2.14}$$

where q_{el1} is the elementary uninsulated conductor diameter. Standard diameters of round conductors with enamel insulation intended for electric machines windings are given in Table 2.2, and in Appendix 7 (Table A 7.1).

Table 2.2 Diameters of insulated and non-insulated round conductors for electric machines windings, and cross-section area of non-insulated round wire

Rated diameter of non-insulated conductor in mm	Mean value of insulated conductor diameter in mm	Cross-section area of non-insulated conductor in mm^2	Rated diameter of non-insulated conductor in mm	Mean value of insulated conductor diameter in mm	Cross-section area of non-insulated conductor in mm^2
0,08	0,10	0,00502	(0,53)	0,585	0,221
0,09	0,11	0,00636	0,56	0,615	0,246
0,10	0,122	0,00785	0,60	0,655	0,283
0,112	0,134	0,00985	0,63	0,69	0,312
0,125	0,147	0,01227	(0,67)	0,73	0,353
0,14	0,162	0,01539	0,71	0,77	0,396
0,15	0,18	0,01767	0,75	0,815	0,442
0,16	0,19	0,0201	0,80	0,865	0,503
0,17	0,20	0,0227	0,85	0,915	0,567
0,18	0,21	0,0255	0,90	0,965	0,636
(0,19)	0,22	0,0284	0,95	1,015	0,709
0,20	0,23	0,0314	1,00	1,08	0,785
(0,212)	0,242	0,0353	1,06	1,14	0,883
0,224	0,259	0,0394	1,12	1,20	0,985
(0,236)	0,271	0,0437	1,18	1,26	1,094
0,25	0,285	0,0491	1,25	1,33	1,227
(0,265)	0,300	0,0552	1,32	1,405	1,368
0,28	0,315	0,0616	1,40	1,485	1,539
(0,30)	0,335	0,0707	1,50	1,585	1,767
0,315	0,350	0,0779	1,60	1,685	2,011
0,335	0,370	0,0881	1,70	1,785	2,27
0,355	0,390	0,0990	1,80	1,895	2,54
0,375	0,415	0,1104	1,90	1,995	2,83
0,40	0,44	0,1257	2,00	2,095	3,14
0,425	0,465	0,1419	2,12	2,22	3,53
0,45	0,49	0,1590	2,24	2,34	3,94
(0,475)	0,515	0,1772	2,36	2,46	4,36
0,50	0,545	0,1963	2,50	2,60	4,91

Notes: 1. Wires, the sizes of which are indicated in brackets, should be applied only in separate cases at a substantiation of technical and economic expediency.

2. The average value of the diameter of the insulated wire is calculated considering the calculated average bilateral thickness of the enamel insulation, taken as a rounded arithmetic mean of the minimum and maximum thickness.

Recommended number of the elementary conductors for fed-in windings is $n_{el1} \leq (5 \ldots 6)$ for hand wounded windings, and $n_{el1} \leq (2 \ldots 3)$ for mechanized wounded machines. Ultimate number of elementary conductors for hand wounded induction motors is $n_{el1} \leq (10 \ldots 12)$. If n_{el1} is greater than recommended, it is necessary to increase the number of parallel circuits in a phase winding a. In two-pole machines at $a = 2$, the number of elementary conductors may be accepted greater than the recommended but less than the ultimate value.

2.2.3. For form-wound windings that are wound of rectangular wire, the conductors ПЭТВП (thermal class B) are recommended for use at the voltage till 660 V. The conductors ПЭТП-155 are used for the machines with class F insulation, and conductors ПЭТП-200 provide thermal class H. In high-voltage machines the conductors ПЭТВСД having enamel insulation made based on polyester and covered by two-layer glass fiber glued and impregnated with thermally stable varnish are applied.

Dimensions of wire with rectangular cross-section and the insulation thickness are given in Appendix 7 (Tables A 7.2 and 7.3).

2.2.4. If q_{ef1} exceeds 20 mm^2, the rectangular conductors are divided into several elementary ones. Cross-section area of the elementary conductor should be $q_{el1} \leq 17 \ldots 20$ mm^2.

In the case of rigid formed coils application, open slots are used. In this case the number of elementary conductors must be $n_{el1} \leq 2$.

In the case of semi-open slots $n_{el1} = 2$.

The coil turn side (i.e., effective conductor) cross-section area must not be greater than 35…40 mm^2. On this reason, at great values of the stator current I_{1r}, greater possible number of parallel circuits in a phase winding a is accepted.

Final selection of the wire dimensions is made concurrently with design of the stator teeth area.

2.2.5. Consider ways of the stator teeth area designing.

First describe the procedure of the teeth area designing for the case of the coils made of rectangular wire. In this case the open or semi-open slots are used (Fig. 2.3 and 2.4). Open and semi-open slots have parallel sides. Therefore, the tooth width is variable, increasing to the tooth base.

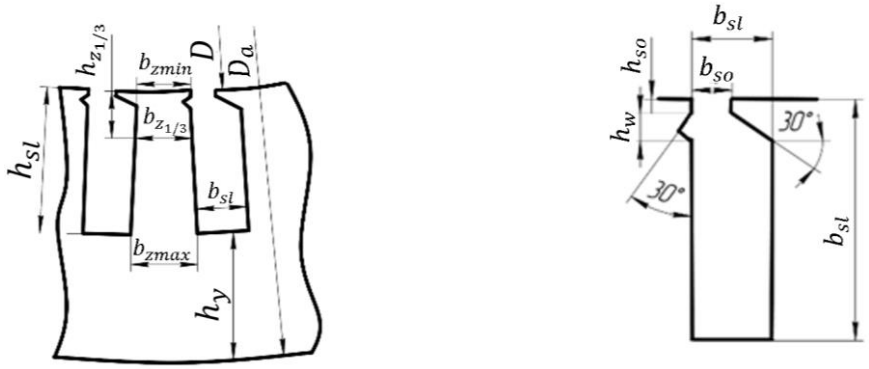

Figure 2.3 Semi-open parallel slot of a stator

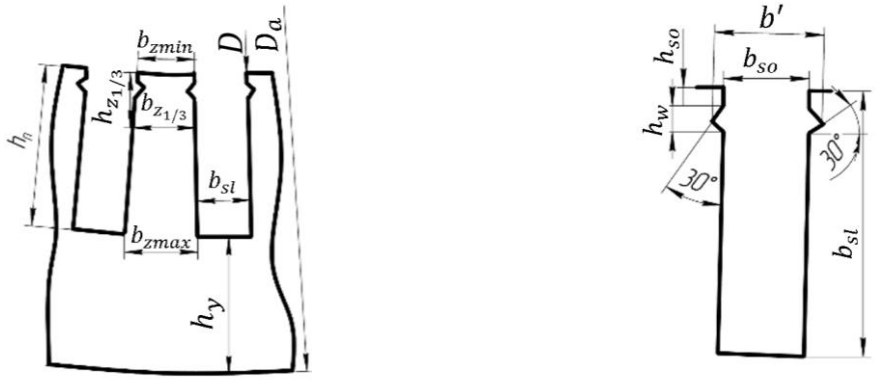

Figure 2.4 Open parallel slot of a stator

2.2.6. Using recommendations given in Table 2.4, the acceptable magnetic flux density in the stator core yoke B_y is taken. Also, is accepted the flux density in the narrowest tooth cross-section $B_{Z1\,max}$.

Next, the stator yoke width in meters is found:

$$h_{y1} = \frac{\Phi}{2B_y l_{cp1} k_{fill}} \tag{2.15}$$

where k_{fill} is the fill (lamination) factor.

Table 2.4 – Permissible values of flux density in different parts of induction motor magnetic circuit

Part of magnetic circuit	Denotation	Degree of protection IP44					Degree of protection IP23					
	$2p$	2	4	6	8	10 and 12	2	4	6	8	10	12
Stator core yoke	B_a	1.4…1.6			1.15…1.35	1.1…1.2	1.45…1.6			1.2…1.4		1.1…1.3
Stator teeth of constant cross-section (fed-in-winding)	B_{z1}	1.7…1.9				1.6…1.8	1.9…2.1	1.8…2.0			1.7…1.9	
Stator teeth in narrowest cross-section, semi-open slots	B_{z1max}	1.75…1.95					1.9…2.1	1.8…2.0				
open slots		1.6…1.8					1.7…1.9					
Rotor yoke:	B_j											
squirrel cage motor		≤ 1.45	≤ 1.25	≤ 1.15	≤ 0.85		≤ 1.55	≤ 1.35	≤ 1.55	≤ 0.95		
wound rotor		–	≤ 1.25	≤ 1.05	≤ 0.75		–	≤ 1.35	≤ 1.15	≤ 0.85		
motor with $U = 6000$ V		–	≤ 1.55	≤ 1.30	≤ 1.00		–	≤ 1.45	≤ 1.20	≤ 1.0		
Rotor teeth with constant cross-section (pear-shaped slots)	B_{z2}	1.75…1.85					1.8…1.95					
Rotor slots in narrowest cross-section:	B_{z2max}											
cage motor		1,5…1.7		1.45…1.69			1.6…1.8		1.55…1.7			
wound motor		1.85…2.05		1.75…1.9			2.0…2.2		1.9…1.05			

Selection of the steel, the method of sheets insulation, and the fill factor value depends on the machine shaft height and voltage and is made with the help of Table 2.5 or Appendix 3 (table 3.1).

2.2.7. Minimum stator tooth width, in meters, is equal to:

$$b_{Z1\,min} = \frac{B_\delta t_1 l_\delta}{B_{Z1\,max} l_{cp1} k_{fill}}. \quad (2.16)$$

Table 2.5. – Recommended steel grades, way of sheets insulation and values of fill factor for induction motors

h, mm	U, V	Steel grade	Stator		Cage rotor		Wound rotor	
			Method of sheets insulation	k_{fill}	Method of sheets insulation	k_{fill}	Method of sheets insulation	k_{fill}
50…250	≤ 660	2013	Oxidation	0.97	Oxidation	0.97	–	–
280…355	≤ 660	2312	Varnish	0.95	Oxidation	0.95	Varnish	0.95
400…560	6000	2411	Varnish	0.95	Varnish	0.95	Varnish	0.95

Preliminary slot dimensions:

- the slot height

$$h_{sl1} = \frac{D_a - D}{Z_1} - h_y \quad (2.17)$$

- the slot width

$$b_{sl1} = t_1 - b_{Z1\,min} \quad (2.18)$$

as a rule, $b_{sl1} \cong (0.4 \ldots 0.5) t_1$.

The obtained value of b_{sl1} is used for selection of dimensions of the wire for the stator winding.

2.2.8. Dimensions of rectangular conductor for the stator winding inserted into slots with parallel sides are determined based on the obtained value of the slot width b_{sl1} and the area of elementary conductor cross-section q_{el1} taking into consideration the wire, coil, and slot insulation thickness.

The uninsulated conductor dimensions are its width b oriented to the width of the slot, and thickness a. From the Appendix7 (Table A 7.2), a

standard wire which has the values of b and q nearest to the calculated values is selected. At this, the conductor height must be $a \leq 2.5 \ldots 3$ mm that provides uniform current distribution in the wire cross-section. The conductor thickness may be some greater in the case of small number of the coil turns.

To avoid difficulties at coils formation it is necessary that $a > 1$ mm. It is also necessary to avoid close values of a and b as in this case the conductor has tendency to twisting.

The sum of the sizes of the uninsulated conductors, of the wire, coil and slot insulation, and interlayers thickness with consideration allowances for the core lamination assembling defines dimensions of the slot part occupied by the winding.

The allowances for laminations assembling are accepted depending on the motor shaft height as follows:

h, mm	Δb_{sl}, mm	Δh_{sl}, mm
50…132	0.1	0.1
160…250	0.2	0.2
280…355	0.3	0.3
400…560	0,4	0,3

The insulation thickness by the slot width and height is accepted according to Table 2.6 or to Appendix 7 (Table A 7.3).

Table 2.6. – Insulation thickness by slot height and width

h, mm	Slot shape	h_{ins}, mm	$2b_{ins}$, mm
280…355	Semi-open	4,5	2,2
280…355	Open	4,5	1,8
400…450	Open	12,4	4,1

In the case of $n_{el1} = 1$, the conductor width is $b = b_{sl1} - \Delta'_{ins}$, where $\Delta'_{ins} = 2b_{ins} + \Delta b_{sl}$, b_{ins} is unilateral total thickness of insulation in the slot

(insulation of the slot, coils, coil turn and conductor), Δb_{sl} is allowance for the core laminations assembling.

In the case of $n_{el1} = 2$, the width $b = 0.5(b_{sl1} - \Delta'_{ins})$.

General cross-sections of AC machine slots are shown in Fig. 2.5.

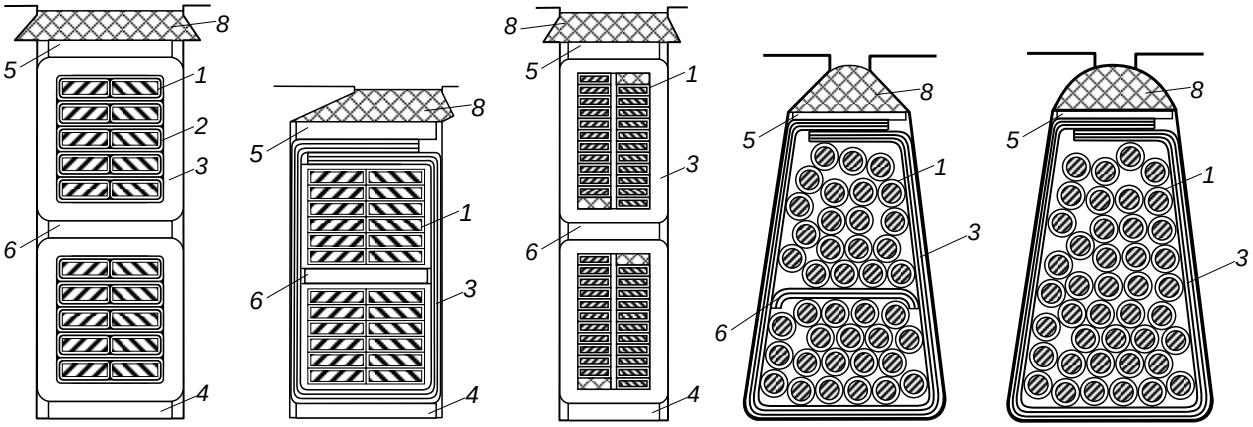

(a) (b) (c) (d) (e)

Figure 2.5 – Cross-section of AC machine slots:
(a) – open slots with inserted coil sides of form-wound winding,
(b) – semi-open slots for insertion of partly form-wound winding,
(c) – open slots of large machine with bar winding,
(d) – semi-closed slot with fed-in two-layer winding,
(e) – semi-closed slot with fed-in one-layer winding.
Reference numerals: 1 – wire insulation, 2 – turn insulation, 3 – slot insulation,
4 – insulating spacer at slot bottom, 5 – insulating spacer under wedge,
6 – interlayer insulation

2.2.9. After the wire selection, ***draw up a table of the slot filling***, indicating the wire dimensions, insulation thickness and layers number, and thickness of interleaving insulation using as a base data given in Appendix 10.

Based on that, ***the slot clear dimensions h_{sl1}, b_{sl1}, b', h_{so} b_{so}, h_w are defined.***

For open slots it is accepted:

$b' - b_{sl} = 2 \dots 5$ mm, $h_{so} = 0.5 \dots 1.0$ mm, $h_w = 3.0 \dots 3.5$ mm.

For semi-open slots

$b_{so} = 0.5 b_{sl} + (1.0 \dots 1.5)$ mm, $h_{so} = 0.5 \dots 0.8$ mm, $h_w = 2.5 \dots 3.5$ mm.

2.2.10. Then, the tooth width is calculated as:

$$b_{Z1\,min} = t_1 - b_{sl1}; \qquad b_{Z1\,max} = t_1\left(1 + \frac{2h_{sl1}}{D}\right) - b_{sl1}. \tag{2.19}$$

The tooth height: $h_{Z1} = h_{sl1}$.

2.2.11. Now consider the procedure of ***determination of the shape and dimensions of slots for fed-in windings***. Slots for such windings are shown in Fig. 2.6.

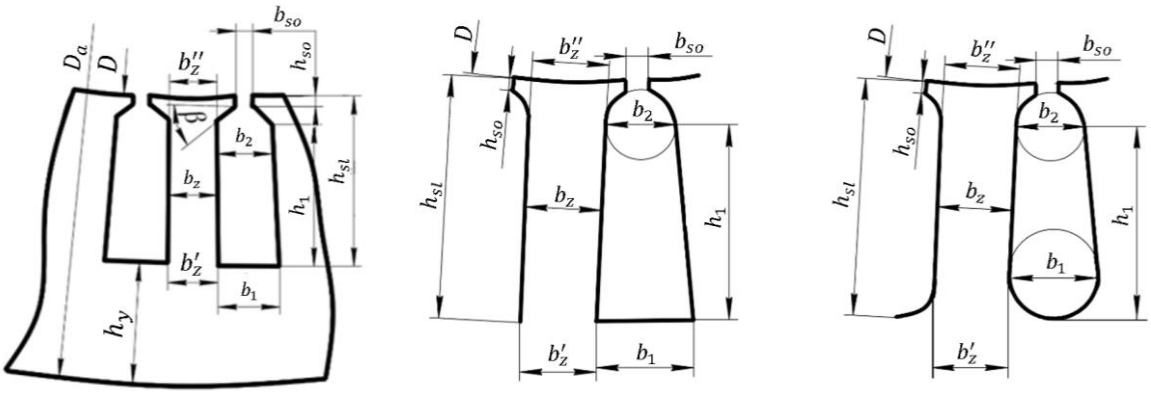

(a) **(b)** **(c)**

Figure 2.6 Slots for fed-in-windings

In induction motors 4A series, trapezoidal slots for placing fed-in-windings are applied. The slope of the wedge part of the slot is accepted equal to $\beta = 45°$ at $h \leq 250$ mm and to $\beta = 30°$ at $h \leq 280$ mm and at $2p = 10$ or 12 regardless of h.

2.2.12. Taking up the assumable values of the magnetic induction from Table 2.4, find the yoke width h_{y1} using (2.15).

2.2.13. After that, the tooth width is determined as

$$b_{Z1} = \frac{B_\delta t_1 l_\delta}{B_{Z1} \cdot l_{cp1} \cdot k_{fill}}. \tag{2.20}$$

The slot dimensions in stamp are:

$$h_{sl1} = \frac{D_a - D}{2} - h_{y1} \qquad b_1 = \frac{\pi(D + 2h_{sl})}{Z_1} - b_{Z1}, \tag{2.21}$$

$$b_2 = \frac{\pi(D+2h_{so}-b_{so})-Z_1 b_{Z1}}{Z_1-\pi} \text{ at } \beta = 45° \quad (2.22)$$

$$b_2 = \frac{\pi\left(D+2h_{so}-b_{so}/\sqrt{3}\right)-Z_1 b_{Z1}}{Z_1-\pi/\sqrt{3}} \text{ at } \beta = 30°. \quad (2.23)$$

The obtained values should be rounded off to the nearest tenth of mm. It is recommended to accept $h_{so} = 0.5$ mm if $h_1 \leq 132$ mm, and $h_{so} = 1$ mm if $h_1 \geq 160$ mm; $b_{so} = d_{ins} + (1.5 \ldots 2.0)$ mm where d_{ins} – diameter of insulated wire, mm.

2.2.14. The slot cross-section area "in stamp" in m^2 is:

$$S_{sl1} = (b_1 + b_2)\, h_1/2 \quad (2.24)$$

where $h_1 = h_{sl} - (h_{so} + h_w)$.

The wedge part of slot height is

$$\begin{aligned} h_w &= (b_2 - b_{so})/2 && \text{if } \beta = 45°; \\ h_w &= (b_2 - b_{so})/\left(2\sqrt{3}\right) && \text{if } \beta = 30°. \end{aligned} \quad (2.25)$$

2.2.15. The slot clear dimensions are:

$$b'_1 = b_1 - \Delta b_{sl}; \quad b'_2 = b_2 - \Delta b_{sl}; \quad h'_1 = h_1 - \Delta h_{sl}$$

where Δb_{sl} and Δh_{sl} are accepted as for parallel slots (see above).
Area occupied by the slot insulation in m^2 is found as

$$S_{ins1} = b_{ins}(2h'_1 + b'_1 + b'_2) \quad (2.26)$$

where b_{ins} is the unilateral thickness of insulation in the slot taken in m. It is accepted depending on the shaft height to:

h, mm	50…80	90…132	160…250	280…315
b_{ins}, mm	0.2	0.25	0.4	0.58

In motors with the shaft height $h = 180 \ldots 250$ mm and having two-layer winding, the area occupied by the interlayer insulation is

$$S_{il} = (0.4b_1 + 0.9b_2) \cdot 10^{-3} \text{ m}^2.$$

In the case of two-layer winding at $h \geq 280$ mm

$$S_{il} = 0.6(b_1 + b_2) \cdot 10^{-3} \text{ m}^2.$$

In one-layer winding, there is no interlayer insulation, and $S_{il} = 0$.

2.2.16. The area of the slot cross-section remaining for the wire placement is equal to

$$S'_{sl1} = \frac{b'_1 + b'_2}{2} h'_1 - S_{ins} - S_{il}. \quad (2.27)$$

Correctness of the slot filing up is checked with the help of the slot fill factor

$$k_{sf} = \frac{d_{ins}^2 u_{sl} n_{el1}}{S'_{sl1}}. \quad (2.28)$$

For hand wounded windings the value must be $k_{sf} = 0.70 \ldots 0.75$. For mechanized wounded windings, the slot fill factor is $k_{sf} = 0.70 \ldots 0.72$.

At less obtained values of k_{sf}, it is necessary to reduce S'_{sl1} by increasing h_{y1} and b_{Z1} that will cause reduction of B_{Z1} and B_{y1}. If the magnetic flux density reduces to lower than indicated in Table 2.4 values, it is necessary to reduce the core length or to accept the near less height of the motor shaft.

At greater values of k_{sf}, when it is impossible to reduce it to the acceptable value by selection h_{y1} and b_{Z1} saving permissible values of B_{y1} and B_{Z1}, or by accepting greater value of q_{el1} at less value of n_{el1}, it is necessary to increase the core length or to design another version of the motor after change of the principal dimensions.

2.2.17. In the case of fed-in windings, the tooth width and height are found by expressions given in Table 2.7. Usually, $b'_Z = b''_Z = b_{z1}$. If the obtained values of b'_Z and b''_Z slightly differ, it is recommended to determine b_Z for further calculations as

$$b_{Z1} = \frac{b'_Z + b''_Z}{2}.$$

If the difference is considerable, it is necessary to change the slot dimensions, or to calculate, in the following computations, the tooth mmf as for the case of parallel slots.

Table 2.7 – To calculation of stator tooth dimensions

Size	Figure 2.6, *a*	Figure 2.6, *b*	Figure 2.6, *c*
b'_z	$\pi\frac{D+2h_{sl}}{z_1} - b_1$	$\pi\frac{D+2h_{sl}}{z_1} - b_1$	$\pi\frac{D+2h_{sl}-b_1}{z_1} - b_1$
b''_z	$\pi\frac{D+2(h_{sl}-h_1)}{z_1} - b_2$	$\pi\frac{D+2h_{so}+b_2}{z_1} - b_2$	$\pi\frac{D+2h_{so}+b_2}{z_1} - b_2$
h_z	h_{sl}	h_{sl}	$h_{sl} - 0{,}1b_1$

2.2.18. After final selection of q_{el1}, n_{el1} and a, the current density is adjusted:

$$J_1 = \frac{I_{1r}}{aq_{el1}n_{el1}}. \qquad (2.29)$$

2.3. Rotor winding and rotor teeth area

2.3.1. First consider the wound rotor.

A winding of the wound rotor has the same number of phases and number of pole pairs that the stator one, i.e., $m_2 = m_1 = m;\ p_2 = p_1 = p$.

The number of rotor slots should be not equal to the number of stator slots. Preliminary value of the rotor number of slots per pole and per phase is taken as $q_2 = q_1 \pm K$ where K is accepted equal $K = 1$ or $^1/_2$. The rotor number of slots preliminary value is found as

$$z_2 = z_1\, q_2/q_1. \qquad (2.30)$$

It is recommended to provide the stator to rotor number of slots ratio as in motor 4A series (Table 2.8). If the preliminary value of q_2 gives another number of Z_2 than indicated in the table, it is recommended to change it according to the Table.

Table 2.8 – Relation of stator and rotor slot numbers in induction motors of 4A series

h, mm	Ratio z_1/z_2 at different values of 2p					
	2	4	6	8	10	12
Squirrel-cage motors						
50…63	24/19	24/18	36/28	–	–	–
71	24/19	24/18	36/28	36/28	–	–
80…100	24/19	36/28	36/28	36/28	–	–
112…132	24/19	36/34	54/51	48/44	–	–
160	36/28	48/38	54/51	48/44	–	–
180…200	36/28	48/38	72/58	72/58	–	–
225	36/28	48/38	72/56	72/56	–	–
250	48/40	60/50	72/56	72/56	–	–
280…355	48/38	60/70	72/82	72/86	90/106	90/106
400…450	–	60/70	72/84	72/86	90/106	90/106
Wound motors						
200	–	48/36	72/54	72/48	–	–
225	–	48/66	72/81	72/84	–	–
250	–	60/72	72/81	72/84	–	–
280…355	–	60/72	72/81	72/84	90/120	90/108
400…450	–	60/72	72/90	72/96	90/120	90/126

2.3.2. As a rule, in induction motors having the rated power till 80…100 kW the two-layer lap windings are used. In machines of higher power, the wave bar windings are applied.

To provide easier mechanical balancing of the rotor, the rotor winding leads are distributed along the circle as uniformly as it is possible.

2.3.3. For determination of the needed number of rotor phase turns w_2, the voltage E_2 induced in a phase of locked rotor is preliminary accepted as follows. The voltage across the slip rings of the locked rotor is usually in the

range of 150…250 V (in some motors till 500 V). As the rotor winding is usually has star connection the phase induced voltage at locked rotor is accepted equal $E_2 = 85 \ldots 145\ (290)$ V. If the rotor winding is connected in delta, the induced voltage E_2 is accepted equal 150…250 (500) V.

The number of turns of the rotor phase is found as

$$w_2 = \frac{E_2}{U_{1r}} w_1. \tag{2.31}$$

The number of effective turns in the rotor slot is equal to

$$u_{sl2} = \frac{2w_2 m_2}{z_2} = \frac{w_2}{p_2 q_2}. \tag{2.32}$$

The obtained value of u_{sl2} must be rounded to the nearest even number. After that the rotor turns number is adjusted according to the expression:

$$w_2 = u_{sl2} p_2 q_2. \tag{2.33}$$

For two-layer wave bar winding

$$u_{sl2} = 2, \qquad w_2 = 2p_2 q_2 = z_2/m_2.$$

2.3.4. After determination w_2 it is necessary to check the condition:

$$U_{sr} = \sqrt{3} U_{1r} \frac{w_2}{w_1} \leq 800 \ldots 1000 \text{ V}. \tag{2.34}$$

If it is necessary to reduce U_{sr} (the voltage between slip rings at stationary rotor), the number of parallel circuits in the rotor phase of wave bar winding may be accepted equal $a = 2$. In this case a wave bar winding is symmetrical only if q_2 is integer).

2.3.5. Preliminary rotor phase current is found as

$$I_{2r} = k_i \cdot I_{1r} \cdot v_i \tag{2.35}$$

where k_i is the coefficient considering influence of no-load current I_0 and the windings impedance onto the ratio I_2/I_1. Its value is accepted according to the curve $k_i = f(\cos\varphi)$ presented in Fig. 2.7. Value of $\cos\varphi$ is accepted according to div.1.2. The current transformation ratio

$$v_i = \frac{m_1 w_1 k_{w1}}{m_2 w_2 k_{w2}}. \quad (2.36)$$

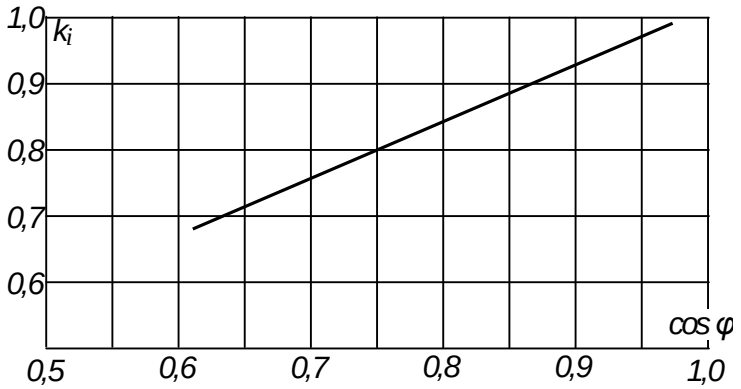

Figure 2.7 – Curve for determination coefficient k_i

2.3.6. The effective rotor conductor cross-section area in m^2:

$$q_{ef2} = I_{2r}/J_2 \quad (2.37)$$

where J_2 – the rotor winding current density in A/m^2. For lap windings of B and F thermal class it is accepted in the limits $J_2 = (5 \dots 6.5) \cdot 10^6$ A/m^2. For bar wave windings, $J_2 = (4.5 \dots 5.5) \cdot 10^6$ A/m^2.

2.3.7. The rotor effective conductors are not divided into elementary ones as at the rated speed the rotor frequency $f_{2r} = s_r f_{1v}$ is very small, and the skin effect is not appreciable.

In wound rotors with the lap windings open slots with parallel sides are used, in the case of the bar wave windings – semi-closed parallel slots are made. These slots are presented in Fig. 2.8.

A parallel slot width is assumed in the range of $b_{sl2} = (0.4 \dots 0.45)t_2$ where t_2 – the tooth pitch at the rotor surface. Subtracting the doubled insulation thickness by the slot width, find preliminary width of the slot for placing the wires as $b_2 = b_{sl2} - 2b_{ins}$. The doubled insulation thickness for lap windings is assumed equal 2.0 mm, for bar windings at $h = 225 \dots 250$ mm - equal 1.4 mm, at $h = 280 \dots 355$ mm - equal 1.6 mm, and at $h = 400 \dots 450$ mm - equal 3.0 mm.

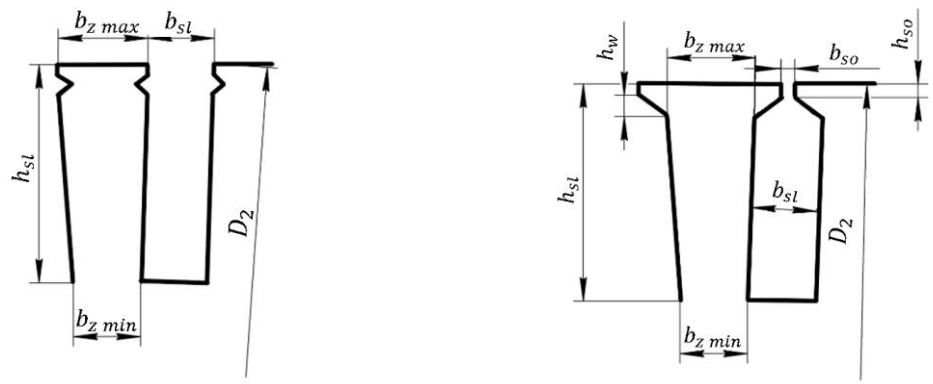

(a) (b)

Figure 2.8 – Open and semi-closed rotor slots

Using the found values of b_2 and q_{ef2}, select the conductor dimensions. After that the slot dimensions are amended.

For rotor lap windings, the same grades of rectangular winding wires that for stators are applied. For bar wave winding bald copper conductors enclosed in a solid insulating sleeve are used.

The wedge height is assumed equal:

- $h_w = 2.5$ mm at $h = 280 \ldots 355$ mm;
- $h_w = 3.5$ mm at $h = 400$ mm.

Width and height of the slot opening are taken equal:

$$b_{so} = 1.5 \text{ mm}, h_{so} = 1.0 \text{ mm}.$$

Then the slot depth h_{sl2} is determined.

After that, the slot dimensions in stamp b_{sl2} and h_{sl2} are calculated by adding the allowances Δb_{sl} and $\Delta h_{sl}$for the core laminations assembling to the slot width and depth found before selection the conductor dimensions. The allowances for the core laminations assembling are assumed as it was described in item 2.2.8.

Next, minimum tooth width and maximum flux density in the rotor tooth are determined:

$$b_{z2min} = \frac{\pi(D_2 - 2h_{sl2})}{z_2} - b_{sl2}\,, \quad B_{z2max} = \frac{B_\delta t_2 l_\delta}{b_{z2min} l_{cp2} k_{fill}}. \qquad (2.38)$$

Maximum rotor tooth width in the case of open slots is

$$b_{z2max} = \frac{\pi D_2}{z_2} - b_{sl2}, \quad (2.39)$$

and in the case of semi-closed slots, it is

$$b_{z2max} = \frac{\pi D_2 - (h_{so} + h_w)}{z_2} - b_{sl2}. \quad (2.40)$$

The teeth height is equal to the depth of the slot, i.e., $h_{z2} = h_{sl2}$.

2.3.8. Now consider the teeth area of a squirrel-cage rotor.

The number of cage rotor slots may be selected from Table 2.9 depending on $2p$ and z_1 and availability the rotor slots skewing. Such selection provides reduction of the field harmonics influence, of noise and vibration at the machine operation.

Rotor slot skewing is recommended for cage motors of not great power having small air gap. In 4A series rotor slots are skewed in motors with $h < 160$ mm. The skew is assumed equal $b_{sc} = t_2$, where t_2 – the rotor tooth pitch.

In motors of small power, the number of rotor teeth is as a rule less the number of stator teeth. In larger motors the number of rotor teeth is sometimes greater than of the stator that is made to decrease the current in cage bars and to provide more uniform conductor distribution around the circle.

2.3.9. Assuming $m_2 = z_2$ and $w_2 = {}^1/_2$ find the current transformation ratio:

$$v_i = \frac{m_1 w_1 k_{w1}}{m_2 w_2 k_{w2}} = \frac{2 m_1 w_1 k_{w1}}{z_2}. \quad (2.41)$$

The rotor phase current being equal the rotor bar current is found as

$$I_2 = I_1 v_i k_i \quad (2.42)$$

where k_i is assumed using Fig. 2.7 as it was made in div. 2.3.5.

The current in sections of end rings between the adjacent bars is equal to

$$I_{ring} = \frac{I_2}{2 \sin \frac{\pi p}{z_2}}. \quad (2.43)$$

Table 2.9 – Recommended number of stator and rotor slots for cage induction motors

$2p$	Z_1	Z_2	
		Slots without skewing	Skewed slots
2	18	15, 21, 22	19, 22, 26, 28, 31,33,34,35
	24	15, 17, 19, 32	19, 26, 31, 33,34,35
	30	22, 38	20, 21, 23, 37,39,40
	36	26, 28, 44,46	25, 27, 28, 29, 43, 45, 47
	42	32, 34, 50, 52	–
	48	38, 40, 56, 58	37, 39, 41, 55, 59
4	24	16, 17	16,18, 28, 30, 33, 34, 36
	36	26, 38, 44, 46	27, 28, 30, 34, 38, 45, 48
	48	34, 38, 56,58, 62, 64	38, 40, 57, 59
	60	50, 52, 68, 70, 74	48, 49, 51, 56, 64, 69, 71
	72	62, 64, 80, 82, 86	61, 63, 68, 76, 81, 83
6	36	26, 46	28, 33, 47, 49, 50
	54	44, 64, 66, 68	42, 43, 51, 65, 67
	72	53, 55, 62, 86, 88	57, 59, 60, 61,83, 85, 87, 90
	90	74, 76, 78, 80, 100, 102, 104	75, 77, 79, 101, 103, 105
8	36	–	28
	48	36, 44, 62, 64	35, 44, 61, 63, 65
	72	56, 58, 86, 88, 90	56, 57, 59, 85, 87, 89
	84	66, 70, 98, 100, 102, 104	–
	96	78, 82, 110, 112, 114	79, 80, 81, 83, 109, 111, 113
10	60	44, 46, 74, 76	57, 69, 77, 78, 79
	90	68, 72, 74, 76, 104, 106, 108, 110	70, 71, 73, 87, 93, 107, 109
	120	86, 88, 92, 96, 98, 102, 104	99, 101, 103, 117, 123, 137
12	72	56, 64, 80, 88	69, 75, 80, 89, 91, 92
	90	68, 70, 74, 88, 98, 106, 108, 110	86, 87, 93, 94
	108	86, 88, 92, 100, 116, 124, 128, 130	84, 89, 91, 104, 105, 111, 112

The rotor bar cross-section area equals:

$$q_b = \frac{I_2}{J_b} \tag{2.44}$$

where the current density J_b in the bar is accepted equal:

- For motors with degree of protection IP44 and aluminum squirrel cage, $J_b = (2.5 \ldots 3.5)10^6\ \mathrm{A/m^2}$
- For motors with degree of protection IP23 and aluminum squirrel cage, J_b is accepted by (10 … 15) % greater than at protection IP44
- For motors with copper squirrel cage J_b is accepted equal $(4.0 \ldots 8.0)10^6\ \mathrm{A/m^2}$.

In the indicated intervals, greater values are accepted for motors of less power.

The end ring cross-section area is found as

$$q_{ring} = \frac{I_{ring}}{J_{ring}} \tag{2.45}$$

where the current density in the ring J_{ring} is accepted by (15 … 20) % less than for the bars.

2.3.10. Dimensions of a cage motor rotor slots are determined with account of their shape (see Fig. 2.9, 2.10, 2.11 and 2.12).

Focusing on 4A series motors, it is recommended to select the rotor slot shape as follows:

- for motors with $h \leq 250$ mm, the pear-shaped slots and cast aluminum squirrel cage are arranged (Fig. 2.9)

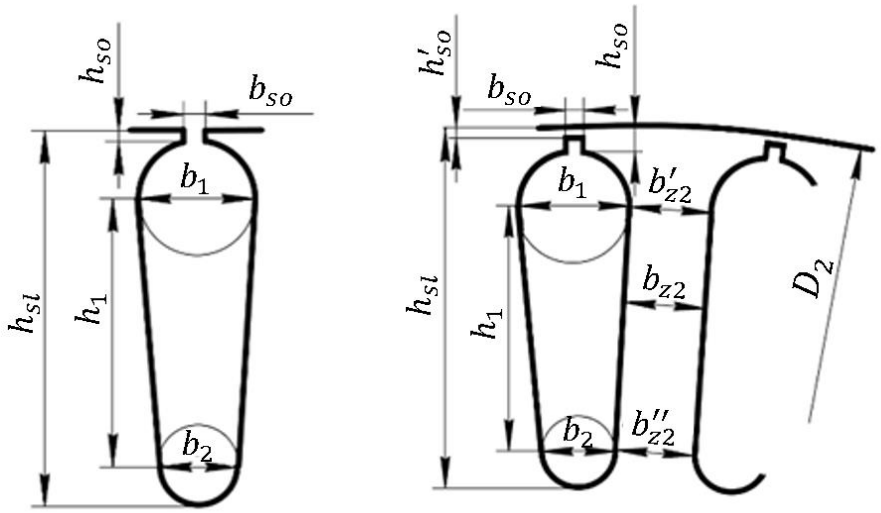

Figure 2.9 – Pear-shaped semi-closed (a) and closed (b) slots

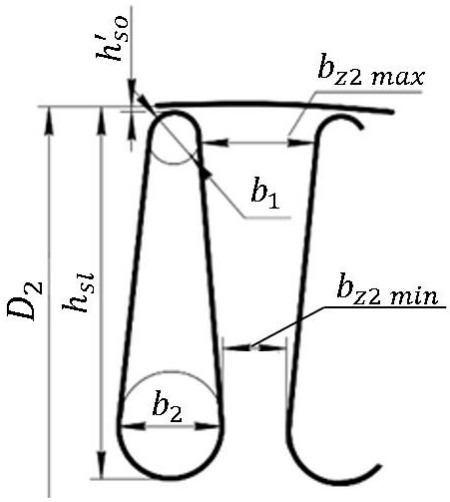

Figure 2.10 – Trapezoidal closed slot

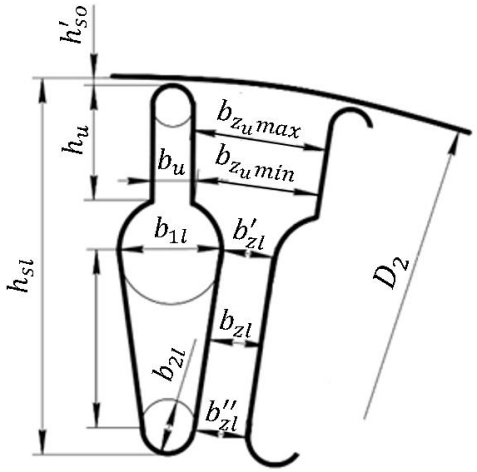

Figure 2.11 – Figured slot

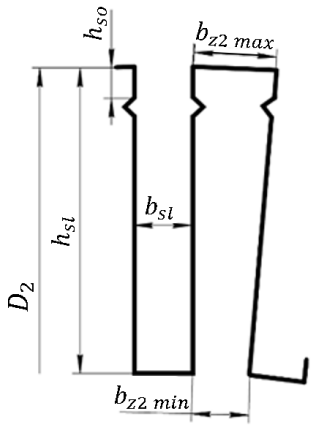

Figure 2.12 – Parallel open slot for inserting aluminum bars

- in motors with $h = 160 \ldots 250$ mm, the pear-shaped closed slots having sizes $b_{so} = 1.5$ mm and $h_{so} = 0.7$ mm are used; at $2p \geq 4$ the dimension h'_{so} equal 0.3 mm and at $2p = 2$ equal 1.0 … 1.5 mm is accepted.
- for motors with $h < 160$ mm, the semi-closed slots are made:
  - at $h < 100$ mm, the slot opening dimensions equal $b_{so} = 1.5$ mm, $h_{so} = 0.5$ mm are excepted.
  - at $h = (112 \ldots 132)$ mm, the slot opening dimensions are accepted equal $b_{so} = 1.5$ mm, $h_{so} = 0.75$ mm
- in motors with $h = 280 \ldots 355$ mm, closed slots are arranged:

- at $2p \geq 4$, the trapezoidal rotor slots (Fig. 2.10) with $h'_{so} = 0.5$ mm are used.
- at $2p = 2$, the rotor slots of shovel shape are used (Fig. 2.11) with $h'_{so} = 1 \ldots 2$ mm and in the case of aluminum cage $h_u = 15 \ldots 16$ mm.

➢ for high-voltage motors with $h = (400 \ldots 450)$ mm, open parallel rotor slots into which rectangular aluminum busses are inserted are used (Fig. 2.12).

2.3.11. Dimensions of pear-shaped slots (Fig. 2.9) are determined to get the needed bar cross-section area q_b and to provide permanent rotor tooth width.

The tooth width is found in this case by the following expression:

$$b_{z2} = \frac{B_\delta t_2 l_2}{B_{z2} l_{cp2} k_{fill}} \tag{2.45}$$

where B_{z2} is accepted according to Table 2.4.

The slot dimensions are found as

$$b_1 = \frac{\pi(D_2 - 2h_{so} - 2h'_{so}) - z_2 b_{z2}}{\pi + z_2},\ b_2 = \sqrt{\frac{b_1^2\left(\frac{z_2}{\pi} + \frac{\pi}{2}\right) - 4q_b}{\frac{z_2}{\pi} - \frac{\pi}{2}}} \tag{2.46}$$

$$h_1 = (b_1 - b_2)\frac{z_2}{2\pi}. \tag{2.47}$$

It is necessary that at $h \leq 132$ mm the width $b_2 \geq (1.5 \ldots 2.0)$mm. At $h \geq 160$ mm it must be $b_2 \geq (2.5 \ldots 3.0)$mm.

The obtained dimension values are to be rounded to the nearest tenth of mm. After that the value of the bar cross-section area is refined:

$$q_b = \frac{\pi}{8}(b_1^2 + b_2^2) + \frac{1}{2}(b_1 + b_2)h_1. \tag{2.48}$$

Then the tooth width in two cross-sections is determined:

$$b'_{z2} = \pi\frac{D_2 - 2(h_{so} + h'_{so}) - b_1}{z_2} - b_1,\ b''_{z2} = \pi\frac{D_2 - 2h_{sl} + b_2}{z_2} - b_2. \tag{2.49}$$

If b'_{z2} and b''_{z2} differ insignificantly, the tooth width is accepted equal:

$$b_{z2} = \frac{b'_{z2}+b''_{z2}}{2}. \quad (2.50)$$

If the difference is considerable the magnetic circuit should be calculated as in the case of trapezoidal rotor slots (see below).

The height of rotor tooth is accepted equal to

$$h_{z2} = h_{sl2} - 0.1b_2. \quad (2.51)$$

2.3.12. In the case of trapezoidal rotor slots (Fig. 2.10) it is expedient to determine their dimensions using a graph-analytical method.

First, minimum tooth width is determined:

$$b_{z2min} = \frac{B_\delta t_2 l_2}{B_{z2max} b_{sc2} k_{fill}} \quad (2.52)$$

where B_{z2max} is found by Table 2.4.

The diameter b_1 must be not less than (3.5 … 4.0) mm.

The slot drawing is made to scale, for example, 10:1. We draw a section of the rotor circle having diameter of D_2 , and the line of a rotor slot axis. Then, the lines of the axes of the teeth adjacent to the slot on the left and right at angle of $180°/z_2$ are drawn.

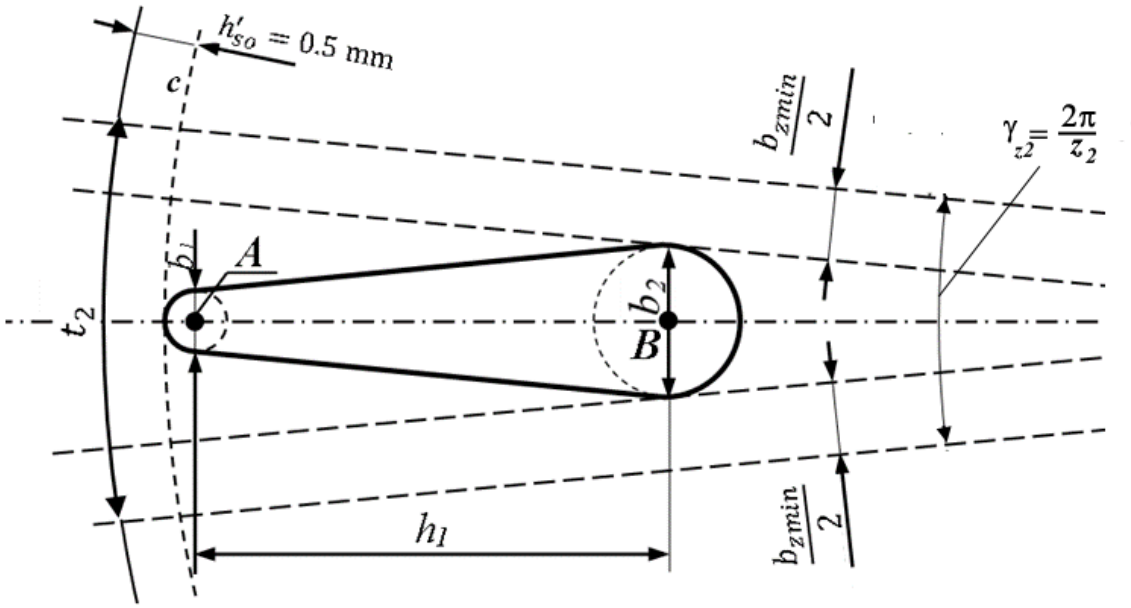

Figure 2.13 – Determination of trapezoidal rotor slot of cage induction motor

After that, straight lines at distance of $b_{z2min}/2$ from the drawn teeth axes and parallel to them are built.

Then the arc c is drawn at $h'_{so} = 0.5$ mm with account of the drawing scale from the rotor circumference, and the circular arc of a diameter equal to b_1 representing the upper slot bound is drawn.

The final stage of geometric constructions for the rotor slot dimensions determination is selection of such a distance AB (or h_1) at which the needed bar cross-section area is provided. The obtained bar cross-section area is found by expression (2.48).

It is possible to vary the minimum tooth width b_{z2min} in the limits which agree with the limiting values of B_{z2max} according to Table 2.4.

The rotor tooth dimensions are found as

$$\begin{cases} b_{z2max} = \pi \frac{D_2 - (2h'_{so} + b_1)}{z_2} - b_1; \\ b_{z2min} = \pi \frac{D_2 - (2h_{sl} - b_2)}{z_2} - b_2; \\ h_{z2} = h_{sl} - 0.1b_2. \end{cases} \quad (2.53)$$

2.4. Construction of rotor core

In the case of $D_2 < 990$ mm the rotor core is fitted to the shaft directly without an intermediate landing bush.

At $h \leq 250$ mm shrink fit is applied without a key. At greater shaft height the core is mounted with a key.

At $D_2 > 990$ mm is assembled from laminated segments on a mounting bush or on longitudinal edges welded to the shaft.

At $h \geq 250$ mm round axial ducts are made in the core to improve its cooling and to reduce its weight and the moment of inertia. The ducts are arranged in one or two rows (Fig. 2.14). The duct numbers and diameter are given in Table 2.10.

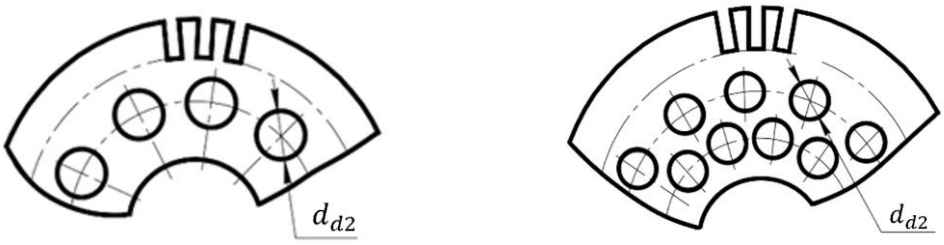

(а) (б)

Figure 2.14 – Axial ducts in rotor cores

Table 2.10 – Number and diameter of axial rotor ducts

h, mm	Number of ducts n_{d2} and their diameter d_{d2} (mm) at different $2p$							
	2		4		6		8,10 and 12	
	n_{d2}	d_{d2}	n_{d2}	d_{d2}	n_{d2}	d_{d2}	n_{d2}	d_{d2}
250	10	15	10	20	10	30	10	30
280	12	20	12	32	12	40	12	40
315	12	20	12	40	12	40	12	40
355	12	20	12	50	12	50	12	50
400	-	-	9	55	9	65	9	75
450	-	-	9	65	9	75	9	90

Radial ducts are made in a rotor at $l_2 > 350$ mm. Their size and number are the same as in the stator core (see div. 1.2.7).

The inner rotor diameter at direct core fitting to the shaft is determined as

$$D_j = k_{sh} D_a \qquad (2.54)$$

where k_{sh} is accepted according to Table 2.11.

Table 2.11 – Values of k_{sh} for induction motor shaft diameter determination

h, mm	50 … 63	71 … 253	280 … 355		400 … 500		
$2p$	2 … 6	2 … 8	2	4 … 12	4	6	8 … 12
k_{sh}	0.19	0.23	0.22	0.23	0.20	0.23	0.25

In the case of fitting the core on a mounting bush or on a finned shaft the rotor core inner diameter D_j is found proceeding from the maximum acceptable flux density B_j in the rotor core yoke:

$$\begin{cases} h_j = \frac{\Phi}{2B_j l_{cs2} k_{fill}}; \\ D_j = D_2 - 2\left(h_{sl2} + h_j\right). \end{cases} \quad (2.55)$$

3. MOTOR MAGNETIC CIRCUIT CALCULATION

To determine the magnetizing current, the mmf per pair of poles of the magnetic field, has to be found.

The values of the magnetic flux density and the magnetic field strength used at the calculation are amplitudes of their fundamental harmonics.

It is assumed that the motor magnetic circuit consists of five homogenous sections connected in series. These are **the air gap between the stator and rotor cores, the stator teeth, the rotor teeth, the stator core yoke, and the rotor core yoke**. Under the calculation of the circuit sections mmf (i.e., the magnetic tension at the sections), it is assumed that the flux density is uniformly distributed along each the section and throughout its cross-section area.

Sequence of the magnetic circuit mmf calculation is the following:

1. Determination the magnetic flux density for each the section
2. Determination of the magnetic field strength for each the section
3. Determination of the magnetic flux path length in the bounds of each the magnetic circuit section along the average field line
4. Determination of mmf along the magnetic circuit sections
5. Determination of the total mmf along the closed average magnetic line.

Saturation of ferromagnetic material of the magnetic circuit causes flattening the flux density curve. To improve the calculation accuracy, the saturation curves which take into consideration non-linear dependence

between the flux density and the magnetic field strength, and flattening the magnetic flux density curves, are used (Appendix 1).

The availability of slots on the stator and rotor cores increases the air gap reluctance. At determination of the magnetic tension (mmf) of the air gap, mmf F_δ is increased by introducing the coefficient of air gap $k_\delta > 1$ in the calculation expression.

Calculation of the induction motor magnetic circuit is performed for no-load conditions under the rated voltage.

3.1. The cross-section areas of the magnetic circuit sections enter the expressions for determination of the sections' flux density as products of appropriate dimensions.

3.2. Values of the flux density amplitude in the sections of the magnetic circuit determination

3.2.1. The flux density in the air gap B_δ was determined in subdivision 2.1.9.

3.2.2. At determination of the flux density in stator or rotor teeth, the distance of any tooth cross-section from the narrowest one is denoted as x, and the flux density in it is B_{zx}.

The calculated values of the flux density in the stator and rotor teeth are determined in the following way:

- in the case when a tooth width is constant (at trapezoidal stator slots or pear-shaped rotor slots) the flux density in itis determined as

$$B_{z1(2)} = \frac{B_\delta t_{1(2)} l_\delta}{b_{z1(2)} l_{cp1(2)} k_{fill}} \quad (3.1)$$

- in the case of parallel slots, the tooth has smoothly varying width, and the flux density in it is determined differently depending on the **maximum** value of the flux density in the tooth

$$B_{z1(2)max} = \frac{B_\delta t_{1(2)} l_\delta}{b_{z1(2)min} l_{cp1(2)} k_{fill}},$$

namely:

- if maximum flux density in the narrowest tooth cross-section $B_{z1(2)max} \leq 2.0\,T$, the tooth mmf can be found using the calculated magnetic strength value in the cross-section area at $x = \frac{1}{3} h_{sl1(2)}$.

In such a case the flux density in the tooth is calculated as

$$B_{z1(2)} = \frac{B_\delta t_{1(2)} l_\delta}{b_{z1(2),1/3} l_{cp1(2)} k_{fill}} \quad (3.2)$$

where $b_{z1(2),1/3}$ – the tooth width at $x = \frac{1}{3} h_{sl1(2)}$

- if maximum flux density in the narrowest tooth cross-section $B_{z1(2)max} > 2.0\,T$, the tooth mmf is found using three magnetic strength values in the narrowest, middle, and widest cross-sections. So, the flux density is calculated in this case for these three tooth cross-sections:

$$B_{z1(2)max} = \frac{B_\delta t_{1(2)} l_\delta}{b_{z1(2)min} l_{cp1(2)} k_{fill}}; \quad (3.3)$$

$$B_{z1(2)middle} = \frac{B_\delta t_{1(2)} l_\delta}{b_{z1(2)middle} l_{cp1(2)} k_{fill}}; \quad (3.4)$$

$$B_{z1(2)min} = \frac{B_\delta t_{1(2)} l_\delta}{b_{z1(2)max} l_{cs1(2)} k_{fill}}, \quad (3.5)$$

where $b_{z1(2)min}$, $b_{z1(2)middle}$, $b_{z1(2)max}$ – minimal, average, and maximal tooth width. The flux density in the middle cross-section may be found as the average value of $B_{z1(2)min}$and $B_{z1(2)max}$.

➢ In the case of figured slots or double cage, the tooth mmf is found as the sum of the mmf of upper and lower tooth parts. Therefore, in the upper and lower tooth parts one or several flux density values are found depending on the tooth shape and maximum values of the flux density.

3.2.3. The flux density in the stator (rotor) core yokes is found by the expression:

$$B_{y1(2)} = \frac{\Phi}{2h'_{y1(2)} l_{cp1(2)} k_{fill}} \quad (3.6)$$

where $h'_{y1(2)}$– design stator (rotor) core yoke height calculated as

$$h'_{y1} = \frac{D_a - D}{2} - h_{sl1} - \frac{2}{3} d_{d1} m_{d1} \quad (3.7)$$

$$h'_{y2} = \frac{D_2 - D_j}{2} - h_{sl2} - \frac{2}{3} d_{d2} m_{d2} \quad (3.8)$$

where $d_{d1(2)}$ – the stator (rotor) axial ventilation ducts diameter, $m_{d1(2)}$ – number of the duct rows in the stator (rotor) core.

3.3. Determination of the magnetic field strength amplitude for each the magnetic circuit section is made with account of the section material and magnetic flux distribution.

The magnetic field strength is found by the saturation curves for the steel grades used for the stator (rotor) cores. At this, phenomena of flattening curves of the flux density in the teeth due to saturation and branching off a part of the tooth flux into the slot, and nonuniformity of the flux density along the length of sections of stator (rotor) yokes are considered.

The flux branching off the teeth is negligible if the calculated flux density value $B_{zx} \leq 1.8\ T$, and must be considered if $B_{zx} > 1.8\ T$.

The magnetic field strength under $B_{zx} \leq 1.8\ T$ is found by the curves without account the flux branching off into the slot. Under $B_{zx} > 1.8\ T$ the curves considering as flattening the magnetic flux distribution, as branching off a part of the flux into the slot are used at determination the magnetic field strength in the tooth.

For determination the magnetic strength in yokes, special saturation curves for yokes are used. These curves are also given in Appendix 1.

The saturation curves are available in the manual text too.

3.3.1. Amplitude of the **magnetic strength fundamental in the air gap** equals

$$H_\delta = \frac{B_\delta}{\mu_0} \quad (3.9)$$

where μ_0 – permeability of vacuum, $\mu_0 = 4\pi 10^{-7}\ \mathrm{H/m}$.

3.3.2. **Amplitude of the magnetic field strength fundamental in the stator and rotor teeth** is found in the following order.

If the flux density in a tooth cross-section is less or equal to 1.8 T the magnetic field strength in this cross-section is determined without considering the flux branching off the tooth, and only the flux distribution curve flattening is taken into consideration. In such a case the field strength H_{zx} is found for the calculated value of the flux density B_{zx} with the help of relevant magnetization curves given in Appendix 1 in compliance with the steel grade.

If the flux density in a tooth cross-section is greater than to 1.8 T the magnetic field strength in this cross-section is determined with account as the flux branching off the tooth as the flux distribution curve flattening. In such a case, the field strength H_{zx} is found at the calculated value of the flux density B_{zx} with the help of magnetization curves given in the Figures of Appendix 1 depending on the steel grade. The magnitude of the branching off flux depends on relation between the slot and tooth width at the given cross-section which is taken in account by means of a coefficient

$$k_{slx} = \frac{b_{slx} l_{\delta}}{b_{zx} l_{cp} k_{fill}} \tag{3.10}$$

where b_{slx} and b_{zx} are respectively the slot and tooth width in the cross-section under consideration. To find the field strength H_{zx} in the cross-section it is necessary to use the magnetization curve corresponding to a value of k_{slx}.

In the case the stator (rotor) tooth has constant width and $B_{z1(2)} >$ 1.8 T, the magnetic strength is found for the tooth cross-section in the middle of the tooth height.

In the case of a tooth with smoothly varying width at 1.8 T $< B_{zmax} \leq$ 2.0 T, the magnetic strength is found for the tooth cross-section being away from its narrowest place by 1/3 of the tooth height.

In the case when the stator (rotor) tooth has smoothly varying width and the flux density $B_{zmax} > 2.0\ T$, the magnetic strength is found according to the expression obtained by means of parabolic interpolation (Simpson's formula):

$$H_{z1(2)} = \frac{1}{6}(H_{z1(2)max} + 4H_{z1(2)middle} + H_{z1(2)min}). \qquad (3.11)$$

Here $H_{z1(2)max}$, $H_{z1(2)midle}$ and $H_{z1(2)min}$ are the magnetic field strength values in the stator (rotor) narrowest, middle, and widest tooth cross-section respectively. These magnetic field strength values are found at the flux density values $B_{z1(2)max,}$ $B_{z1(2)middle}$ and $B_{z1(2)min}$with the help of magnetization curves (Tables 3.1, 3.2, 3.3 or Fig. 3.1, 3.2 of the manual text, or relevant curves of Appendix 1) depending on the steel grade and the coefficient k_{slx} for each of the indicated tooth cross-sections.

3.3.3. Amplitude of the magnetic field strength in the stator (rotor) core yokes $H_{y1(2)}$ is determined with the help of magnetization curve for induction motor core yokes at the calculated value of the yoke magnetic flux density $B_{y1(2)}$ (Tables 3.4, 3.5, 3.6 in the text of the Manual, or relevant Tables of the Appendix) choosing the curve for a proper steel grade.

3.4. Determination of the magnetomotive force of magnetic circuit sections

Amplitude of magnetomotive force produced by the magnetizing current at no-load is determined as the total mmf of the motor magnetic circuit sections along the medial design magnetic line per a pair of poles. The total mmf is determined to calculate the magnetizing current.

Amplitudes of the sections mmf per a pair of poles are found as it is described below.

3.4.1. **Mmf of the air gap** is found as

$$F_\delta = 2H_\delta \delta k_\delta \qquad (3.12)$$

where k_δ – the air gap coefficient equal to the product of the coefficients $k_{\delta 1}$ and $k_{\delta 2}$ accounting teeth structure of the stator and rotor cores respectively:

$$k_\delta = k_{\delta 1} k_{\delta 2} \qquad (3.13)$$

$$k_{\delta 1} = \frac{t_1}{t_1 - \gamma_1 \delta} \qquad k_{\delta 2} = \frac{t_2}{t_2 - \gamma_2 \delta} \qquad (3.14)$$

$$\gamma_1 = \frac{(b_{so1}/\delta)^2}{5+b_{so1}/\delta} \qquad \gamma_2 = \frac{(b_{so2}/\delta)^2}{5+b_{so2}/\delta}\,. \tag{3.15}$$

3.4.2. **Mmf of the stator (rotor) teeth** is calculated as

$$F_{z1(2)} = 2H_{z1(2)}h_{z1(2)}. \tag{3.16}$$

3.4.3. **After determination of the magnetomotive forces** F_δ, F_{z1} and F_{z2} the teeth area saturation factor k_z should be assessed with the help of the expression

$$k_z = 1 + \frac{F_{z1}+F_{z2}}{F_\delta}. \tag{3.17}$$

If teeth saturation is in acceptable bounds, the saturation factor is in the limits of $1.2 \le k_z \le 1.5 \ldots 1.6$. When $k_z < 1.2$, the teeth area is insufficiently used. When $k_z > 1.5 \ldots 1.6$, the teeth are excessively saturated. In both cases it is necessary to make proper changes into the previous calculations.

3.4.4. **Mmf of the stator (rotor) core yokes** equals

$$F_{y1(2)} = H_{y1(2)}L_{y1(2)} \tag{3.18}$$

where L_{y1} – design length of the magnetic flux path in the stator core yoke:

$$L_{y1} = \frac{\pi(D_a-h_{y1})}{2p}. \tag{3.19}$$

Design stator core yoke height calculated by the expression

$$h_{y1} = \frac{D_a-D}{2} - h_{sl1}. \tag{3.20}$$

Design length of the magnetic flux path in the rotor yoke and the rotor yoke height is found depending on the way of fitting the rotor core to the shaft by the formulae:

- at fitting the core to the shaft directly without a bush and $2p \neq 2$:

$$h_{y2} = \frac{D_2-D_j}{2} - h_{sl2} \qquad L_{y2} = \frac{\pi(D_j+h_{y2})}{2p} \tag{3.21}$$

where D_j is defined by (2.54)

- at fitting the core to the shaft on a mounting bush or to the finned shaft and $2p \neq 2$:

$$h_{y2} = \frac{D_2 - D_j}{2} - h_{sl2} \qquad L_{y2} = \frac{\pi(D_j + h_{y2})}{2p} \tag{3.22}$$

whereD_j is defined by (2.55)

- at fitting the rotor core directly to the shaft and $2p = 2$, the length of the magnetic flux path in the rotor core yoke is accepted equal to $L_{y2} = 2h_{y2}$ where h_{y2} is defined by (3.21) or (3.22) in accordance with the method of the rotor core fitting to the shaft.

3.5. Amplitude of total magnetomotive force

Amplitude of magnetomotive force produced by the magnetizing current is found as

$$F = F_\delta + F_{z1} + F_{z2} + F_{y1} + F_{y2}. \tag{3.23}$$

3.6. Rms value of the magnetizing current

The magnetizing current is determined by the expression:

$$I_\mu = \frac{\pi p F/2}{m_1\sqrt{2}w_1 k_{w1}} = \frac{pF}{0.9 m_1 w_1 k_{w1}}\,. \tag{3.24}$$

Relative value

$$I_\mu^* = {I_\mu}\Big/{I_{1r}}.$$

If the machine dimensions are determined properly, the relative value of the magnetizing current must be in the limits of 0.18…0.35 for motors of medium rated power (15…400 kW) and in the limits of 0.2…0.6 for small machines (<10 kW).

4. DETERMINATION OF MOTOR PARAMETERS FOR RATED OPERATING CONDITIONS

The phase windings resistance R_1 and R_2, their leakage reactance X_1 and X_2, resistance R_{12}, and the magnetization branch reactance X_{12} are referred to the motor parameters. Their determination is necessary for definition of the equivalent circuit parameters, data of no-load condition, the motor ratings, its performance and starting characteristics. At starting conditions calculation, effects of current displacement (skin effect) in the squirrel cage bars and of the stator and rotor tooth tips saturation must be taken into consideration, but for the rated conditions these effects are not considerable.

4.1. Calculation of the winding resistance

4.1.1. Windings resistance of induction motor stators and wound rotors.

For the indicated windings the resistance is found by the expression:

$$R = k_r \rho_\theta \frac{L}{q_{ef} a} \tag{4.1}$$

where L – total length of the phase winding effective conductors in meters,

q_{ef} – cross-section area of the effective conductor in m^2,

a – the number of a phase winding parallel paths,

ρ_θ – specific resistance of the winding material at the design temperature in Ω·m,

k_r – a coefficient considering increase of the resistance due to current displacement; under rated conditions, it equals $k_r = 1$ for both stator and rotor windings.

For conductors with insulation of A, E and B temperature classes, the design temperature is assumed equal $\theta = 75℃$, and with insulation of F and H classes $\theta = 115℃$. Values of ρ_θ are given in Table 4.1.

The total length of the winding effective conductors is

$$L = l_{av}w \tag{4.2}$$

where l_{av} – a coil turns average length in m,

w – the phase winding turns number.

The average turn length

$$l_{av} = 2(l_{sl} + l_{ec}), \tag{4.3}$$

where l_{sl} – the length of the part of effective conductor located in a slot in m,

l_{ec} – the length of the end connection in meters (see Fig. 4.1 and 4.2).

Table 4.1 – Specific resistance of winding conductors

Winding kind	Material	Specific resistance (in Ω·m) under temperature (in˚C)		
		20	75	115
Windings of copper	Copper	$0.01754 \cdot 10^{-6}$	$0.02128 \cdot 10^{-6}$	$0.02439 \cdot 10^{-6}$
Squirrel-cage windings	Aluminum busses	$0.02857 \cdot 10^{-6}$	$0.03571 \cdot 10^{-6}$	$0.03846 \cdot 10^{-6}$
	Casted aluminum	$0.03333 \cdot 10^{-6}$	$0.04167 \cdot 10^{-6}$	$0.04545 \cdot 10^{-6}$

Note: The casted aluminum specific resistance should be taken some greater than indicated in the Table due to arising air bulbs in the material while casting and changing the material structure at it hardening in the narrow space of slots. On these reasons the specific resistance for casted aluminum conductors of a squirrel-cage is accepted equal $\rho_\theta = 0.04651 \cdot 10^{-6}\ \Omega \cdot \text{m}$ under temperatures θ=75 and 115 ˚C.

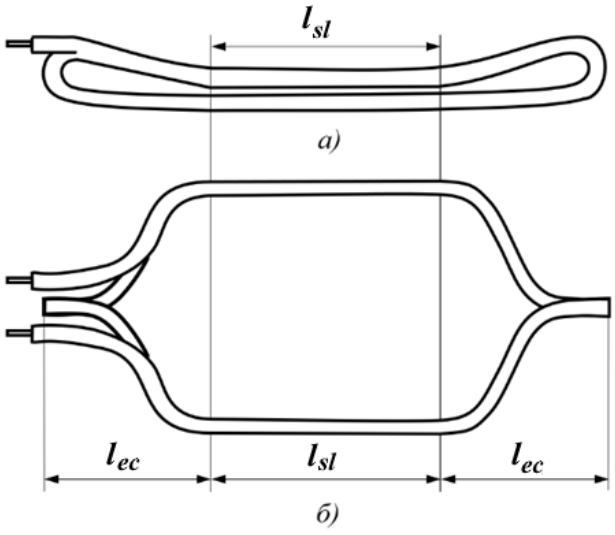

Figure 4.1 – Coil of two-layer stator winding

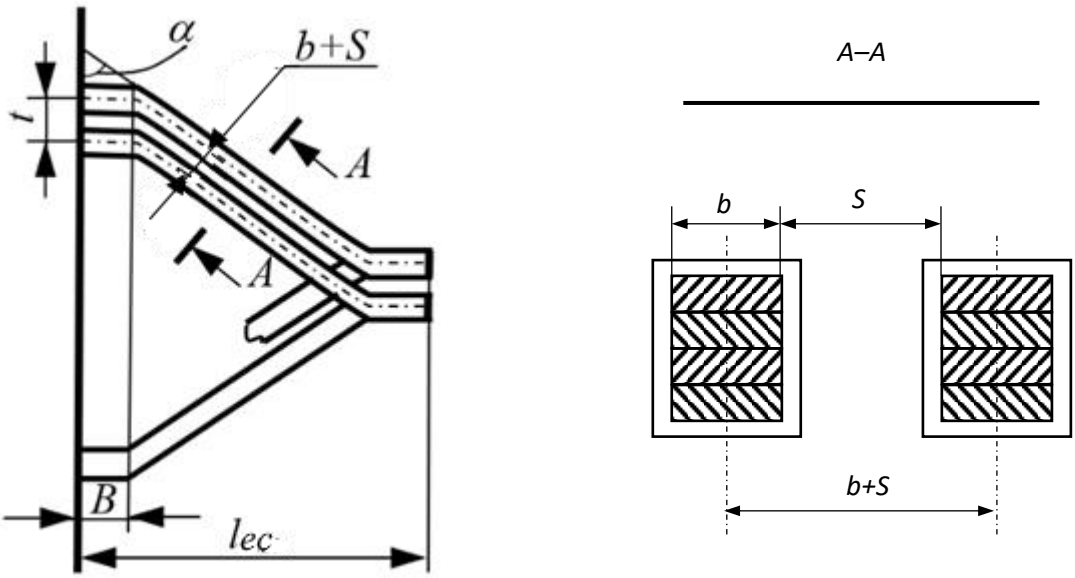

Figure 4.2 – Dimensions of a coil end connections

For fed-in stator windings

$$l_{ec} = k_{ec} b_{coil} + 2B \tag{4.4}$$

where

$$b_{coil} = \frac{\pi(D+h_{sl1})}{2p}\beta_1, \qquad \beta_1 = y_1/\tau_1 \tag{4.5}$$

k_{ec} – a coefficient which values are given in Table 4.2,

B – the straight part of slot conductor overhang; it is accepted equal 0.01 m if the winding is wound before the core insertion into the frame, and 0.015 m if it is wounded after the core inserted into the frame.

The end connections overhang is

$$l_{oh} = k_{oh} b_{coil} + B$$

where k_{oh} is taken from Table 4.2

***For stator and rotor coils wound of the wire of rectangular cross-section*:**

$$l_{ec} = k_{ec} b_{coil} + 2B + h_{sl} \qquad l_{oh} = k_{oh} b_{coil} + B + 0.5 h_{sl} \tag{4.6}$$

where B is accepted by Table 4.3,

Table 4.2 – Coefficients for calculation of fed-in-winding end connections

Number of poles $2p$	Stator coils			
	End connections non-insulated with tape		End connections insulated with tape	
	k_{ec}	k_{oh}	k_{ec}	k_{oh}
2	1.20	0.26	1.45	0.44
4	1.30	0.40	1.55	0.50
6	1.40	0.50	1.75	0.62
≥ 8	1.50	0.50	1.90	0.72

Table 4.3 – Dimensions of end connections for coils wound with rectangular wire

Rated voltage, V	S, m	B, m
≤660	0.0035	0.025
3000 … 3300	0.005 … 0.006	0.035 … 0.04
6000 … 6600	0.006 … 0.007	0.035 … 0.05
≥10000	0.007 … 0.008	0.06 … 0.065

$b_{coil} = \frac{\pi(D+h_{sl1})}{2p}\beta_1$ – for stator windings,

$b_{coil} = \frac{\pi(D_2-h_{sl2})}{2p}\beta_2$ – for rotor windings,

$$\beta_1 = y_1/\tau_1 \qquad \beta_2 = y_2/\tau_2 \qquad k_{ec} = 1/\sqrt{1-m^2}$$

$$k_{0h} = \frac{1}{2}k_{ec}m \qquad m = (b+S)/t$$

t - the tooth pitch,

b – the copper width in the end connection,

S – permissible minimum distance between the adjacent coils copper at the end connections (Table 4.3).

For bar wave windings of wound rotors

$$l_{ec} = k_{ec}b_{coil} + 2B_b \qquad l_{oh} = k_{oh}b_{coil} + B_b \qquad (4.7)$$

where

$$b_{coil} = \frac{\pi(D_2-h_{sl2})}{2p}, \qquad k_{ec} = \frac{1}{\sqrt{1-m^2}}, \qquad m = \frac{b_2+S_2}{t_2'},$$

$t_2' = \frac{\pi(D_2 - 2h_{sl2})}{z_2}$ is the tooth pitch at the slots bottom,

b_2 – width of the rotor bar copper,

S_2 – distance between copper of two adjacent bars in the end connections taken from Table 4.4,

$B_b = 0.05 \ldots 0.1$ m (for high-voltage machines with $P_r = 800 \ldots 1000$ kW it is accepted $B_b = 0.12 \ldots 0.16$ m).

Table 4.4 – Distance between copper of adjacent bars in end connections for coils of rotor bar wave winding

U_{sr}, V	till 500	500…1000	1000…1500	1500…2000
S_2, m	0.0017	0.002	0.0026	0.0029

Resistance of the wound rotor phase referred to the stator side equals

$$R_2' = R_2 \upsilon_{12} \tag{4.8}$$

where

$$\upsilon_{12} = \frac{m_1 (w_1 k_{w1})^2}{m_2 (w_2 k_{w2})^2}. \tag{4.9}$$

4.1.2. Resistance of induction motor cage-rotors

Resistance of a cage-rotor phase equals

$$R_2 = R_b + \frac{2R_{ring}}{\Delta^2} \tag{4.10}$$

where R_b – the bar resistance, R_{ring} – resistance of the rotor end ring part between two adjacent bars, $\Delta = 2\sin(\pi p/z_2)$.

The bar and end ring section resistance are found by the expressions:

$$R_b = \rho_b \frac{l_b}{q_b} k_r \qquad R_{ring} = \rho_{ring} \frac{\pi D_{ring,av}}{z_2 q_{ring}} \tag{4.11}$$

where ρ_b, ρ_{ring} are the bar and end ring material specific resistance under the design temperature (Table 4.1 and the note to it),

l_b is the bar length,

q_b and q_{ring} are the bar and end ring cross-section area (see div. 2.3.9).

Average end ring diameter is

$$D_{ring,av} = D_2 - b_{ring}$$

where D_2 – the rotor diameter,

b_{ring} – the ring height which in rotors with plug-in bars equals $b_{ring} = (1.1 \dots 1.25)h_{sl2}$ and in rotors with casted squirrel cage is $b_{ring} \geq 1.2h_{sl2}$.

The coefficient k_r considers the cage bar resistance growth due to current displacement; for slip values in the range of 0 ... s_r it is accepted equal $k_r = 1$.

The rotor phase resistance referred to the stator side is found by the expression:

$$R_2' = R_2 v_{12} \tag{4.12}$$

where

$$v_{12} = {[4m_1(w_1 k_{w1})^2]}/{[z_2 k_{sk}]} \qquad \mathrm{k_{sk}} = {\left[\sin\frac{\pi}{2}\frac{b_{sk}}{z_2 t_2}\right]}/{\left[\frac{\pi b_{sk}}{2z_2 t_2}\right]}. \tag{4.13}$$

b_{sk}, t_2 – the rotor slot skew in mm and tooth pitch in mm respectively.

4.2. Calculation of windings leakage reactance

4.2.1. Leakage reactance of wound-rotor induction motor

The stator and rotor reactance of a wound rotor induction motor is calculated by the expression:

$$X_{1(2)} = 15.8\frac{f}{100}\left(\frac{w}{100}\right)^2 \frac{l_\delta'}{pq}(\lambda_{sl} + \lambda_{ec} + \lambda_d) \tag{4.14}$$

where λ_{sl}, λ_{ec}, λ_d – coefficients of leakage permeance for slot part of coils, end connections and differential leakage respectively.

The coefficient of slot leakage permeance is calculated by an expression selected from Table 4.5 depending on the slot shape (Fig. 4.3).

Coefficients k_β and k_β' depend on the coil span $\beta = \frac{y}{\tau}$

- at $\beta = 1$, $k_\beta = k_\beta' = 1$ for one- and two-layer windings.

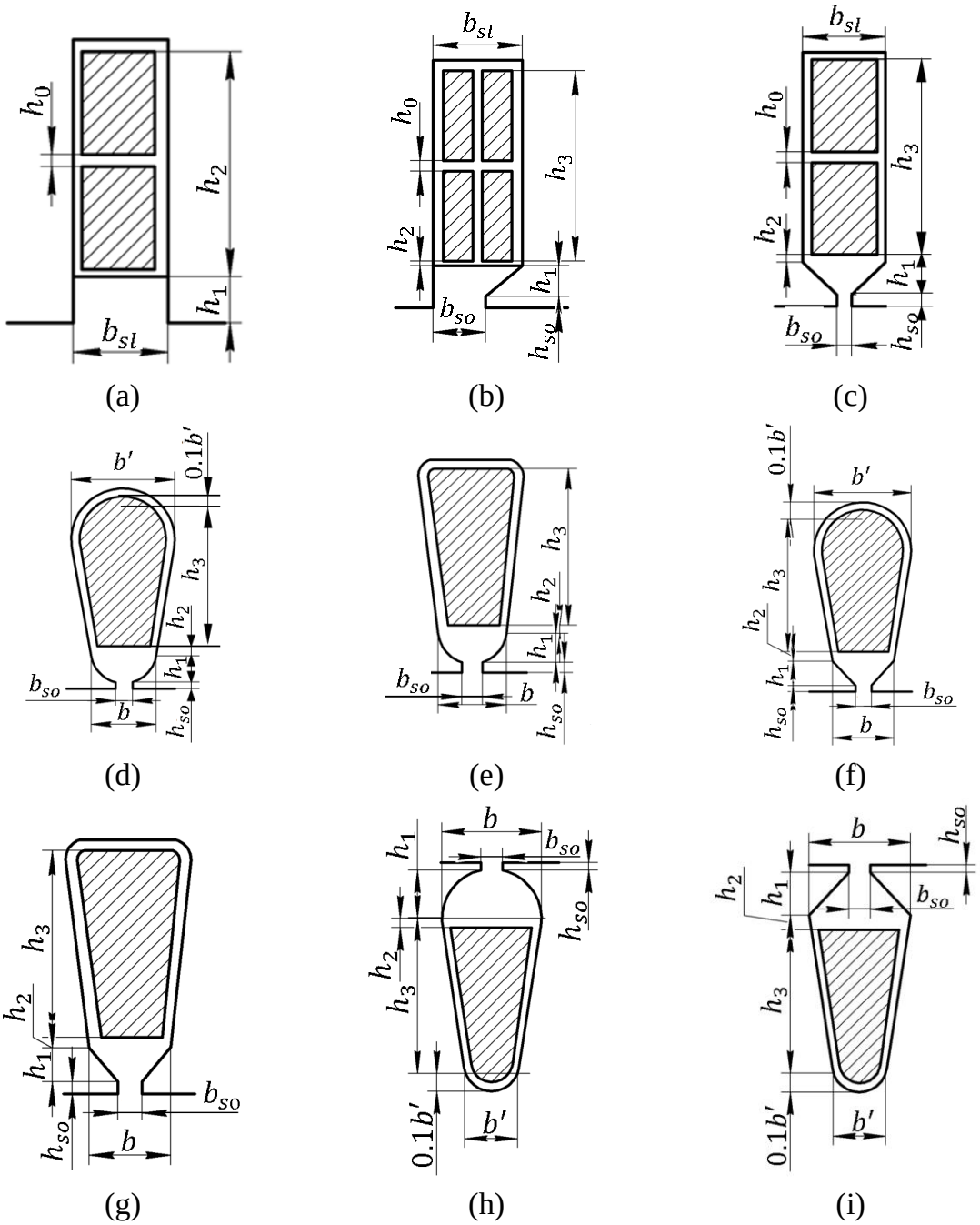

Figure 4.3 – To calculation coefficients of slot leakage permeance

- at $\frac{2}{3} \le \beta < 1,\ \ k'_\beta = 0.25(1 + 3\,\beta)$;
- at $\frac{1}{3} \le \beta < \frac{2}{3},\ k'_\beta = 0.25(6\,\beta - 1)$;
- coefficient $k_\beta = 0.25(1 + 3k'_\beta)$.

The leakage permeance coefficient for end connections:

$$\lambda_{ec} = 0.34\,\frac{q}{l'_\delta}\,(l_{ec} - 0.64\beta\tau)\ . \qquad (4.15)$$

Table 4.5 – Expressions for calculation of coefficients of slot leakage permeance λ_{sl} for phase windings of induction motors

Figure	Winding type	Expression for calculation
4.3 (a)	two-layer	$\frac{h_2 - h_0}{3b_{sl}} k_\beta + \frac{h_1}{b_{sl}} k'_\beta + \frac{b_0}{4b_{sl}}$
	one-layer	$\frac{h_2}{3b_{sl}} + \frac{h_1}{b_{sl}}$
4.3 (b)	two-layer	$\frac{h_3 - h_0}{3b_{sl}} k_\beta + (\frac{h_2}{b_{sl}} + \frac{3h_1}{b_{sl} + 2b_{so}} + \frac{h_{so}}{b_{so}})\, k'_\beta$
4.3 (c)	two-layer	$\frac{h_3 - h_0}{3b_{sl}} k_\beta + (\frac{h_2}{b_{sl}} + \frac{3h_1}{b_{sl} + 2b_{so}} + \frac{h_{so}}{b_{so}})\, k'_\beta$
	one-layer	$\frac{h_3}{3b_{sl}} + \frac{h_2}{b_{sl}} + \frac{3h_1}{b_{sl} + 2b_{so}} + \frac{h_{so}}{b_{so}}$
4.3 (d), (e), (f)	one-layer and two-layer	$\frac{h_3}{3b} k_\beta + (0.785 - \frac{b_{so}}{2b} + \frac{h_2}{b} + \frac{h_{so}}{b_{so}})\, k'_\beta$
4.3 (g), (h), (i)	one-layer and two-layer	$\frac{h_3}{3b} k_\beta + (\frac{h_2}{b} + \frac{3h_1}{b + 2b_{so}} + \frac{h_{so}}{b_{so}})\, k'_\beta$

In (4.14) and (4.15) quantity l'_δ is respectively determined by the expressions:

$$l'_\delta = l_1 - 0.5 n_{rd1} b_{rd1}, \quad l'_\delta = l_2 - 0.5 n_{rd2} b_{rd2},$$

where $n_{rd1(2),}$ $b_{rd1(2)}$ – number and width of the stator (rotor) radial ventilation ducts accordingly.

The coefficient of differential leakage permeance for the stator and rotor windings is calculated by the expression:

$$\lambda_d = \frac{t_{1(2)}}{12\delta k_{\delta 1(2)}} \xi \qquad (4.16)$$

where coefficient ξ is determined depending on the number of slots per phase and per pole by the expressions:

- at integer $q \geq 2$ and $\beta = 1$

$$\xi = 2 + 0.022q^2 - k_w^2(1 + \Delta_z);$$

- at integer $q \geq 2$ and $\beta < 1$

$$\xi = k''q^2 + 2k'_\beta - k_w^2(1 + \Delta_z);$$

- at fractional $q > 2$

$$\xi = k''q^2 + 2k''_\beta - k_w(\frac{1}{d^2} + \Delta_z);$$

- at fractional $1 < q < 2$

$$\xi = k''q^2 + 2k''_\beta - \frac{k'}{q} - k_w(\frac{1}{d^2} + \Delta_z).$$

In the above expressions $\Delta_z, k', k'', k''_\beta$ are determined by the curves of Fig. 4.4. The coefficient k'_β is the same as was used for determination of λ_{sl}. The quantity d is the denominator of the fractional part of the number of slots per phase and per slot q.

The rotor reactance referred to the stator side equals

$$X'_2 = X_2 v_{12}. \tag{4.17}$$

4.2.2. Stator leakage reactance of a cage induction motor

The leakage reactance of the stator of a cage motor is calculated by expression 4.14, the same as for a wound-rotor induction motor.

The permeance coefficients for the slot part of coils and for the end connections of the stator phase winding of a cage motor are found by expressions given in Table 4.5 and by expression (4.15) respectively.

The permeance coefficient of differential leakage for the stator winding of a cage motor is calculated by the expression:

$$\lambda_{d1} = \frac{t_1}{12\delta k_\delta}\xi. \tag{4.18}$$

Here, coefficient ξ is found by expressions given in Table 4.6.

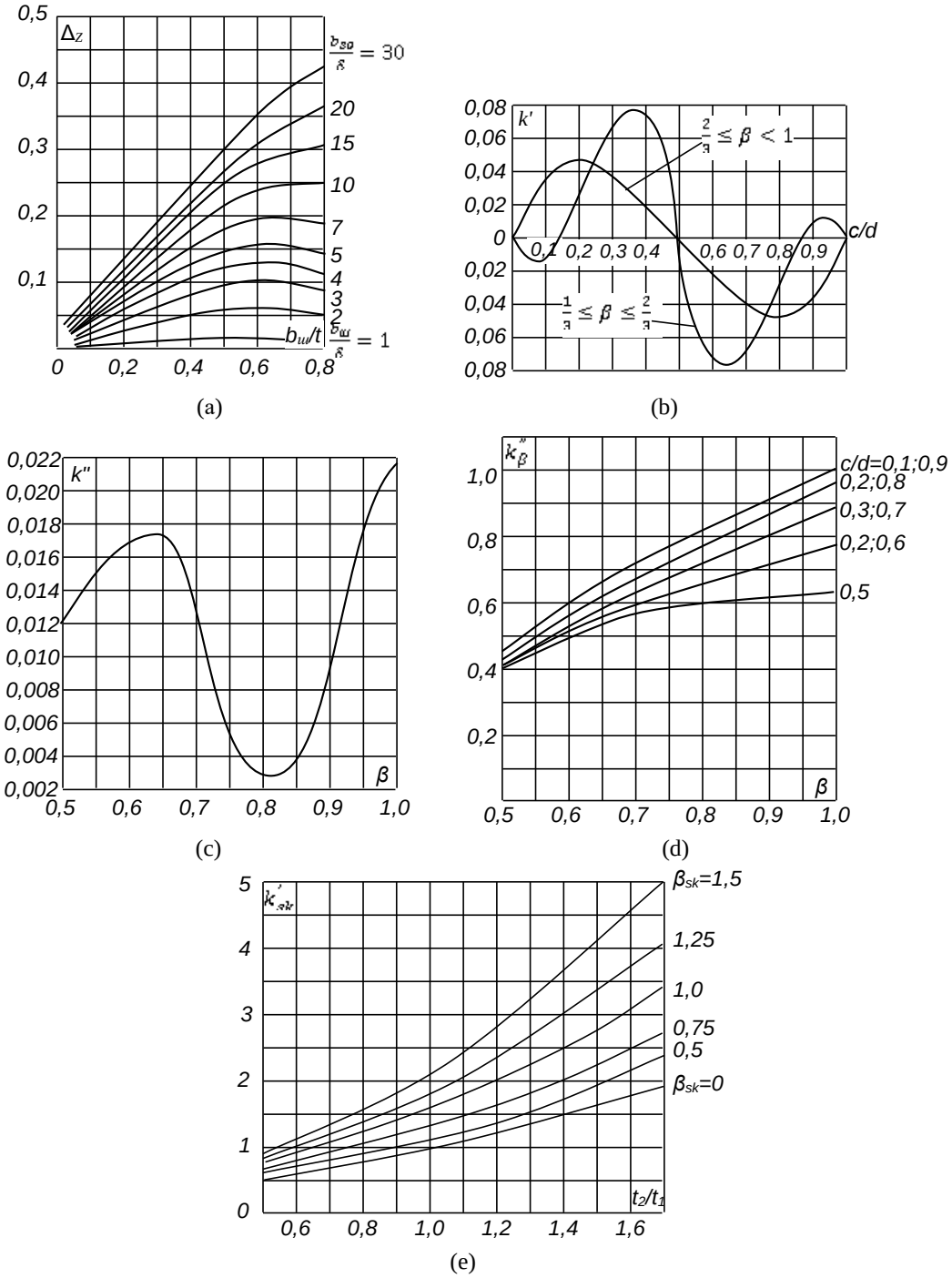

Figure 4.4 – Curves to calculate the coefficient of differential leakage permeance:

(a) – dependence of coefficient Δ_z on ratios b_{so}/t and b_{so}/δ;

(b) – dependence of coefficient k' on the fractional part of the number of slots per pole and per phase q;

(c) – dependence of coefficient k'' on relative coil span β;

(d) – dependence of coefficient k'_β on relative coil span β and fractional part of q;

(e) – dependence of coefficient k'_{sk} on ratio t_2/t_1 and relative slots skewing β_{sk}

Table 4.6 – Calculation of coefficient ξ for stator windings of cage motors

Feature of slots	Expression for calculation
Open stator slots. Stator and rotor slots are not skewed	$\xi = \left(2\frac{t_2}{t_1} - \frac{t_1}{t_2}\right)\Delta_z - k_{w1}^2\left(\frac{t_2}{t_1}\right)^2$
Semi-closed or semi-open stator slots. Slots may be skewed	$\xi = 2k'_{sk}k_\beta - k_{w1}^2\left(\frac{t_2}{t_1}\right)^2(1+\beta_{sk}^2)$

In expressions of Table 4.6 t_1 and t_2 are stator and rotor tooth pitches; Δ_z is found from Fig 4.4 (a); k_β is calculated as for the stators of wound-rotor machines; $\beta_{sk} = \frac{b_{sk}}{t_2}$; k'_{sk} is found from Fig. 4.4 (e).

4.2.3. Leakage reactance of cage rotor

The leakage reactance of a cage rotor is found as

$$X_2 = 7.9 f_1 l'_\delta 10^{-6}(\lambda_{sl2} + \lambda_{ec2} + \lambda_{d2}). \qquad (4.18)$$

The slot leakage permeance coefficient is calculated by an expression selected from Table 4.7 depending on the slot shape (Fig. 4.5).

The leakage permeance coefficient for end connections for rotors with casted cage:

$$\lambda_{ec2} = \frac{2.3\, D_{ring,av}}{z_2 l'_\delta (2\sin(\pi p/z_2))^2} lg \frac{4.7 D_{ring,av}}{2a_{ring} + b_{ring}}.$$

For welded rotor cages with copper or brass bars brazed to the end rings, and bars projecting out the slots:

$$\lambda_{ec2} = \frac{2.3\, D_{ring,av}}{z_2 l'_\delta (2\sin(\pi p/z_2))^2} lg \frac{4.7 D_{ring,av}}{2\left(a_{ring} + b_{ring}\right)},$$

where $a_{ring} = q_{ring}/b_{ring}$. In these expressions $D_{ring,av}$ is average diameter of end rings; $D_{ring,av} - D_2 - b_{ring}$.

Table 4.7 – Calculation of slot leakage permeance of cage rotors

Figure	Expression for calculation
4.5 a	$\left[\frac{h_1}{3b}\left(1-\frac{\mathrm{p}b^2}{8q_{sl}}\right)^2+0.66-\frac{b_{so}}{2b}\right]k_d+\frac{h_{so}}{b_{so}}$
4.5 b	$\left(\frac{h_1}{3b}+\frac{3h_2}{b+2b_{so}}\right)k_d+\frac{h_{so}}{b_{so}}$
4.5 c	$\frac{h_1}{3b}k_d+\frac{h_{so}}{b_{so}}$、
4.5 d	$\frac{h_1}{3b}k_d+\frac{h_2}{b}+\frac{2h_2}{b+2b_{so}}+\frac{h_{so}}{b_{so}}$
4.5 e	$\frac{h_1}{3b}k_d+\frac{h_2}{b}+0.785-\frac{b_{so}}{2b}+\frac{h_{so}}{b_{so}}$
4.5 f	$\left[\frac{h_1}{3b}\left(1-\frac{\mathrm{p}b^2}{8q_{sl}}\right)^2+0.66-\frac{b_{so}}{2b}\right]k_d+\frac{h_{so}}{b_{so}}$
4.5 g	$\left(0.785-\frac{b_{so}}{2b}\right)k_d+\frac{h_{so}}{b_{so}}$

Notes: 1. For rated conditions $k_d = 1$.

2. For closed slots (Fig. 4.5, (h), (i)), it is necessary to substitute instead of $\frac{h_{so}}{b_{so}}$:

- for slots in Fig. 4.5, (h) - the expression $0.3 + 1.12\, h'_{so}/I_2\, 10^6$;
- for slots in Fig. 4.5, (i) – the expression $h_{so}/b_{so} + 1.12\, h'_{so}/I_2\, 10^6$ where h'_{so} – thickness of the bridge above the slot in meters, I_2 – the rotor phase current in Amperes.

The differential leakage permeance coefficient:

$$\lambda_{d2} = \frac{t_2}{12\delta k_\delta}\xi, \qquad \xi = 1 + \frac{1}{5}\left(\frac{\pi p}{z_2}\right)^2 - \frac{\Delta_z}{1-\left(p/z_2\right)^2},$$

where Δ_z is determined with the help of curves in Fig. 4.4, a.

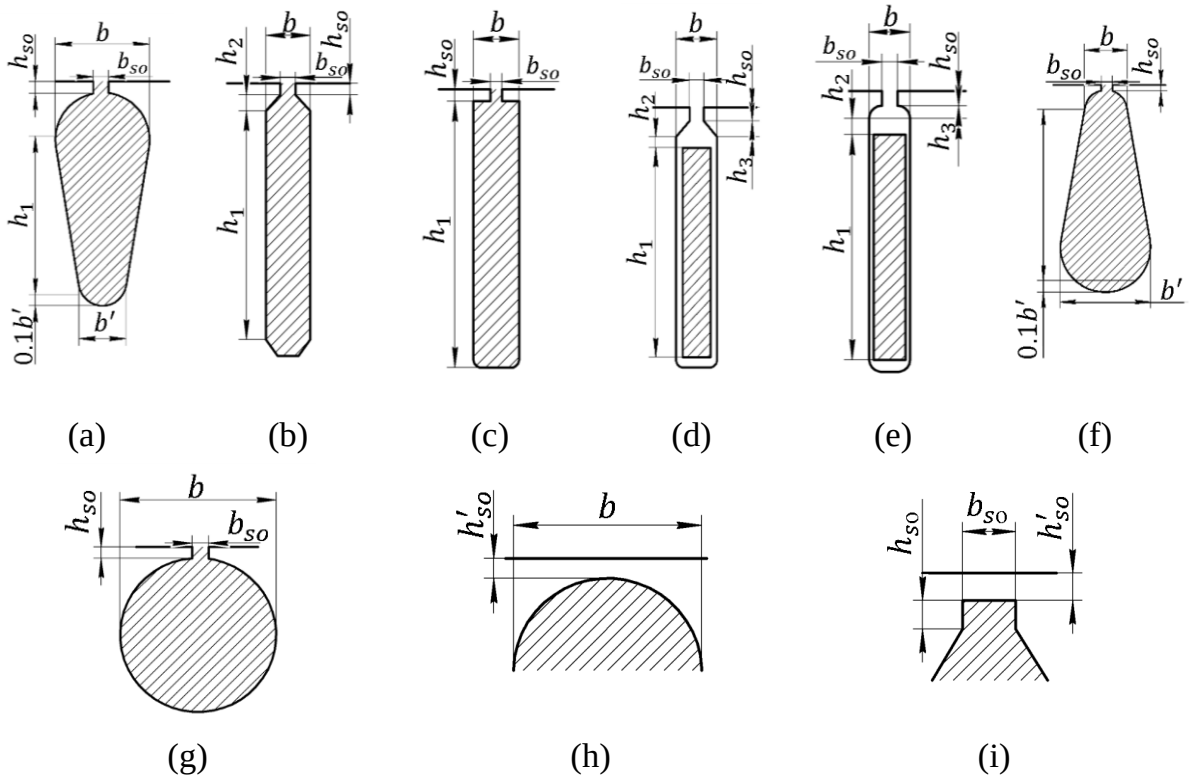

Figure 4.5 – Before calculating the magnetic conductivity of the rotor grooves

4.3 Relative values of windings parameters

Relative values of a motor stator and rotor windings parameters are found by the following equalities:

- for a stator

$$R_1^* = R_1 \frac{I_{1r}}{U_{1r}}, X_1^* = X_1 \frac{I_{1r}}{U_{1r}} \tag{4.20}$$

- for a rotor (referred values)

$$R_2'^* = R_2'^* \frac{I_{1r}}{U_{1r}}, \quad X_2'^* = X_2'^* \frac{I_{1r}}{U_{1r}}. \tag{4.21}$$

As a rule, these quantities values are in the ranges:

$$R_1^* \cong R_2'^* = 0.02 \ldots 0.03, \quad X_1^* = 0.08 \ldots 0.14, \quad X_2'^* = 0.1 \ldots 0.16.$$

5. POWER LOSSES IN INDUCTION MOTORS

5.1 Total power loss in an induction motor equals

$$\Sigma(\Delta P) = P_{c,main} + P_{c,add} + P_{w1} + P_{w2} + P_{br} + P_{mech} + P_{bf} + P_{add} \quad (5.1)$$

where $P_{c,main}$ – the main magnetic loss caused by eddy currents and hysteresis stipulated by the magnetic field in the machine magnetic cores,

$P_{c,add}$ – the additional magnetic losses,

P_{w1} and P_{w2} – the resistance (copper) losses in the stator and rotor winding respectively,

P_{br} – the electrical loss in wound rotor brush contacts,

P_{mech} –the losses for friction in bearings and for ventilation,

P_{bf} – the loss for friction in brush contacts of a wound rotor motor,

P_{add} – the additional loss under load.

5.2 Main magnetic loss

At the main magnetic loss determination, the magnetic loss in the rotor is neglected. The following equality is used:

$$P_{c,main} = p_{1.0/50}\left(\frac{f_1}{50}\right)^{\beta}\left(k_{dy}B_{y1}^2 m_{y1} + k_{dz}B_{z1middle}^2 m_{z1}\right) \quad (5.2)$$

where $p_{1.0/50}$ – the specific loss in the steel of given grade and the laminations thickness under the flux density amplitude $B_m = 1\,T$ and frequency $f = 50\,Hz$ in W/kg (Table 5.1),

β – exponent (Table 5.1),

k_{dy} and k_{dz} – the coefficients taking into account ununiform distribution of the magnetic flux in stator yoke and in teeth, and manufacturing process influence; for motors of $P_r < 250\,kW$, $k_{dy} = 1.6$ and $k_{dz} = 1.8$; for motors of $P_r \geq 250\,kW$ $k_{dy} = 1.4$ and $k_{dz} = 1.7$,

B_{y1} and $B_{z1middle}$ – the flux density in the stator yoke and middle tooth cross-section expressed in T,

m_{y1} and m_{z1} - the magnetic circuit sections (the stator yoke and teeth) masses in kg.

The stator yoke and teeth masses are found as:

$$m_{y1} = \pi(D_a - h_{y1})h_{y1}l_{cp1}k_{fill}\gamma_{st}; \qquad h_{y1} = 0.5(D_a - D) - h_{sl1};$$

$$m_{z1} = h_{z1}b_{z1middle}z_1 l_{cp1}k_{fill}\gamma_{st}; \qquad b_{z1middle} = \frac{b_{z1max}+b_{z1min}}{2};$$

$\gamma_{st} = 7.8 \cdot 10^3\ kg/m^3$ – the steel density.

Table 5.1 – Specific losses $p_{1.0/50}$ and exponent β at lamination thickness of 0.5 mm

Steel grade	$p_{1.0/50}$, W/kg	β
2013	2.5	1.5
2211	2.6	1.5
2312	1.75	1.4
2411	1.6	1.3

5.3 Additional magnetic losses

These losses are caused by fluctuation of the flux density in the magnetic cores surface layer (surface magnetic loss) and in the stator and rotor cores teeth (pulsating loss). Total additional magnetic losses are found as the sum:

$$P_{c,add} = P_{s1} + P_{p1} + P_{s2} + P_{p2}$$

where and $P_{s1}$and P_{s2} – the surface magnetic losses in the stator and rotor cores, P_{p1} and P_{p2} – pulsation losses in the stator and rotor teeth.

The surface magnetic losses may be found in terms of the specific surface magnetic loss per $1m^2$ of a core surface:

$$P_{s1} = p_{s1}(t_1 - b_{so1})z_1 l_{cs1};\ P_{s2} = p_{s2}(t_2 - b_{so2})z_2 l_{cs2}, \qquad (5.3)$$

where p_{s1} and p_{s2} – the specific surface magnetic loss in the stator and rotor cores in $\mathrm{W/m^2}$:

$$p_{s1} = 0.5k_{01}\left(\frac{z_2 n}{10000}\right)^{1.5}(B_{01}t_2 10^3)^2;$$

$$p_{s2} = 0.5k_{02}\left(\frac{z_1 n}{10000}\right)^{1.5}(B_{02}t_1 10^3)^2.$$

Here coefficients k_{01}, k_{02} take the values in the range of 1.4 … 1.8 for motors of $P_r \leq 160\ kW$ and in the range of 1.7 … 2.0 for motors $P_r > 160\ kW$; the rotating frequency is accepted equal to the synchronous one in rpm. B_{01} and B_{02} – amplitudes of the magnetic flux density in the air gap above the stator and rotor teeth edges equal to

$$B_{01(2)} = \beta_{01(2)} k_\delta B_\delta$$

where $\beta_{01(2)}$ are the coefficients found by curves of Fig. 5.1.

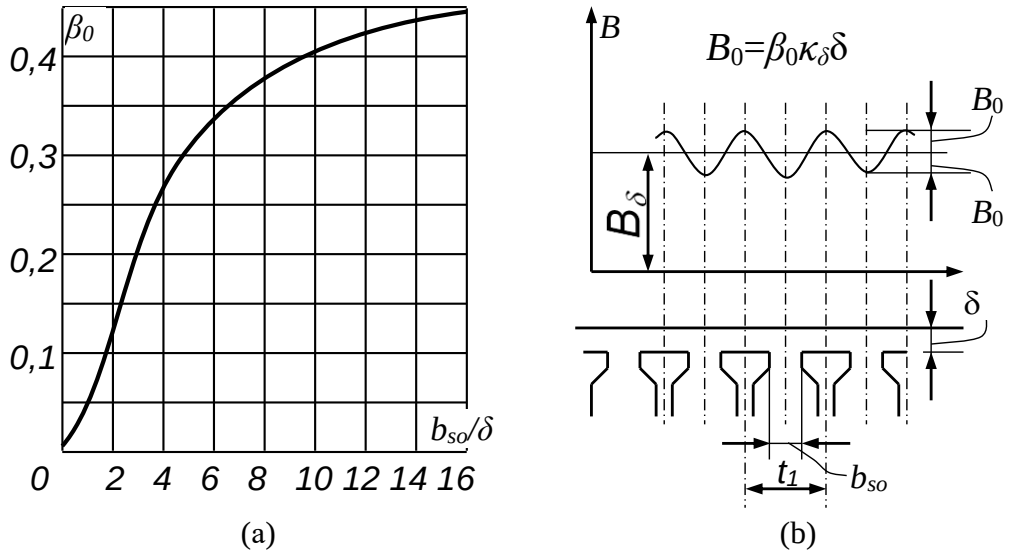

Figure 5.1 – Curve for determination of coefficient β_0 (a), ripples of magnetic flux density in air gap (b)

Pulsation losses in the stator and rotor core teeth are calculated by expressions:

$$P_{p1} = 0.11\left(\frac{z_2 n}{1000}B_{p1}\right)^2 m_{z1}, \quad P_{p2} = 0.11\left(\frac{z_1 n}{1000}B_{p2}\right)^2 m_{z2},$$

where B_{p1} and B_{p2} – amplitudes of the magnetic flux density in the air gap above the stator and rotor teeth edges equal:

$$B_{p1} \cong \frac{\gamma_2 \delta}{2t_1} B_{z1middle}; \quad B_{p2} \cong \frac{\gamma_1 \delta}{2t_2} B_{z2middle};$$

$$\gamma_1 = \frac{(b_{so1}/\delta)^2}{5+b_{so1}/\delta}; \ \gamma_2 = \frac{(b_{so2}/\delta)^2}{5+b_{so2}/\delta}.$$

In the case of open slots, at determination of γ_1 and γ_2, the design values of the slot openings are taken instead of b_{so1} and b_{so2}:

$$b'_{so1(2)} = \frac{b_{so1(2)}}{3}\left(1 + \frac{0.5t_{1(2)}}{t_{1(2)}b_{so1(2)} + \kappa_\delta}\right)$$

where κ_δ – is accepted by the curve in Fig. 5.2.

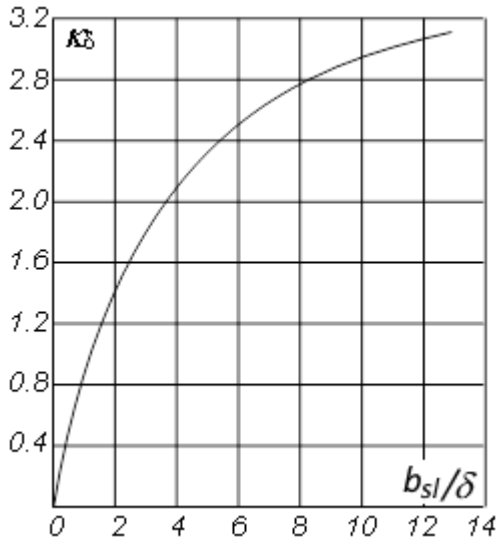

Figure 5.2 – Determination of κ_δ for open slots

Mass of the rotor teeth is determined as

$$m_{z2} = h_{z2} b_{z2middle} z_2 l_{cs2} k_{fill} \gamma_{st}, \quad b_{z2middle} = \frac{b_{z2max}+b_{z2min}}{2}.$$

Losses P_{s1} and P_{p1} in wound-rotor motors with bar wave winding and in squirrel cage motors are negligible and must not be calculated for such machines.

5.4 Total magnetic loss in the motor steel cores is

$$P_c = P_{c,main} + P_{c,add}. \tag{5.4}$$

Usually, additional steel core loss is by order of magnitude less than the main steel loss.

5.5 Resistance loss in windings

The resistance losses depend on the motor load.

For rated load, preliminary resistance losses are found as

$$P_{w1} = m_1 I_{1r}^2 R_1, \quad P_{w2} = m_2 I_{2r}^2 R_2. \tag{5.5}$$

The rated values of stator and rotor currents had been found at previous calculations.

5.6 Friction and ventilation losses (mechanical losses)

Calculation of this kind of losses is made in different ways depending on the method of cooling.

5.6.1 Mechanical losses in motors with radial ventilation without radial ducts and in cage motors with ventilation blades on the cage end rings

$$P_{mech} = K_T \left(\frac{n}{1000}\right)^2 (10D)^3 \tag{5.6}$$

where D – the stator inner diameter in m,

- $K_T = 5$ at $2p = 2$,
- $K_T = 6$ at $2p \geq 4$ for motors with $D_a \leq 0.25$ m,
- $K_T = 6$ at $2p \geq 4$ for motors with $D_a > 0.25$ m.

5.6.2 Mechanical loss in self-cooled motors with external fan

Such ventilation method is applied for motors with $0.1 \leq D_a \leq 0.5$ m. The mechanical losses:

$$P_{mech} = K_T \left(\frac{n}{10}\right)^2 D_a^4 \tag{5.7}$$

where $K_T = 1$ at $2p = 2$; $K_T = 1.31(1 - D_a)$ at $2p \geq 4$. Here D_a is the outside stator core diameter.

5.6.3 Mechanical loss in motors of large and medium power with radial ventilation ducts

$$P_{mech} = 1.2 \cdot 2p\tau^3(n_{rd} + 11)10^3 \tag{5.8}$$

where n_{rd} – number of radial ventilation ducts.

5.6.4 Mechanical loss in motors with axial ventilation

$$P_{mech} = K_T \left(\frac{n}{1000}\right)^2 \left(10D_{fan}\right)^3 \tag{5.9}$$

where D_{fan} – the external diameter of the fan in m (it is accepted $D_{fan} \cong D_a$);

$K_T = 2.9$ at $D_a \leq 0.25$ m, $K_T = 3.6$ at $D_a = (0.25 \ldots 0.5)$ m.

5.6.5 Mechanical loss in motors with outside stator core diameter $0.5 < D_a < 0.9\ m$

$$P_{mech} = K_T(10D_a)^3$$

where coefficient K_T is accepted according to Table 5.2.

Table 5.2 – Coefficient K_T for induction motors of large power

$2p$	2	4	6	8	10	12
K_T	3.65	1.5	0.7	0.35	0.2	0.2

5.7 Electrical loss in brush contacts and loss for brushes friction

5.7.1 The brush dimensions and grade are selected based on the following data:

1. The brush grade is selected from the grades intended for current collection with slip rings of ac machines. The selected brushes should meet the value of speed on external surface of the slip ring.

2. From possible grades, the brushes with less values of voltage drop in the brush contacts are preferable.

3. The brush dimensions are selected from the standard range. The brush contact area $S_{br} = b_{br} l_{br}$ must provide the current density in the brush contact not exceeding but close to its specified value. It is possible to install 2 (3) brushes for each the slip ring.

4. Previously selected slip ring width may be corrected if necessary to fit it to possible dimensions of the brushes. It is better to locate the slip rings at external side of the end shield. It is desirable that the slip ring diameter was less than the outer diameter of the machine bearing that permit to take the end shield off without the slip rings removal. Usually, the slip ring diameter is accepted equal $D_{sr} = (0.4 \ldots 0.5)D$.

5. The brush holders must provide reliable brush keeping in proper position. The needed pressure in the current collecting contact is specified for the selected brush grade.

The brushes grades, the brush data and the brush dimension see Application 8 (Tables A8.1 and A8.2)

5.7.2 Electrical loss in the brush contacts is

$$P_{br} = m_2 \Delta U_{br} I_{sr} \qquad (5.10)$$

where ΔU_{br} – voltage drop in the brush contact, I_{sr} – current flowing through a slip ring. If the rotor winding has Y-connection, the current $I_{sr} = I_2$, at Δ-connection $I_{sr} = \sqrt{3} I_2$.

5.7.3 The loss for friction in brush contacts

$$P_{bf} = k_{fr}\rho_{br}S_{br}v_{sr} \quad (5.11)$$

where $k_{fr} = 0.16 \ldots 0.17$ is friction factor; ρ_{br} – pressure in the brush contacts in Pa; S_{br} – total contact area at all the rings in m^2 equal

$$S_{br} = 3n_{br}b_{br}l_{br},$$

$$n_{br} \geq \frac{I_{sr}}{J_{br}b_{br}l_{br}}$$

where J_{br} – the brush contacts current density specified for the selected brush grade in A/m^2,

b_{br} and l_{br} – the brush dimensions in m^2, selected by data of Appendix 8.

The line speed of the brush contact surface equals

$$v_{sr} = \frac{\pi n}{60}D_{sr}.$$

5.8 Additional losses under load

Additional losses under rated load $P_{add,r}$ caused by influence of the leakage flux, the flux density in the air gap fluctuation and magnetic flux harmonics are accepted equal to 0.5% of the motor rated power.

Under load which differs from the rated one

$$P_{add} = P_{add,r}(I_1/I_{1r})^2. \quad (5.12)$$

6. PARAMETERS AND DATA OF NO-LOAD MODE

Resistance, reactance, and impedance of the magnetizing circuit are approximately defined as:

$$R_m = \frac{P_{c,main}}{m_1 I_\mu^2}, \quad X_m = \frac{U_{1r}}{I_\mu} - X_1, \quad Z_m = \sqrt{R_m^2 + X_m^2}. \quad (6.1)$$

Relative values of the parameters:

$$R_m^* = R_m \frac{I_{1r}}{U_{1r}}, \quad X_m^* = X_m \frac{I_{1r}}{U_{1r}}. \tag{6.2}$$

For most asynchronous machines these relative parameters are in the range:

$$R_m^* = 0.05 \ldots 0.2; \quad X_m^* = 2 \ldots 4. \tag{6.3}$$

Components of the no-load current:

$$I_{0act} = \frac{P_c + P_{mech} + P_{w10}}{m_1 U_{1r}}, \; I_{0react} \cong I_\mu \tag{6.4}$$

where $P_{w10} \cong m_1 I_0^2 R_1$ is electrical loss in the stator winding at no-load.
The motor no-load current equals

$$I_0 = \sqrt{I_{0act}^2 + I_{0react}^2}. \tag{6.5}$$

The motor power factor under no-load:

$$\cos \varphi_0 = \frac{I_{0act}}{I_0}. \tag{6.6}$$

7. MOTOR PERFORMANCE CHARACTERISTICS

The motor performance characteristics are the relationships

$$P_1 = f(P_2), I_1 = f(P_2), \cos \varphi = f(P_2), \eta = f(P_2), \; s = f(P_2).$$

It is recommended to determine the performance characteristics using the applied software such as Mathcad, Mathematica, etc., or programs composed in one of programming languages.

As the source data, the previously determined values of quantities are used. The calculations are carried out for the slip values in the range of $(0 \ldots 1.5)s_r$.

7.1 The resistance and reactance of the right path of Γ-shaped equivalent circuit

Real and imaginary components of complex coefficient $\underline{c_1}$:

$$c_{1Re} = \frac{R_m(R_1+R_m)+X_m(X_1+X_m)}{R_m^2+X_m^2};\ c_{1Im} = \frac{X_1R_m-R_1X_m}{R_m^2+X_m^2};\ c_1 = \sqrt{c_{1Re}^2 + c_{1Im}^2}. \quad (7.1)$$

This coefficient squared $\underline{c_1^2}$ and it's real and imaginary parts are:

$$\underline{c_1^2} = a' + jb',\ a' = c_{1Re}^2 - c_{1Im}^2, \quad b' = 2c_{1Re}c_{1Im}. \quad (7.2)$$

Component of impedance of the right path of Γ-shaped equivalent circuit, which does not depend on the slip, equals $\underline{c_1}(R_1 + jX_1) + j\underline{c_1^2}X_2' = a + jb$. Its real and imaginary components are:

$$a = c_{1Re}R_1 - c_{1Im}X_1 - b'X_2', \quad b = c_{1Re}X_1 + c_{1Im}R_1 + a'X_2'. \quad (7.3)$$

Component of this impedance being dependent on the slip is

$$a'\frac{R_2'}{s} + jb'\frac{R_2'}{s} \quad (7.4)$$

7.2 Calculations for plotting performance characteristics

It is recommended to tabulate the calculations into the table (Table 7.1).

Calculation is made for the slip values in the range of $(0.1s_r \ldots 1.5s_r)$ with the step of $0.1s_r$. Before the calculation, the rated value of the slip is taken equal approximately to

$$s_r \approx R_2'\frac{I_{1r}}{U_{1r}}. \quad (7.5)$$

Table 7.1 – Calculations of induction motor performance characteristics

Calculated quantity	Unit of measurements	Formula	Slips s					
			$0.1s_r$	$0.2s_r$	$0.3s_r$	…	$1.5\ s_r$	Refined s_r
Resistance, reactance and impedance of right path of equivalent circuit	Ω	$R = a + a' \frac{R_2'}{s}$						
	Ω	$X = b + b' \frac{R_2'}{s}$						
	Ω	$Z = \sqrt{R^2 + X^2}$						
Current of the right path	A	$I_2'' = \frac{U_{1r}}{Z}$						
Stator current and its components	A	$I_{1act} = I_{0act} + I_2'' \frac{R}{Z}$						
	A	$I_{1react} = I_\mu + I_2'' \frac{X}{Z}$						
	A	$I_1 = \sqrt{{I_{1act}}^2 + {I_{1react}}^2}$						
Consumed active power	kW	$P_1 = 3U_{1r}I_{1act}10^{-3}$						
Electrical losses	kW	$P_{w1} = 3I_1^2 R_1 10^{-3}$						
	kW	$P_{w2} = 3I_2''^2 c_1^2 R_2' 10^{-3}$						
Loss in brush contact	kW	$P_{br=}P_{br,\ r}\ \frac{I_1}{I_{1r}}$						
Additional losses	kW	$P_{add} = P_{add,r}\left(\frac{I_1}{I_{1r}}\right)^2$						
Total losses	kW	$\Sigma(\Delta P) = P_{c,main} + P_{c,add} + {+}P_{w1} + P_{w2} + P_{br} + {+}P_{mech} + P_{bf} + P_{add}$						
Power on shaft	kW	$P_2 = P_1 - \Sigma(\Delta P)$						
Efficiency	%	$\eta = \frac{P_2}{P_2} \cdot 100$						
Power factor	–	$\cos\varphi = \frac{I_{1act}}{I_1}$						

After obtaining data for all specified slip values, it is necessary to refine data for the rated conditions. For that, a more accurate value of the rated slip

s_r is found by linear interpolation of the slip values for which the obtained power on the shaft is the nearest less and the nearest greater to the rated motor power P_{2r} specified in the task. Then the data for the rated operating conditions are calculated using the found refined value s_r in the order given in the table. At this, if obtained value of P_2 differs of the value P_{2r} specified in the task not more than for 1 … 2 %, it is assumed that this operation condition is the rated one. If the difference is grater, it is necessary to repeat interpolation and calculation using the newly received data.

8. CALCULATION OF CAGE MOTORS STARTING CHARACTERISTICS

Starting properties of a squirrel cage induction motor are assessed by the torque on the shaft and the stator current during the starting period. The starting torque and current of squirrel-cage motors at zero speed (i.e., under the motor short-circuit condition) are standardized (Table 8.1).

Table 8.1 – Standard relative values of starting torque and current of squirrel-cage induction motors of 4A series at zero speed

Motor version	2p	$h \leq 132$ mm		$h = (160 \ldots 250)$ mm		$h \geq 280$ mm	
		M_{st}^*	I_{1st}^*	M_{st}^*	I_{1st}^*	M_{st}^*	I_{1st}^*
A	2	1.7...2.0	6.5...7.5	1.2...1.4	7.0...7.5	1.0...1.2	6.5...7.0
	4	2.0...2.2	5.0...7.5	1.2...1.4	6.5...7.5	1.2...1.3	5.5...7.0
	6	2.0...2.2	4.0...5.5	1.2 –1.3	5.0...6.5	1.4	5.5...6.5
	8	1.6...1.9	4.0...5.5	1.2...1.4	5.5...6.0	1.2	5.5...6.5
	10	–	–	1.2	6.0	1.0	6.0
	12	–	–	–	–	1.0	6.0
AH	2	–	–	1.2...1.3	7.0	1.0...1.2	6.5...7.0
	4	–	–	1.2...1.3	6.5	1.0...1.2	6.0...7.0
	6	–	–	1.2	6.0...7.0	1.2	6.0
	8	–	–	1.2...1.3	5.5...6.0	1.2	5.0...5.5
	10	–	–	–	–	1.0	5.5
	12	–	–	–	–	1.0	5.5

Note: Some motors with $h \leq 80$ mm are manufactured with reduced starting current: till $I_{1st}^* = 4.0$ at 2p=2, till $I_{1st}^* = 2.5$ at 2p=4, and till $I_{1st}^* = 3.0$ at greater number of poles.

In wound-rotor motors the starting torque and current are determined by resistance of the starting rheostat and, therefore, are not standardized. Calculation of starting characteristics for them is not performed.

Overloading capacity of an induction motor is defined by its maximum torque (breakdown torque) M_m which should be not less than 1.8 in per unit.

8.1 Starting characteristics of squirrel-cage induction motors

The starting characteristics are relationships $M^* = f(s)$ and $I_1^* = f(s)$ where M^* and I_1^* are the electromagnetic torque and the stator current expressed in per unit. Starting characteristics should be plotted in the same common coordinate axes for the slip values between

Determination of the starting characteristic of a squirrel-cage motor is made for the slip range of 1.0 … s_r. The characteristics should be plotted in the same common coordinate axes.

The calculations are performed in two stages:

- Calculations with account the displacement of current in the cage bars without consideration the teeth area saturation.
- Redetermination the data with account as the current displacement as the teeth area saturation.

8.1.1 Calculation of starting characteristics considering the current displacement

In this stage it is recommended to make calculation for the slip values $s = 1, 0.8, 0.5, 0.3,\ s_{cr}$.

The reduced cage bar height is determined considering decrease of equivalent bar cross-section due to the current displacement. It is determined for working temperature of 75 or 115 °C depending on the thermal class of insulation and found by expressions accordingly:

- For a copper squirrel cage

$$\xi = 96.32 h_b \sqrt{s} \sqrt{\frac{b_b}{b_{sl}}}\,,\ \xi = 89.96 h_b \sqrt{s} \sqrt{\frac{b_b}{b_{sl}}} \qquad (8.1)$$

- For casted aluminum squirrel cage

$$\xi = 65.15 h_b \sqrt{s},\ \ \xi = 63.61 h_b \sqrt{s}\,. \qquad (8.2)$$

Here h_b and b_b are the bar height and width, b_{sl} is the slot width, the ratio $\frac{b_b}{b_{sl}}$ is accepted equal 0.9 for cases of bars inserted into slots, and equal 1 for casted cages.

At the starting characteristics determination, it is assumed that under the bar current displacement the current is uniformly distributed in the upper part of the bar limited by the height h_r which is called the current penetration depth (or the skin depth). The penetration depth is indicated at the slot drawings (Fig. 8.1). The penetration depth is found by the expression:

$$h_r = \frac{h_b}{1+\varphi} \qquad (8.3)$$

where φ is a parameter found from the chart in Fig. 8.2.

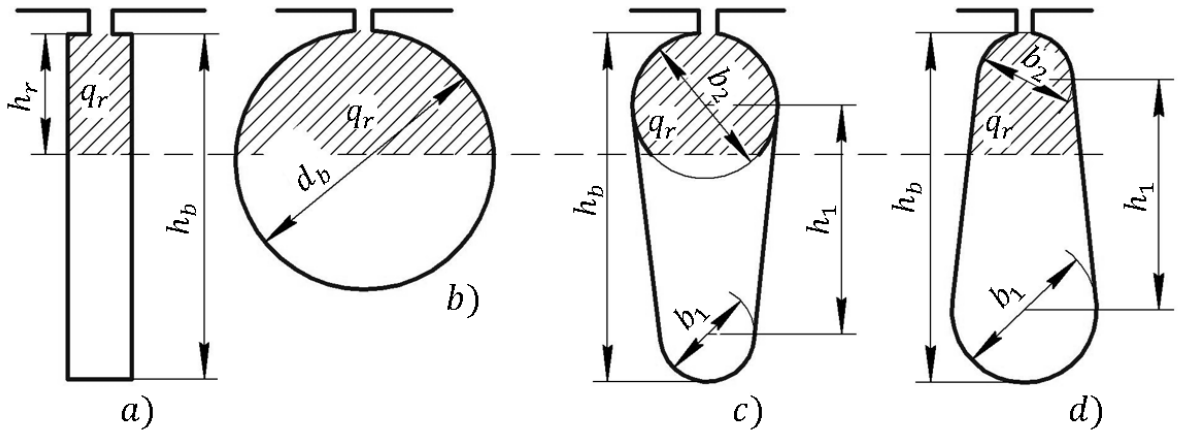

Figure 8.1 – Depth of current penetration into bars of different shape

The current displacement effect causes increase of the bars effective resistance $R_{b\xi} = R_b K_r$ and decrease of the leakage reactance of the slot part of a squirrel cage $X_{b\xi}$ resulting in a decrease of the rotor phase reactance

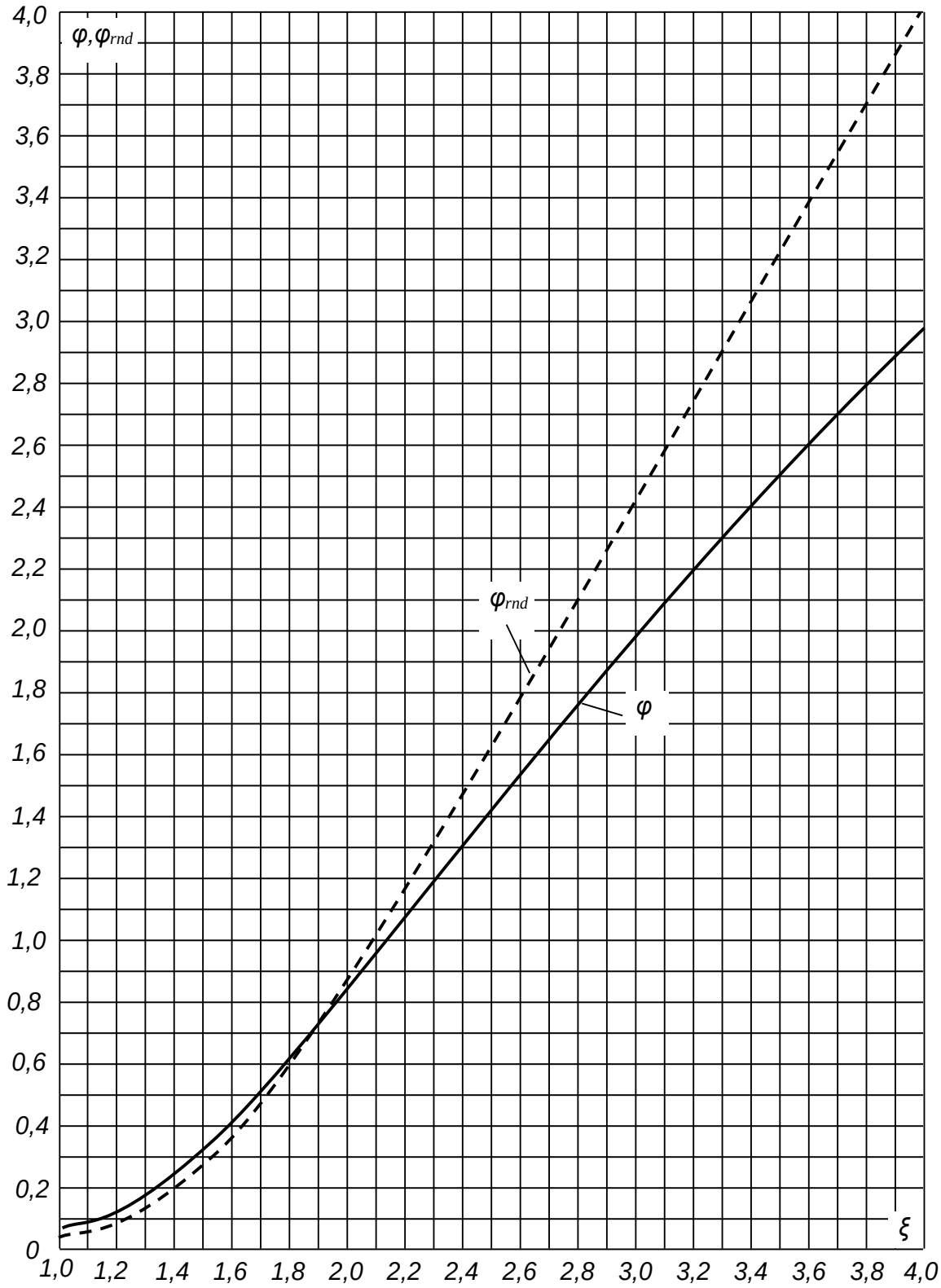

Figure 8.2 – Curves of φ and φ_{rnd}as dependence of ξ
($\varphi \cong \xi - 1$ at $\xi > 4$; $\varphi \cong (4\xi^4)/45$ at $\xi < 1$)

$$X_{2\xi} = X_2 K_X \tag{8.4}$$

where the coefficients are $K_r > 1$, $K_X < 1$.

As the end rings resistance does not change at the current in bars displacement, the rotor phase resistance changes in some less degree than the resistance of bars:

$$R_{2\xi} = R_2 K_R, \qquad K_R = 1 + (K_r - 1)\frac{R_b}{R_2} < K_r\ . \tag{8.5}$$

The rotor phase resistance and reactance determined with account of the current displacement influence referred to the stator winding equal:

$$R'_{2\xi} = R_2 K_R, \qquad X'_{2\xi} = X_2 K_X. \tag{8.6}$$

Consider determination of coefficients K_R and K_X.

Determination of K_R

Coefficient K_R is found by expression (8.5). To calculate it, the coefficient K_r is to be known. Its determination depends on the bar shape.

For bars of rectangular shape (Fig. 8.1, a)

$$K_r = \frac{q_b}{q_r} = \frac{h_b}{h_r} = 1 + \varphi. \tag{8.7}$$

For bars of round shape (Fig. 8.1, b)

$$K_r = 1 + \varphi_{rnd} \tag{8.8}$$

where φ_{rnd} is a parameter found by the chart $\varphi_{rnd} = f(\xi)$ given in Fig 8.2.

For pear-shaped bars (Fig. 8.1, c)

$$K_r = \frac{q_b}{q_r} \tag{8.9}$$

where

$$q_b = \frac{\pi(b_1^2 + b_2^2)}{8} + \frac{b_1 + b_2}{2} h_1. \tag{8.10}$$

The part of the bar cross-section area corresponding to the penetration depth q_r is found in different ways depending on the value of h_r:

- At $\frac{b_2}{2} \le h_r \le h_1 + \frac{b_2}{2}$

$$q_r = \frac{\pi b_2^2}{8} + \frac{b_2+b_r}{2}\left(h_r - \frac{b_2}{2}\right), \quad b_r = b_2 - \frac{b_2-b_1}{h_1}\left(h_r - \frac{b_2}{2}\right). \qquad (8.11)$$

- At $h_r < \frac{b_2}{2}$

$$q_r = \frac{\pi b_2^2}{4(\varphi_{rnd}+1)} \qquad (8.12)$$

where φ_{rnd} is found by Fig. 8.2.

For the trapezoidal bars (Fig. 8.1, d) the same relations that for the pear-shaped bars are used except for expression for b_r. In this case

$$b_r = b_2 + \frac{b_1+b_2}{h_1}\left(h_r - \frac{b_2}{2}\right). \qquad (8.13)$$

For bars of other shapes K_r is found by (8.9) where q_b is determined as cross-section area for the bar of the specified shape and q_r as this bar cross-section part area in bounds of the penetration depth h_r.

Determination of K_X

The coefficient which considers decrease of the rotor reactance due to the current in bars displacement is determined based on the expression:

$$K_X = \frac{X'_{2\xi}}{X'_2} = \frac{X_{2\xi}}{X_2} = \frac{\lambda_{sl2\xi}+\lambda_{ec2}+\lambda_{d2}}{\lambda_{sl2}+\xi_{ec2}+\lambda_{d2}} = \frac{\lambda_{sl2}k_d+\lambda_{ec2}+\xi_{d2}}{\lambda_{sl2}+\lambda_{ec2}+\lambda_{d2}} \qquad (8.14)$$

where $k_d = \lambda_{sl2\xi}/\lambda_{sl2}$. The coefficient $k_d = \varphi'$ where φ' is found by the chart in Fig. 8.3.

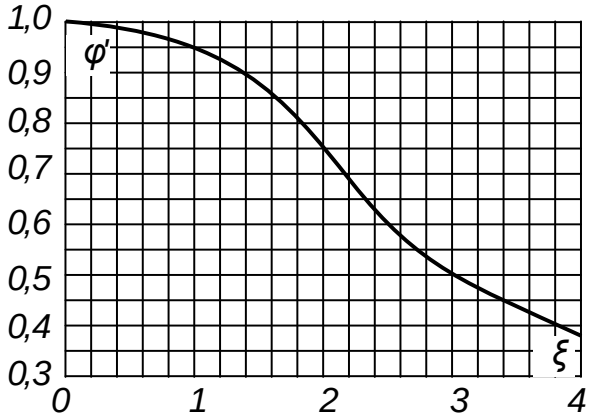

Figure 8.3 – Dependence of coefficient φ' on reduced cage bar height ξ

($\varphi' \cong {}^{3\xi}/_{2}$ at $\xi > 4$)

To find K_X it is necessary to determine the value of $\lambda_{sl2\xi}$ using expressions given in Table 4.7 and value of $k_d = \varphi'$. After that the coefficient K_X is calculated by (8.14).

Under starting conditions, the main magnetic flux decreases, the machine magnetic circuit saturation weakens and the equivalent circuit magnetizing branch impedance increases. At the starting characteristics calculation, it is assumed that impedance Z_m in the range of slip taking place during the starting period is equal to

$$X_{m,st} = X_m \frac{F}{F_\delta}. \tag{8.15}$$

In this stage of calculation, provisional value of the critical slip is found as

$$s_{cr} = \frac{R_2'}{\frac{X_1}{c_{1st}} + X_2'} \tag{8.16}$$

where

$$c_{1st} = 1 + \frac{X_1}{X_m}. \tag{8.17}$$

In farther stage, at calculation with account saturation of the teeth area, more exact values of the coefficient c_{1st} and the critical slip are used.

It is recommended to tabulate the calculations of the starting curves into the table (Table 8.2).

8.1.2 Redetermination the starting characteristics with account the current displacement and the teeth area saturation

Redetermination of starting characteristics is made based on data obtained in the previous stage of calculation.

During the starting period, the stator and rotor currents considerably exceed the values under rated conditions that causes increase of the windings leakage fluxes. The teeth become more saturated, especially in the areas of the teeth edges, and the slot coil parts leakage permeance λ_{sl1} and λ_{sl2} decrease. With account the saturation, the slot parts leakage permeance is found as

$$\lambda_{sl1sat} = \lambda_{sl1} - \Delta\lambda_{sl1}, \qquad \lambda_{sl2\xi sat} = \lambda_{sl2\xi} - \Delta\lambda_{sl2}. \tag{8.18}$$

Table 8.2 – Result of starting characteristics of cage induction motor calculation with considering current displacement in cage bars

Quantity	Unit	Value at slip					
		1	0.8	0.5	0.3	s_{cr}	s_r
ξ	-						
φ	-						
K_r	-						
$K_R = 1 + (K_r - 1)\frac{R_b}{R_2}$	-						
$R'_{2\xi} = R'_2 \cdot K_R$	Ω						
$k_d = f(\xi)$	-						
$\lambda_{sl2\xi} = \lambda_{sl2} \cdot k_d$	-						
$K_X = \frac{\lambda_{sl2\xi} + \lambda_{ec2} + \lambda_{d2}}{\lambda_{sl2} + \lambda_{ec2} + \lambda_{d2}}$	-						
$X'_{2\xi} = X'_2 \cdot K_X$	Ω						
$X_{m,st} = X_m \frac{F}{F_\delta}$	Ω						
$c_{1st} = 1 + \frac{X_1}{X_{m,st}}$	-						
$R = R_1 + \frac{c_{1st} \cdot R'_{2\xi}}{s}$	Ω						
$X = X_1 + c_{1st} \cdot X'_{2\xi}$	Ω						
$I'_2 = \frac{U_{1r}}{\sqrt{R^2 + X^2}}$	A						
$I_1 = I'_2 \frac{\sqrt{R^2 + (X + X_{m,st})^2}}{c_{1st} \cdot X_{m,st}}$	A						
$I_1^* = \frac{I_1}{I_{1r}}$	-						
$M^* = M/M_r = \left(\frac{I'_2}{I'_{2r}}\right)^2 \cdot \frac{s_r}{s} \cdot K_R$	-						

Reduction of the stator and rotor leakage permeance $\Delta\lambda_{sl1}$ and $\Delta\lambda_{sl2}$ caused by saturation is determined by means of introduction the slots additional openings C_1 and C_2 being equivalent by their influence on the permeance to the saturation effect.

Calculation of starting characteristics is carried out using $k_{sat1(2)}$ - the multiples of increase in the current of the stator and rotor due to saturation of their tooth areas that are

$$k_{sat1(2)} = \frac{I_{1(2)sat}}{I_{1(2)}}$$

where $I_{1(2)}$ is the stator (or rotor) current value found without taking saturation into account, $I_{1(2)sat}$ is these current values considering effect of saturation.

As value of k_{sat} is not known beforehand, calculation of starting characteristics is made using the iteration method. Initially the saturation factor may be assumed equal $k_{sat1(2)} = 1.25 \ldots 1.4$ for $s = 1$ and $k_{sat!1)2)} = 1.1 \ldots 1.2$ for $s = s_{cr}$.

Decrease in coefficients of leakage permeance for stator and rotor $\Delta\lambda_{sl1}$ and $\Delta\lambda_{sl2}$ due to saturation are determined separately for each of the indicated values of the slip.

To find C_1 and C_2, first, the average stator winding mmf per slot is calculated:

$$F_{sl,av} = 0.7\frac{k_{sat}I_1u_{sl1}}{a}(k'_\beta + k_{p1}k_{w1}\frac{z_1}{z_2}) \qquad (8.19)$$

where I_1 is the stator current at given value of the slip s taken from data of Table 8.2, k'_β is the coefficient considering decrease of voltage induced in the slot conductors due to the coil pitch shortening which is taken equal to the value found at the slot leakage permeance calculation (see div. 4.2.1). Coefficient k_{sat} is the saturation factor taking into consideration the teeth saturation caused by the leakage fluxes.

After that the fictitious leakage magnetic flux density in the air gap is calculated:

$$B_{\delta f} = \frac{F_{sl,av}}{1.6\delta C_N}10^{-6},\ T \qquad (8.20)$$

where δ is measured in meters, coefficient $C_N = 0.64 + 2.5\sqrt{\frac{\delta}{t_1+t_2}}$.

Further, with the help of curve in Fig. 8.4 the coefficient κ_δ specifying ratio of the leakage fluxes in saturated and non-saturated tooth area are determined by the found value of $B_{\delta f}$. Then additional slots opening equivalent in its effect to the tooth area saturation (Fig.8.5) is calculated as

$$C_1 = (t_1 - b_{so1})(1 - \kappa_\delta), \quad C_2 = (t_2 - b_{so2})(1 - \kappa_\delta)\ . \tag{8.21}$$

Reduction of the leakage permeance $\Delta\lambda_{sl1}$ and $\Delta\lambda_{sl2}$ caused by saturation are defined by expressions depending on the slots shape.

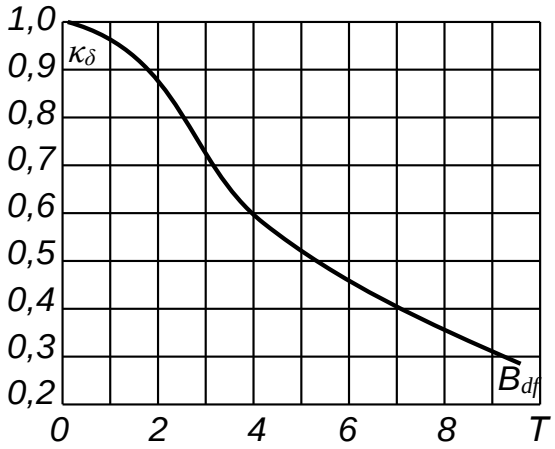

Figure 8.4 – Coefficient κ_δ as a function of fictitious leakage magnetic flux density

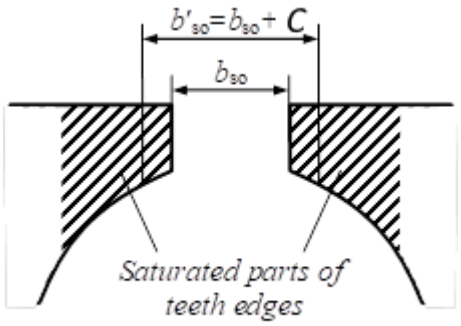

Figure 8.5 – Equivalent additional slot opening considering teeth edges saturation

For stator slots (Fig. 8.6) it is found as:

- For open parallel slots (Fig. 8.6, a)

$$\Delta\lambda_{sl1} = \frac{h'}{b_{so}} \frac{C_1}{b_{so}+C_1}. \tag{8.22}$$

- For semi-open parallel slots (Fig. 8.6, b)

$$\Delta\lambda_{sl1} = \frac{h_{so}}{b_{so}} \frac{C_1}{b_{so}+C_1} + \frac{h'_{so}}{b_{so}+b} \frac{C_1}{b_{so}+b+C_1}. \quad (8.23)$$

- For semi-closed slots (Fig. 8.6, c and d)

$$\Delta\lambda_{sl1} = \frac{h_{so}+0.58h'}{b_{so}} \frac{C_1}{1.5b_{so}+C_1}. \quad (8.24)$$

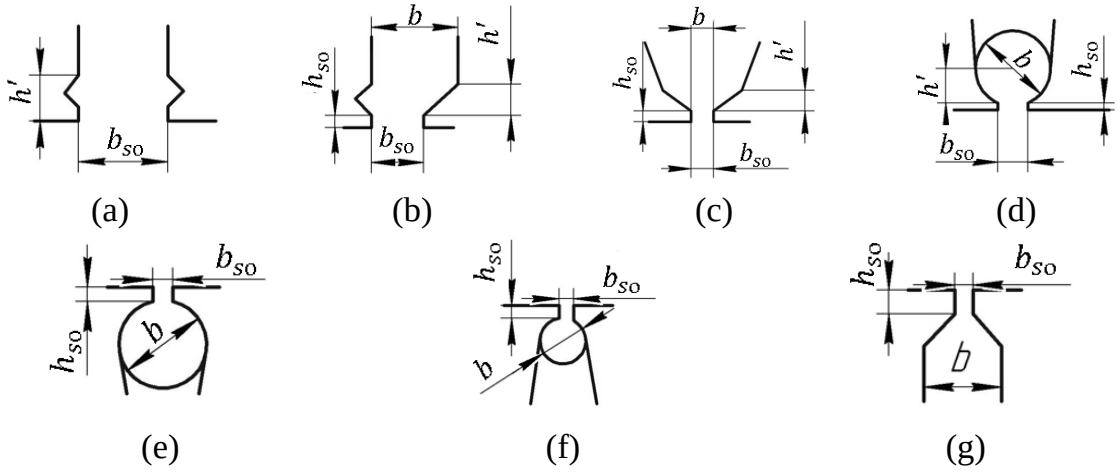

(a) (b) (c) (d)

(e) (f) (g)

Figure 8.6 – Slot dimensions considered at calculation of leakage permeance reduction

For rotor slots (Fig. 7.6) it is found as:

- For semi-closed slots (Fig. 8.6, e, f, and g)

$$\Delta\lambda_{sl2} = \frac{h_{so}}{b_{so}} \frac{C_2}{b_{so}+C_2}. \quad (8.25)$$

- For closed slots (Fig. 8.7)

$$\Delta\lambda_{sl2} = 0.4\pi\left(\frac{h_s}{0.05} \frac{C_2}{C_2+0.05} + \frac{C_2-0.15d}{C_2+0.6d}\right). \quad (8.26)$$

Dimensions are substituted into (8.26) in centimeters.

Differential leakage permeance is also influenced by the teeth area saturation:

$$\lambda_{d1sat} = \lambda_{d1}\kappa_\delta, \quad \lambda_{d2sat} = \lambda_{d2}\kappa_\delta. \quad (8.27)$$

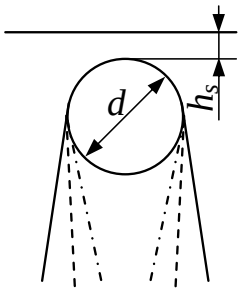

Figure 8.7 – Closed slot of squirrel-cage rotor

Total leakage permeance for the stator and rotor windings determined with account of saturation and rotor current displacement equal:

$$\Sigma\lambda_{1sat} = \lambda_{sl1sat} + \lambda_{d1sat} + \lambda_{ec1} \tag{8.28}$$

$$\Sigma\lambda_{2\xi sat} = \lambda_{sl2\xi sat} + \lambda_{d2sat} + \lambda_{ec2}. \tag{8.29}$$

Redetermination the starting characteristics considering the current displacement and the teeth area saturation is carried out for the same values of slip that are indicated in Table 8.2. For each value of slip the values of quantities, needed for plotting the starting characteristics considering as the current displacement as the teeth area saturation, are found. Calculation is made in the following order:

- The calculation is begun from the slip $s = 1$ at which the saturation factor is accepted in the range of 1.25 …1.40.

For $s = 1$ values of $F_{sl,av}$, $B_{\delta f}$, κ_δ, c_1, c_2, $\Delta\lambda_{sl1}$, $\Delta\lambda_{sl2}$, λ_{sl1sat}, $\lambda_{sl2\xi sat}$, λ_{d1sat}, λ_{d2sat}, $\Sigma\lambda_{1sat}$, $\Sigma\lambda_{2\xi sat}$ are found.

Then the reactance of the stator and rotor phase windings with considering effect of current displacement in rotor bars and teeth saturation are found as

$$X_{1sat} = X_1 \frac{\Sigma\lambda_{1sat}}{\Sigma\lambda_1} \qquad X'_{2\xi sat} = X'_2 \frac{\Sigma\lambda_{2\xi sat}}{\Sigma\lambda_2} \tag{8.30}$$

where X_1, X'_2 $\Sigma\lambda_1$ and $\Sigma\lambda_2$ are taken by data of div.4.2, $\Sigma\lambda_{1sat}$ and $\Sigma\lambda_{2\xi sat}$ are calculated by expressions (8.28) and (8.29).

After that, the resistance and reactance needed for the current calculation with considering the current displacement and saturation are found as

$$R_{st} = R_1 + c_{1st,sat}\frac{R'_{2\xi}}{s} \tag{8.31}$$

$$X_{st} = X_{1sat} + c_{1st,sat}X'_{2\xi sat} \tag{8.32}$$

where the quantities are taken: R_1 – from div. 4.1, $R'_{2\xi}$ - from Table 8.2, X_{1sat} and $X'_{2\xi sat}$ - calculated by (8.30). Starting saturated value of coefficient $c_{1st,sat}$ used at calculation parameters of $\Gamma-$ shaped equivalent circuit is found as

$$c_{1st,sat} = 1 + \frac{X_{1sat}}{X_{m,st}} \tag{8.33}$$

where X_{1sat} is calculated by (8.30), $X_{m,st}$ is calculated by (8.15) or taken from Table 8.2.

After R_{st} and X_{st} determination, the referred rotor current and stator current with considering current in the rotor bars displacement and saturation are found:

$$I'_{2\xi sat} = \frac{U_{1r}}{\sqrt{R_{st}^2+X_{st}^2}}. \tag{8.34}$$

$$I_{1\xi sat} = I'_{2\xi sat}\frac{\sqrt{R_{st}^2+\left(X_{st}+X_{m,st}\right)^2}}{c_{1st,sat}X_{m,st}}. \tag{8.35}$$

The saturation factor obtained as

$$k'_{sat} = \frac{I_{1\xi sat}}{I_1} \tag{8.36}$$

must be compared with the initially accepted its value. If difference between them does not exceeds 10% the currents calculation for the specified value of the slip (in this case – for $s = 1$) is over. If not, it is necessary to change the preliminary accepted value of k_{sat}, taking it between k_{sat} and k'_{sat}, and repeat calculation.

When difference of the saturation factor values satisfies the requirement the relative values of the stator current, and torque are determined:

$$I_1^* = \frac{I_{1\xi sat}}{I_{1r}} \tag{8.37}$$

$$M^* = \left(\frac{I'_{2\xi sat}}{I'_{2r}}\right)^2 K_R \frac{s_r}{s}. \quad (8.38)$$

Next, the determination of the saturation factor at the critical slip is performed. The preliminary value of s_{cr}r is determined according to (8.17). The preliminary value of the saturation factor at s_{cr}r is accepted in the range of $k_{sat} = 1.1 - 1.2$. Then, the determination of k'_{sat}at the critical slip is performed in the order that has been described above and, if necessary, the calculation is repeated till obtaining the difference between k'_{sat} and $k_{sat}$is not more than 10%.

After obtaining satisfactory value of difference between k'_{sat} and k_{sat} at critical slip, adjust the critical slip value by the expression

$$s_{cr} = \frac{R'_{2\xi}}{\frac{X_{1sat}}{c_{1st,sat}} + X'_{2\xi sat}} \quad (8.39)$$

using the quantities values received at the preliminary value of s_{cr}. For this refined value of the critical slip, determine the proper values of I_1^* and $M^* = M_{max}^*$.

Carry out calculations of I_1^* and $M^*$for the remaining specified values of the slip $s-$ $0.8, 0.5, 0.3$ in the above-described order accepting that the saturation factor linearly depends on slip in the range between s_{cr} and 1.

The results of calculation are recommended to tabulate (Table 8.3).

8.2 Multiplicity of wound-rotor motor maximum torque

It is determined with account of the teeth edge saturation as described in div. 8.1.2. In comparison with calculation for a cage motor, difference is that the current displacement in the rotor conductors is not considered, and instead of $R'_{2\xi}$ and $X'_{2\xi}$ the values R'_2 and X'_{2sat} are applied.

Initially the critical slip of a wound-rotor induction motor is found using (8.17), without account the teeth area saturation:

Table 8.3 – Result of starting characteristics of cage induction motor calculation with considering current displacement in cage bars and saturation

Quantity	Unit	Value at slip					
		1	0.8	0.5	0.3	s_{cr}	s_r
k_{sat}	-						
$F_{sl,av}$	A						
$B_{\delta f}$	T						
κ_δ	-						
c_1	-						
c_2	-						
$\Delta\lambda_{sl1}$	-						
$\Delta\lambda_{sl2}$	-						
λ_{sl1sat}	-						
$\lambda_{sl2osat}$	-						
λ_{d1sat}	-						
λ_{d2sat}	-						
$\Sigma\lambda_{1sat}$	-						
$\Sigma\lambda_{2\xi sat}$	-						
X_{1sat}	Ω						
$X'_{2\xi sat}$	Ω						
$c_{1st,sat}$	-						
R_{st}	Ω						
X_{st}	Ω						
$I'_{2\xi sat}$	A						
$I_{1\xi sat}$	A						
k'_{sat}	-						
I_1^*	-						
M^*	-						

$$s_{cr} = \frac{R'_2}{\frac{X_1}{c_{1st}} + X'_2}.$$

Then calculation of currents I'_2 and I_1 with account the effect of saturation is carried out.

After that, using the motor parameters X_{1sat}, X'_{2sat}, $c_{1st,sat}$, found under the above determined critical slip value with account of teeth edge saturation (8.31), the motor critical slip value is refined:

$$s_{cr} = \frac{R'_2}{\frac{X_{1sat}}{c_{1st,sat}} + X'_{2sat}}. \quad (8.40)$$

Finally, the torque M^*_{max} is determined under the critical slip value found with account the teeth area saturation but without account of the rotor current displacement:

$$M^* = \left(\frac{I'_{2sat}}{I'_{2r}}\right)^2 \frac{s_r}{s}. \quad (8.41)$$

9. THERMAL AND VENTILATION CALCULATIONS

9.1 Calculation of motor heating

Calculations of the machine heating are carried out to determine the temperature rise of the machine windings above the ambient temperature to be sure that they do not exceed allowable values.

For motor with wound rotor, temperature rises are calculated for windings as of the stator as the rotor.

In squirrel-cage motors, the allowable temperature rise of the rotor winding is defined by the temperature of the rotor and the material of the adjacent parts which usually does not exceed their allowable values. For that reason, the temperature rise of the rotor winding for the cage motors is not needed.

The rise of temperature for the stator winding above the ambient temperature is found in °C as

$$\Delta\vartheta_1 = \Delta\vartheta'_1 + \Delta\vartheta_{air}$$

where $\Delta\vartheta'_1$ is the temperature rise of the stator winding above the temperature of the air inside the machine in °C,

$\Delta\vartheta_{air}$ is the temperature rise of air inside the machine above the ambient temperature.

The rise of temperature for the rotor winding above the ambient temperature is found in °C as

$$\Delta\vartheta_2 = \Delta\vartheta_2' + \Delta\vartheta_{air}$$

where $\Delta\vartheta_2'$ is the temperature rise of the stator winding above the temperature of the air inside the machine in °C.

Calculations the quantities $\Delta\vartheta_1'$, $\Delta\vartheta_2'$ and $\Delta\vartheta_{air}$ are found in the following order.

In this training project, an approximate method of thermal calculations based on the use of average values of coefficients of heat transfer from a surface and heat conduction of insulation for specific production technology and construction of 4A series of induction motors is recommended.

9.1.1 Calculation of stator winding temperature rise above ambient temperature

Resistance power loss in the stator winding is divided into two components – the loss in slot parts $P_{w1,sl}$ and in end connections of the stator winding coils $P_{w1,ec}$:

$$P_{w1,sl}' = k_\rho P_{w1} \frac{2l_{sl1}}{l_{av1}} \quad (9.1)$$

$$P_{w1,ec}' = k_\rho P_{w1} \frac{2l_{ec1}}{l_{av1}}. \quad (9.2)$$

Quantities l_{sl1}, l_{ec1} and l_{av1}had been found in div. 4, and power loss P_{w1} under recommended working temperature at rated conditions of operation for the specified insulation thermal class – in div. 5.

In the thermal calculations, it is recommended to consider some greater values of resistance loss that take place due to windings resistance increase at the possible rise of the temperature to the maximum level permitted for the specified thermal class of insulation of the given machine. This increase of power loss is considered by means of coefficient k_ρ which is accepted

depending on the maximum winding temperature permitted for the specified thermal class: for thermal class B - temperature 120 ℃, $k_\rho = 1.15$; for thermal class F - temperature 140 ℃, $k_\rho = 1..07$; for thermal class H -temperature 165 ℃, $k_\rho = 1.45$.

The stator core inner surface temperature rise above the air temperature inside the machine in °C equals:

$$\Delta\vartheta_{surf1} = K\frac{P'_{w1,sl}+P_{c,main}}{\pi D l_1 \alpha_1} \quad (9.3)$$

where α_1 – coefficient of heat transfer from the core surface in W/(m^2·°C) (Fig. 9.1, 9.2)

K– coefficient considering part of the losses that is transferred through the motor case to the environment directly, its value is taken from Table 9.1

$P_{c,main}$ – the main magnetic loss in W (div. 5)

D – the inner stator core diameter in m

l_1 – full stator core design length l_1 in m (subdivision. 1.2.7).

Table 9.1 – Average values of coefficient K for 4A induction motors series

Degree of protection	Poles number $2p$					
	2	4	6	8	10	12
IP44	0.22	0.20	0.19	0.18	0.17	0.16
IP23	0.84	0.80	0.78	0.76	0.74	0.72

Temperature drop in insulation of the slot parts of the stator winding coils in °C:

$$\Delta\vartheta_{sl\ ins,1} = \frac{P'_{w1,sl}}{z_1 \Pi_{sl1} l_1}\left(\frac{b_{ins1}}{\lambda_{eqv}} + \frac{b_1+b_2}{16\lambda'_{eqv}}\right) \quad (9.4)$$

where Π_{sl1} – calculated perimeter of the stator slot cross-section in m which is found by expressions:

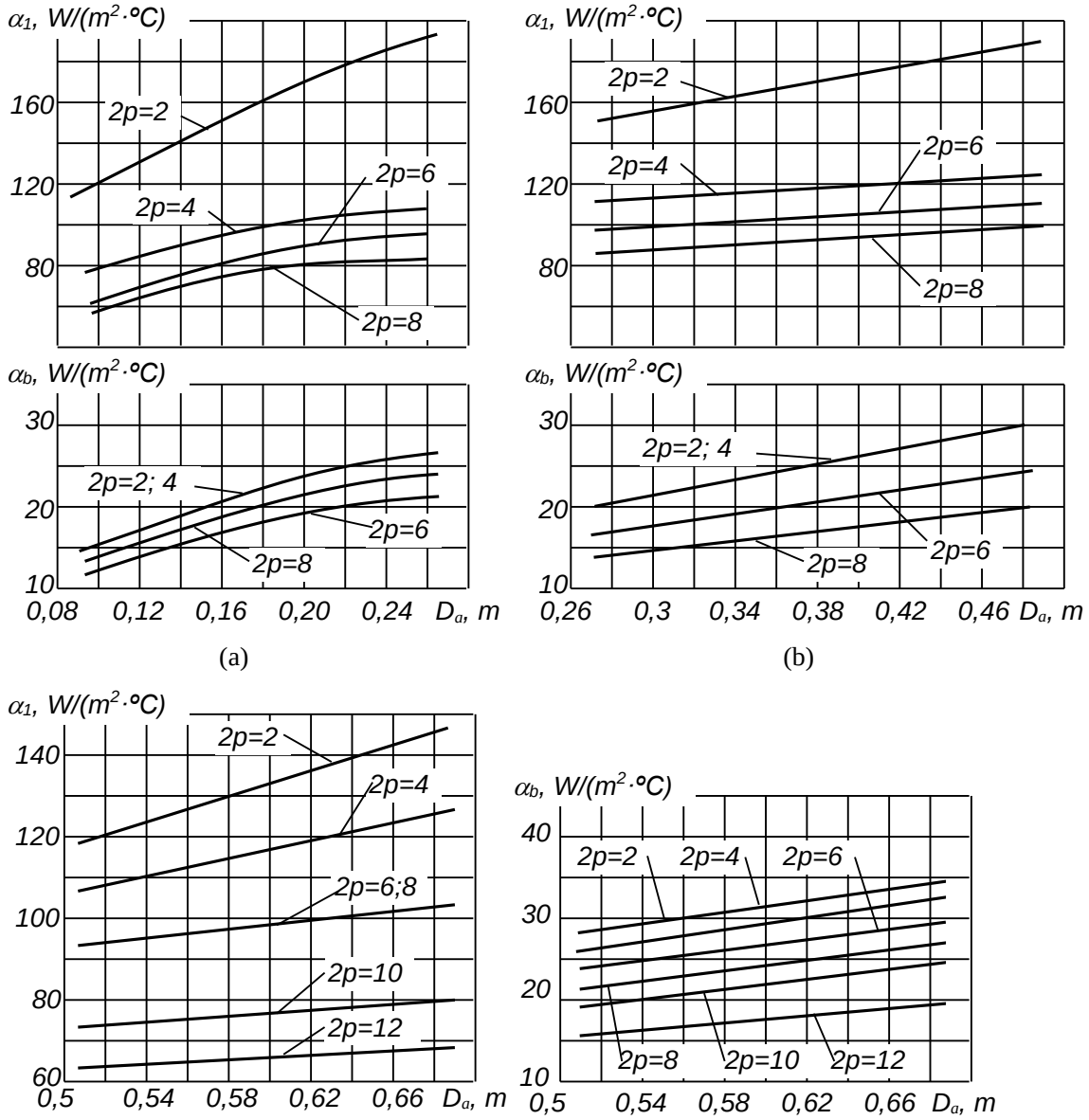

Figure 9.1 – Coefficients of heat transfer from the surface α1 and of air heating αb for motors of 4A series, degree of protection IP44:
a – for $h < 160$ mm; b – for $160 \le h \le 250$ mm; c – for $h \ge 280$ mm

- for semi-closed trapezoidal slots

$$\Pi_{sl1} = 2h_{sl1} + b_1 + b_2 \qquad (9.5)$$

- for parallel open and semi-open slots

$$\Pi_{sl1} = 2(h_{sl1} + b_{sl1}). \qquad (9.6)$$

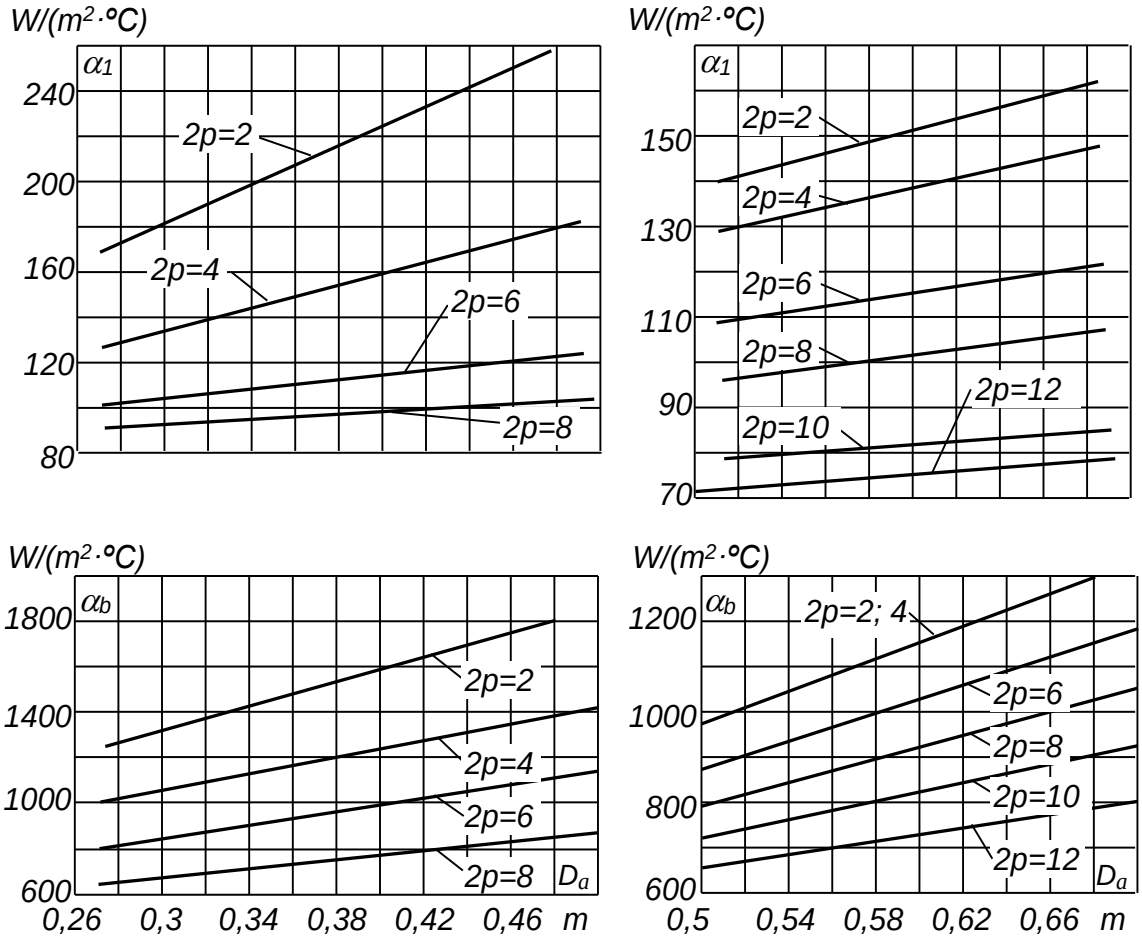

(a) (b)

Figure 9.2 – Coefficients of heat transfer from the surface α_1 and of air heating α_b for motors of 4A series, degree of protection IP23: a – for $160 \leq h \leq 250$ mm; b – for $h \geq 280$ mm

In the above expressions b_{ins1} – unilateral (one-sided) insulation thickness in the slot which value for fed-in windings is taken from previous calculation of the slot dimensions, and for windings made of rectangular wire is calculated as

$$b_{ins1} = 0.5(b_{sl} - n_{el}b) \tag{9.7}$$

n_{el} and b – the number and width of non-insulated elementary conductors placed in one layer by the slot width;

λ_{eqv}– average values of coefficient of thermal conductivity for the slot insulation. For insulation of thermal classes B, F and H $\lambda_{eqv} = 0.16$ W/(m · °C);

λ'_{eqv} – average value of coefficient of thermal conductivity for inner insulation of fed-in-winding coil made of enameled wire in $\mathrm{W/(m \cdot °C)}$ determined considering looseness of the conductors to each other (Fig. 9.3).

For windings of rectangular conductors, it is assumed that $\frac{b_1+b_2}{16\lambda'_{eqv}} = 0$.

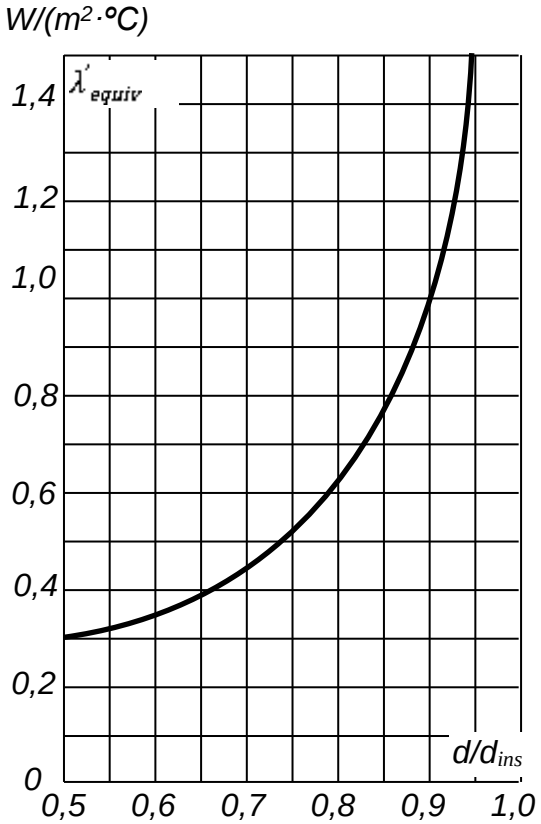

Figure 9.3 – Coefficient of thermal conductivity of coils internal insulation for fed-in windings wound of enamel-covered wire

The drop of temperature across the thickness of insulation of coil end connections in °C is found by the expression:

$$\Delta\vartheta_{ec\ ins,1} = \frac{P'_{w1,ec}}{2z_1\Pi_{ec1}lec_1}\left(\frac{b_{ins\ ec1}}{\lambda_{eqv}} + \frac{h_{sl1}}{12\lambda'_{eqv}}\right) \qquad (9.8)$$

where Π_{ec1} – the perimeter of conditional cooling surface of one coil end connections in m that is assumed equal $\Pi_{ec1} \cong \Pi_{sl1}$;

$b_{ins\ ec1}$ – unilateral thickness of the coil end connections insulation in m (see tables of Appendix 10). If the insulation is not available, it is accepted $b_{ins\ ec1} = 0$;

λ'_{eqv} is taken from Fig. 9.3 for coils of fed-in windings; for coils of rectangular wire, it is accepted $\frac{h_{sl1}}{12\lambda'_{eqv}} = 0$.

The temperature rise of external surface of the stator winding end connections above temperature of the air inside the machine in °C:

$$\Delta\vartheta_{ec,surf1} = K\frac{P'_{w1,ec}}{2\pi D l_{oh1}\alpha_1} \tag{9.9}$$

where l_{oh1} – the stator winding coils overhang in m found in subdivision 4.1.1 (Fig. 4.2); quantities K and α_1 were found above at determination of $\Delta\vartheta_{surf1}$ in this subdivision.

The temperature rise of the stator winding above temperature of the air inside the machine in °C:

$$\Delta\vartheta'_1 = \frac{(\Delta\vartheta_{surf1}+\Delta\vartheta_{sl\,ins,1})2l_1+(\Delta\vartheta_{ec\,ins,1}+\Delta\vartheta_{ec,surf1})2l_{ec1}}{l_{av1}} \tag{9.14}$$

where l_1 have been found in subdivision 1.2.7 and l_{ec1}, l_{av1}– in subdivision 4.1.1.

The temperature rise of air inside the machine above the ambient temperature in °C:

$$\Delta\vartheta_{air} = \frac{\Sigma P'_{air}}{S_h\alpha_b} \tag{9.15}$$

where $\Sigma P'_{air}$ – the total loss dissipated to the air inside the motor, in W

α_b – the coefficient of air heating in $\mathrm{W/(m^2 \cdot °C)}$, its values are given in Fig. 9.1, 9.2

S_h – the equivalent motor housing cooling surface, in $\mathrm{m^2}$.

The total loss dissipated to the air inside the motor is calculated as follows.

For motors with protection IP23

$$\Sigma P'_{air} = \Sigma P' - (1-K)\left(P'_{w1,ec} + P_{c,main}\right) \tag{9.16}$$

where

$$\Sigma P' = \Sigma P + \left(k_\rho - 1\right)(P_{w1} + P_{w2}) \qquad (9.17)$$

ΣP – the motor total power loss under rated operation conditions and temperature adopted for their calculation.

For motors with protection IP44, power consumed by the external ventilator, mounted on the rotor shaft, and equal roughly 0.9 of total mechanical loss is not considered. Therefore

$$\Sigma P'_{air} = \Sigma P' - (1 - K)\left(P'_{w1,ec} + P_{c,main}\right) - 0.9\, P_{mech} \qquad (9.18)$$

where $\Sigma P'$ is calculated by (9.17).

The equivalent motor housing cooling surface in m^2 is found as:

- For motors with protection IP23:

$$S_h = \pi D_a (l_1 + 2l_{ec1}) \qquad (9.19)$$

- For motors with protection IP44:

$$S_h = (\pi D_a + 8\Pi_{rib})(l_1 + 2l_{ec1}) \qquad (9.20)$$

where Π_{rib} – the housing ribs cross-section perimeter which may be roughly found from Fig. 9.4.

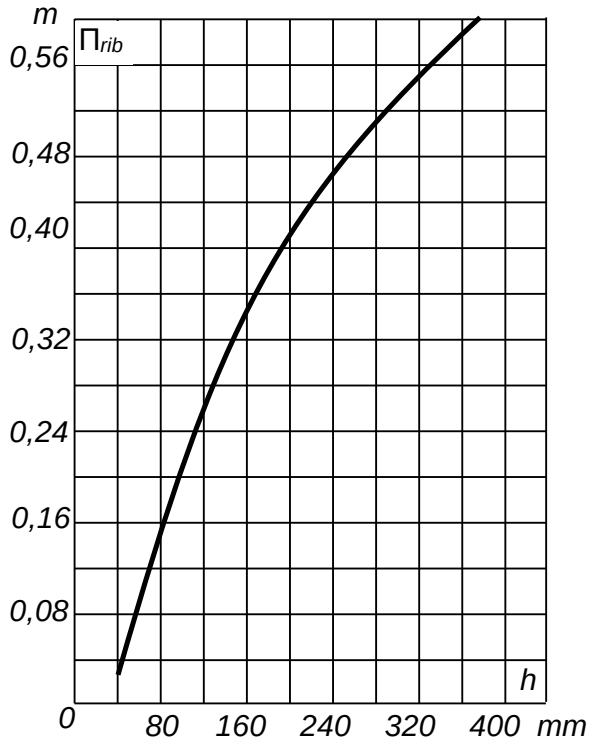

Figure 9.4 – Average value of the cooling ribs cross-section perimeter for induction motors of 4A series

The temperature rise of the stator winding above the ambient temperature in °C:

$$\Delta\vartheta_1 = \Delta\vartheta_1' + \Delta\vartheta_{air}. \quad (9.21)$$

As the described calculation is simplified, the obtained value of $\Delta\vartheta_1$ is approximate. Therefore, it should be at least 10% less than allowable for the thermal class of the machine insulation.

9.1.2 Calculation of the rotor winding temperature rise above ambient temperature for a wound-rotor machine

The wound–rotor winding temperature rise is calculated in the same order that for the stator winding.

The rotor core surface temperature rise above the air temperature inside the machine in °C equals

$$\Delta\vartheta_{surf2} = \frac{P'_{w2,sl}}{\pi D_2 l_2 \alpha_2} \quad (9.22)$$

where α_2 – coefficient of heat transfer from the wound rotor surface (Fig. 9.5)

$P'_{w2,sl}$ – the resistance loss in the slot part of the rotor winding equal

$$P'_{w2,sl} = k_\rho P_{w2} \frac{2l_{sl2}}{l_{av2}}. \quad (9.23)$$

The average turn length l_{av2} was found in div. 4.1.

Temperature drop in insulation of the slot parts of the rotor winding coils in °C:

$$\Delta\vartheta_{sl\ ins,2} = \frac{P'_{w2,sl}}{z_2 \Pi_{sl2} l_2 \lambda_{eqv}} \quad (9.24)$$

where Π_{sl2} – the calculated perimeter of the rotor slot cross-section which is found for slots with parallel sides by expression:

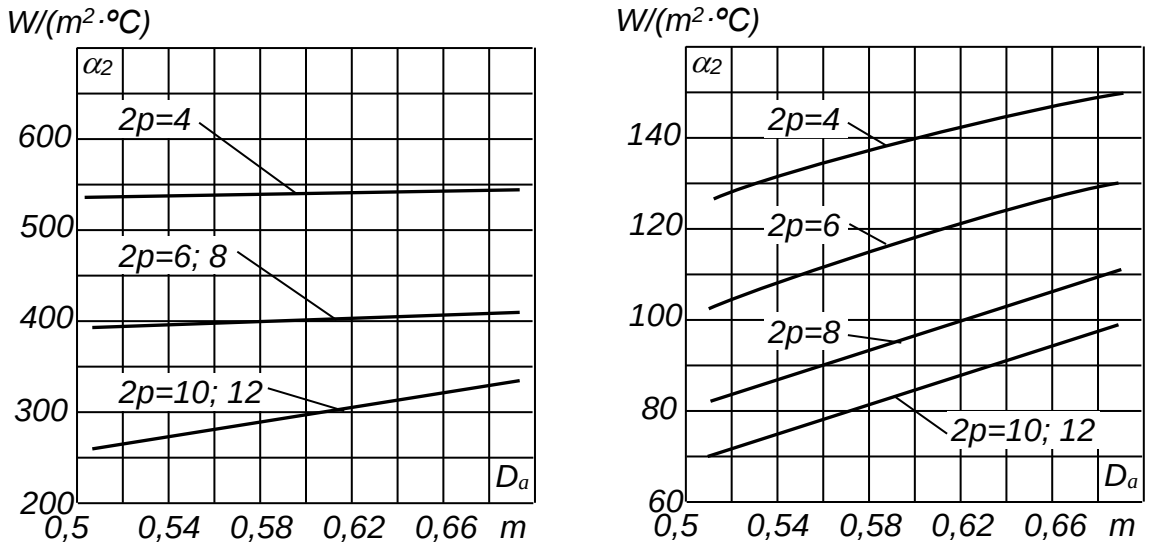

Figure 9.5 – Average values of coefficient of heat transfer from the wound rotor surface at voltage of 680 V and less: a – for blown through rotors, degree of protection IP44; b - for motors with degree of protection IP23

$$\Pi_{sl2} = 2(h_{sl2} + b_{sl2}). \tag{9.25}$$

The temperature's rise of external surface of the rotor winding end connections above temperature of the air inside the machine in °C:

$$\Delta\vartheta_{ec,surf2} = \frac{P'_{w2,ec}}{2\pi D_2 l_{oh2}\alpha_2} \tag{9.26}$$

where $P'_{w2,ec}$ – the loss in end connections of the rotor winding coils in W:

$$P'_{w2,ec} = k_c P_{w2} \frac{2l_{ec2}}{l_{av2}}. \tag{9.27}$$

The temperature drop by thickness of the coil end connections insulation in **°C** is found by the expression:

$$\Delta\vartheta_{ec\ ins,2} = \frac{P'_{w2,ec}}{2z_2\Pi_{ec2}lec_2\lambda_{eqv}} \tag{9.28}$$

where Π_{ec2} – the perimeter of conditional cooling surface of one coil end connections that is assumed equal $\Pi_{ec2} \cong \Pi_{sl2}$;

$b_{ins\ ec2}$ – unilateral thickness of the coil end connections insulation (see tables of Appendix 10).

The average temperature rise of the rotor winding above temperature of the air inside the machine in °C:

$$\Delta\vartheta_2' = \frac{(\Delta\vartheta_{surf2}+\Delta\vartheta_{sl\ ins,2})2l_2+(\Delta\vartheta_{ec\ ins,2}+\Delta\vartheta_{ec,surf2})2l_{ec2}}{l_{av1}} \qquad (9.29)$$

where l_2 have been found in subdivision 1.2.7 and l_{ec2}, l_{av2} – in subdivision 4.1.1.

The temperature rise of the rotor winding above the ambient temperature in °C:

$$\Delta\vartheta_2 = \Delta\vartheta_2' + \Delta\vartheta_{air}. \qquad (9.30)$$

The obtained value of $\Delta\vartheta_2$ is approximate. Therefore, it should be at least 10% less than allowable for the thermal class of the machine insulation.

9.3 Motor ventilation calculation

Effectiveness of the motor ventilation is assessed by comparison of **the air consumption needed** for the machine cooling, and **the air consumption which may be provided** at the given motor design and dimensions. Below the calculation method applicable for motors designed on the base of induction motors of 4A series construction is described.

9.3.1 Calculation of the needed air consumption

The air consumption Q_{air} needed for the designed motor cooling is calculated with account its degree of protection.

For motors with protection IP23 its value in m^3/s is found as:

$$Q_{air} = \frac{\Sigma P'_{air}}{1100\,\Delta\vartheta'_{air}}, \qquad (9.31)$$

where$\Sigma P'_{air}$ in W is determined by (9.16); $\Delta\vartheta'_{air}$ – the temperature rise of the output air above the input air temperature in ºC, $\Delta\vartheta'_{air} \cong \Delta\vartheta_{air}$.

For motors with protection IP44 the needed air consumption in m^3/s is found as:

$$Q_{air} = \frac{k_m \Sigma P'_{air}}{1100\ \Delta\vartheta_{air}} \tag{9.32}$$

where $\Sigma P'_{air}$ is determined by (9.18); k_m – the coefficient considering changing of cooling conditions along the motor housing. It equals

$$k_m = m\sqrt{\frac{n}{100} D_a} \tag{9.33}$$

where $m = 2.6$ for motors with $2p = 2$ at $h \leq 132$ mm, $m = 3.3$ at $h \geq 160$ mm; $m = 1.8$ for motors with $2p \geq 4$ at $h \leq 132$ mm, and $m = 2.5$ at $h \geq 160$ mm. The motor rotational frequency n is substituted in rpm, D_a – in m.

9.3.2 Calculation of the provided air consumption

The air consumption provided by the motor ventilation system Q'_{air} is also calculated differently for motors with different degree of protection.

For motors with protection IP23 its value in m^3/s is found as:

$$Q'_{air} = m(n_{rd} b_{rd} + 0.1)\frac{n}{100} D_a^2 \tag{9.34}$$

where $n_{rd}$and b_{rd} are the number and width of radial air ducts, b_{rd} in m; n – in rpm; $m = 2.6$ for motors with $2p = 2$ and $m = 3.15$ for motors with $2p \geq 4$; D_a – in m.

For motors with protection IP44 the air consumption provided by the motor ventilation system in m^3/s is found as:

$$Q'_{air} = 0.6 D_a^3 \frac{n}{100}. \tag{9.35}$$

9.3.3 Comparison of the needed and provided by the motor ventilation system air consumption

Effectiveness of the motor ventilation is satisfactory if

$$Q'_{air} \geq Q_{air}. \tag{9.36}$$

APPENDIXES

Appendix 1
Magnetizing curves of electrical steel

STEEL GRADE 2013

Table A1.1

Basic magnetizing curve

B, T	0	0,01	0,02	0,03	0,04	0,05	0,06	0,07	0,08	0,09
	H, A/m									
0,4	56	56	57	58	59	60	60	61	61	62
0,5	63	63	64	65	66	67	67	68	68	69
0,6	70	70	71	72	73	74	74	75	76	77
0,7	78	79	80	81	82	83	84	85	86	87
0,8	88	89	90	91	92	93	94	95	96	97
0,9	99	100	101	102	103	104	105	106	107	108
1,0	110	111	113	114	115	117	118	120	121	123
1,1	125	126	127	128	129	132	133	134	136	138
1,2	141	146	152	158	164	170	176	182	188	194
1,3	200	210	220	230	240	250	260	270	280	290
1,4	300	320	350	380	410	430	460	500	540	580
1,5	620	670	780	890	1 000	1 130	1 240	1 350	1 460	1 580
1,6	1 700	1 860	2 020	2 180	2 340	2 500	2 700	2 800	3 000	3 200
1,7	3 400	3 700	4 000	4 300	4 700	5 000	5 400	5 800	6 200	6 600
1,8	7 000	7 500	8 000	8 500	9 200	10 000	10 600	11 200	11 800	12 400
1,9	13 000	13 600	14 200	14 800	15 600	16 500	17 300	18 100	18 900	19 800
2,0	20 700	22 600	24 400	26 300	28 100	30 000	36 000	42 000	48 000	54 000
2,1	60 000	67 000	74 000	81 000	88 000	95 000	102 000	109 000	116 000	123 000
2,2	130 000	138 000	146 000	154 000	162 000	170 000	178 000	186 000	194 000	202 000
2,3	210 000	218 000	226 000	234 000	242 000	250 000	258 000	266 000	274 000	282 000
2,4	290 000	298 000	306 000	314 000	322 000	330 000	338 000	346 000	354 000	362 000

Table A1.2

Magnetizing curve for yokes of asynchronous machines

B, T	0	0,01	0,02	0,03	0,04	0,05	0,06	0,07	0,08	0,09
	H, A/m									
0,4	52	53	54	55	56	58	59	60	61	62
0,5	64	65	66	67	69	71	72	74	76	78
0,6	80	81	83	85	87	89	91	93	95	97
0,7	100	102	104	106	108	111	113	115	118	121
0,8	124	126	129	132	135	138	140	143	146	149
0,9	152	155	158	161	164	168	171	174	177	181
1,0	185	188	191	195	199	203	206	209	213	217
1,1	221	225	229	233	237	241	245	249	253	257
1,2	262	267	272	277	283	289	295	301	307	313
1,3	320	327	334	341	349	357	365	373	382	391
1,4	400	410	420	430	440	450	464	478	492	506
1,5	520	542	564	586	608	630	654	678	702	726
1,6	750	788	826	864	902	940	982	1 020	1 070	1 110
1,7	1 150	1 220	1 290	1 360	1 430	1 500	1 600	1 700	1 800	1 900
1,8	2 000	2 160	2 320	2 490	2 650	2 810	2 960	3 110	3 270	3 420
1,9	3 570	3 800	4 030	4 260	4 490	4 720	4 930	5 140	5 350	5 560
2,0	5 770	6 000	6 300	6 600	7 000	7 400	7 900	8 400	9 000	9 700

Table A1.3

Magnetizing curve for teeth of induction motors

B, T	0	0,01	0,02	0,03	0,04	0,05	0,06	0,07	0,08	0,09
	H, A/m									
0,4	124	127	130	133	136	138	141	144	147	150
0,5	154	157	160	164	167	171	174	177	180	184
0,6	188	191	194	198	201	205	208	212	216	220
0,7	223	226	229	233	236	240	243	247	250	253
0,8	256	259	262	265	268	271	274	277	280	283
0,9	286	290	293	297	301	304	308	312	316	320
1,0	324	329	333	338	342	346	350	355	360	365
1,1	370	375	380	385	391	396	401	406	411	417
1,2	424	430	436	442	448	455	461	467	473	479
1,3	486	495	504	514	524	533	563	574	584	585
1,4	586	598	610	622	634	646	658	670	683	696
1,5	709	722	735	749	763	777	791	805	820	835
1,6	850	878	906	934	962	990	1020	1050	1080	1 110
1,7	1150	1180	1220	1250	1290	1330	1360	1400	1440	1 480
1,8	1520	1570	1620	1670	1720	1770	1830	1890	1950	2 010
1,9	2070	2160	2250	2340	2430	2520	2640	2760	2890	3 020
2,0	3150	3320	3500	3680	3860	4040	4260	4480	4700	4 920
2,1	5140	5440	5740	6050	6360	6670	7120	7570	8020	8 470
2,2	8920	9430	9940	10460	10980	11500	12000	12600	13200	13 800
2,3	14400	15100	15800	16500	17200	18000	18800	19600	20500	21 400

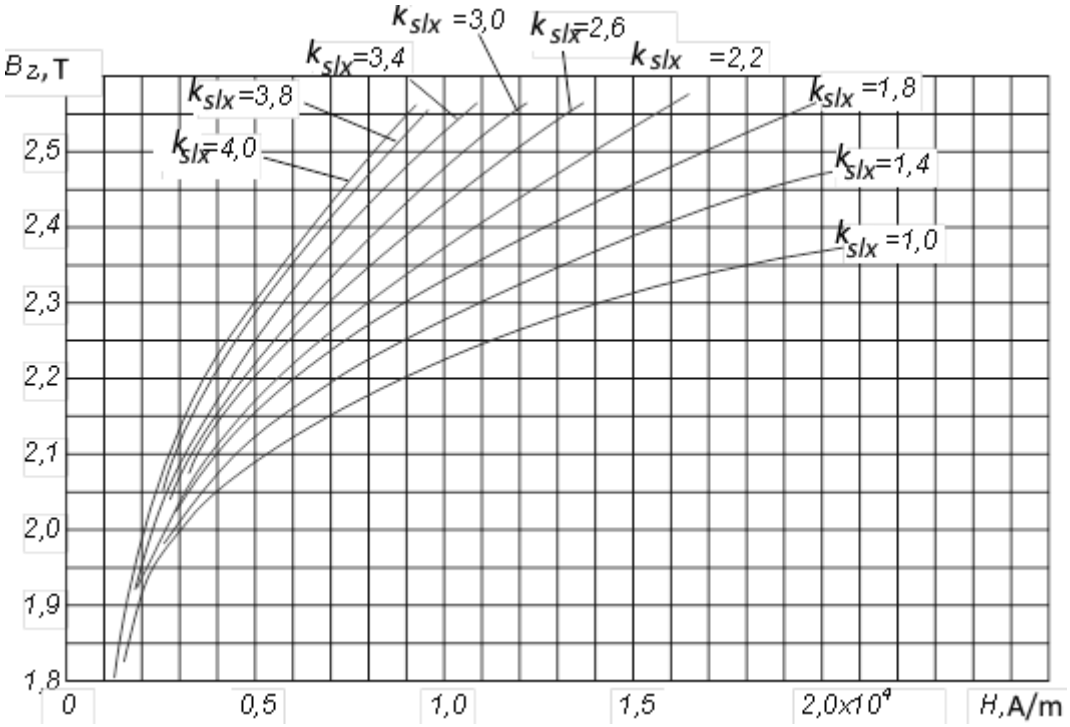

Figure A1.1 Magnetizing curves for teeth of induction motors
Considering branching off the magnetic flux into slots

STEEL GRADES 2211, 2212, 2214, 2312, 2411

Table A1.4

Basic magnetizing curve

B, T	0	0,01	0,02	0,03	0,04	0,05	0,06	0,07	0,08	0,09
	H, A/m									
0,4	68	69	70	71	72	73	73	74	75	75
0,5	76	77	78	79	80	81	82	83	84	85
0,6	86	87	88	89	90	91	92	93	94	95
0,7	.96	99	103	108	113	118	122	126	131	135
0,8	140	145	150	155	160	165	170	175	180	185
0,9	190	195	200	205	210	215	220	225	230	235
1,0	240	246	252	258	264	270	276	282	288	294
1,1	300	310	320	330	340	350	360	370	380	390
1,2	400	410	420	430	440	460	470	480	500	520
1,3	550	580	610	650	690	730	780	830	880	940
1,4	1 000	1 060	1 120	1 180	1 240	1 300	1 360	1 420	1 480	1 540
1,5	1 600	1 750	1 900	2 050	2 200	2 350	2 500	2 700	2 900	3 100
1,6	3 400	3 600	3 800	4 100	4 400	4 700	5 300	5 900	6 500	7 100
1,7	7 700	8 200	8 900	9 400	10 000	10 600	11 100	11 700	12 200	12 800
1,8	13 400	14 000	14 600	15 200	15 800	16 400	17 000	17 600	18 200	18 800
1,9	19 400	20 000	21 800	23 700	25 700	27 800	30 000	32 200	34 400	36 600
2,0	38 800	41 000	43 200	45 400	47 600	49 800	52 000	54 500	57 500	60 500
2,1	65 500	72 500	80 000	88 000	96 000	104 000	112 000	120 000	128 000	136 000
2,2	144000	152 000	160 000	168 000	176 000	184 000	192 000	200 000	208 000	216 000
2,3	224000	232 000	240 000	248 000	256 000	264 000	272 000	280 000	288 000	296 000
2,4	304000	312 000	320 000	328 000	336 000	344 000	352 000	360 000	368 000	376 000

Table A1.5

Magnetizing curve for yokes of asynchronous machines

B, T	0	0,01	0,02	0,03	0,04	0,05	0,06	0,07	0,08	0,09
	H, A/m									
0,4	89	91	93	94	96	98	100	102	104	106
0,5	108	110	113	115	118	120	122	124	126	128
0,6	131	134	136	139	141	144	147	150	153	156
0,7	159	162	166	169	172	176	180	183	186	190
0,8	194	198	201	204	208	212	216	220	223	227
0,9	231	235	239	243	248	252	255	260	265	269
1,0	274	279	284	289	295	300	305	311	318	323
1,1	332	338	344	351	357	367	374	382	390	398
1,2	410	418	426	435	444	455	466	475	487	498
1,3	509	52!	533	546	558	572	585	600	618	635
1,4	656	675	695	717	740	763	789	815	843	870
1,5	905	934	965	1000	1040	1090	1130	1190	1240	1290
1,6	1370	1440	1520	1590	1660	1720	1820	1910	2010	2100
1,7	2180	2310	2410	2550	2610	2720	2840	2980	3130	3290
1,8	3460	3630	3800	3970	4140	4301	4490	4670	4850	5040
1,9	5220	5600	6000	6400	6900	7400	7900	8500	9100	9700
2,0	10400	11100	11800	12500	13300	14100	14900	15800	16700	17600

Table A1.6

Magnetizing curve for teeth of induction motors

B, T	0	0,01	0,02	0,03	0,04	0,05	0,06	0,07	0,08	0,09
	H, A/m									
0,4	140	143	146	149	152	155	158	161	164	171
0,5	174	177	180	184	186	190	192	196	198	202
0,6	204	209	213	216	221	224	229	233	237	241
0,7	245	249	253	257	262	267	272	277	282	287
0,8	292	297	302	306	311	316	322	326	331	337
0,9	342	347	353	360	366	372	379	384	390	396
1,0	403	409	417	425	433	440	450	460	470	477
1,1	488	497	509	517	527	537	547	559	570	582
1,2	593	602	613	626	638	651	663	677	695	710
1,3	724	738	755	770	790	804	820	840	857	870
1,4	897	917	936	955	977	1 000	1 020	1 040	1 060	1 090
1,5	1 120	1 150	1 170	1 210	1 240	1 270	1 310	1 330	1 370	1 410
1,6	1 450	1 490	1 530	1 560	1 610	1 650	1 690	1 750	1 790	I 840
1,7	1 900	1 940	2 000	2 070	2 140	2 220	2 300	2 380	2 500	2 600
1,8	2 700	2 800	2 920	3 050	3 220	3 330	3 490	3 610	3 710	4 000
1,9	4 160	4 350	4 600	4 800	5 030	5 330	5 430	5 790	6 130	6 420
2,0	6 750	7 170	7 400	7 790	8 150	8 520	9 000	9 400	9 750	10 200
2,1	10 600	11 000	11 500	12 100	12 600	13 000	13 500	14 100	14 700	15 400
2,2	15 900	16 500	17 300	17 800	18 500	19 100	19 600	20 300	21 100	22 000
2,3	23 100	24 300	25 500	26 800	28 100	29 500	30 900	32 400	33 900	36 400

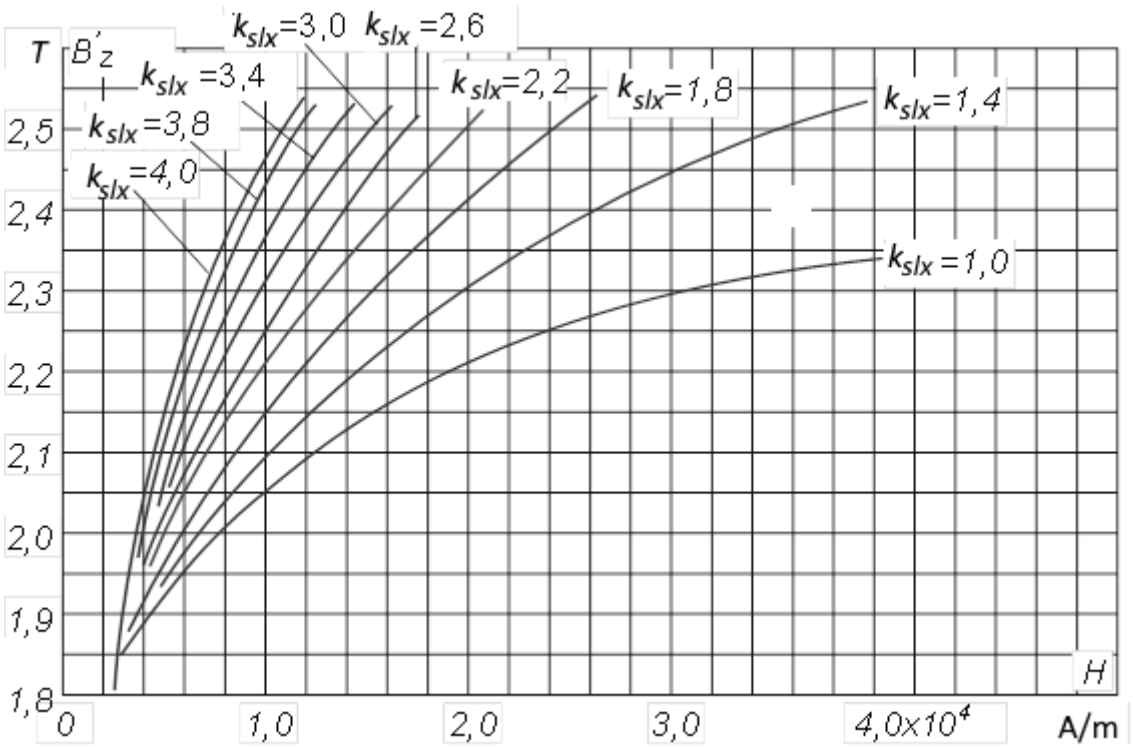

Figure A1.2. Magnetizing curves for teeth of induction motors
Considering branching off the magnetic flux into slots

STEEL GRADE 2412

Table A1.7

Basic magnetizing curve

B, T	0	0,01	0,02	0,03	0,04	0,05	0,06	0,07	0,08	0,09
	H, A/m									
0,4	67	68	69	70	71	72	73	74	75	76
0,5	77	78	79	80	81	83	84	86	87	89
0,6	90	92	94	96	97	99	101	103	105	107
0,7	109	111	113	115	117	119	122	124	127	130
0,8	133	135	138	141	144	147	150	154	158	162
0,9	166	170	174	179	184	187	194	199	205	211
1,0	217	223	230	237	244	252	260	269	277	286
1,1	295	304	314	324	334	344	355	366	377	388
1,2	399	411	423	435	447	460	473	486	500	540
1,3	585	630	680	735	795	860	930	1 000	1 070	1 150
1,4	1 230	1 320	1 420	1 520	1 630	1 750	1 870	2 010	2 160	2 320
1,5	2 500	2 680	2 870	3 080	3 300	3 540	3 800	4 090	4 380	4 700
1,6	5 000	5 380	5 760	6 200	6 650	7 120	7 650	8 200	8 800	9 400
1,7	10 000	10 500	11 000	11 500	12 000	12 500	13 100	13 700	14 300	14 900
1,8	15 600	16 200	16 800	17 500	18 300	19 100	20 000	20 900	21900	22 900
1,9	23 900	25 000	26 200	27 400	28 700	30 000	32 000	36 000	42 000	50 000
2,0	59 000	68 000	77 000	86 000	95 000	104 000	113 000	122 000	131 000	140 000
2,1	149 000	158 000	167 000	176 000	185 000	194 000	203 000	212 000	221 000	230 000

Table A1.8

Magnetizing curve for yokes of asynchronous machines

B, T	0	0,01	0,02	0,03	0,04	0,05	0,06	0,07	0,08	0,09
	H, A/m									
0,4	48	48	49	50	51	51	52	53	53	54
0,5	55	56	56	57	58	59	60	61	61	62
0,6	63	63	65	66	67	68	69	69	70	71
0,7	72	72	73	74	75	76	76	77	78	79
0,8	81	82	83	84	85	87	88	90	92	94
0,9	96	98	100	102	104	105	107	109	112	114
1,0	116	118	121	124	126	129	132	136	139	143
1,1	146	150	154	158	162	167	172	176	182	188
1,2	192	198	204	210	216	222	230	238	246	260
1,3	272	288	300	316	330	340	358	370	386	399
1,4	410	440	460	490	530	570	610	660	710	770
1,5	820	890	960	1 030	1 100	1 170	1 230	1 310	1 400	1 480
1,6	1 560	1 640	1 730	1 820	1 920	2 000	2 100	2 260	2 440	2 600
1,7	2 800	2 960	3 100	3 260	3 400	3 580	3 740	3 900	4 100	4 300
1,8	4 500	4 700	5 000	5 300	5 500	5 800	6 100	6 400	8 800	7 200
1,9	7 600	8 000	8 500	9 100	9 700	10 300	11 100	11 900	13 100	14 200
2,0	16 000	18 000	20 000	22 000	23 800	25 500	27 600	29 600	31 500	33 800

Table A1.9

Magnetizing curve for teeth of induction motors

B, T	0	0,01	0,02	0,03	0,04	0,05	0,06	0,07	0,08	0,09
	H, A/m									
0,4	72	73	74	75	77	78	79	80	81	82
0,5	83	84	85	86	87	88	89	90	91	92
0,6	93	94	95	96	97	98	99	101	102	104
0,7	105	106	108	110	111	113	115	117	118	120
0,8	122	124	126	128	130	132	134	136	138	140
0,9	142	144	147	149	151	155	158	160	163	165
1,0	168	171	175	177	180	184	188	191	196	200
1,1	204	207	212	216	222	227	232	237	242	247
1,2	254	259	265	272	277	284	291	298	307	316
1,3	323	333	341	351	361	372	383	394	404	421
1,4	425	432	461	480	497	518	537	554	573	596
1,5	622	644	673	700	728	756	795	828	859	890
1,6	932	976	1 020	1 070	1 130	1 180	1 260	1 350	1 440	1 520
1,7	1 630	1 740	1 870	2 020	2 130	2 300	2 450	2 630	2 830	3 040
1,8	3 190	3 410	3 590	3 830	4 100	4 400	4 600	4 800	5 100	5 400
1,9	5 700	5 900	6 300	6 600	6 900	7 200	7 700	8 100	8 300	8 700
2,0	9 200	9 700	10 000	10 500	10 900	11 400	12 000	12 700	13 100	13 700
2,1	14 200	15 000	15 800	16 500	17 200	17 900	18 700	19 800	20 600	21 600
2,2	22 600	23 700	24 600	26 100	26 900	28 700	30 000	31 400	33 200	35 400
2,3	37 600	39 900	42 200	44 600	47 000	49 500	52 000	54 600	57 200	59 800

Appendix 2

Table A2.1

Specific losses in electrical steel

Grade	Thickness, mm	Specific loss, W/kg,, not more than		
		$p_{1.0/50}$	$p_{1.5/50}$	$p_{1.5/50}$
1211	1,0	5,8	13,4	
	0,5	3,3	7,7	
1212	1,0	5,4	12,5	
	0,5	3,1	7,2	
1213	1,0	4,7	10,7	
	0,5	2,8	6.5	
1311	0,5	2,5	6.1	
1312	0,5	2,2	5.3	
1313	0,5	2,1	4,6	
1411	0,5	2,0	4,4	
1442	0,5	1,8	3,9	
1413	0,5	1,55	3,5	
1511	0,5	1,55	3,5	
1512	0,5	1,4	3,1	
1513	0,5	1,25	2,9	
1514	0,5	1,15	2,7	
2011	0,5	3,5	8.0	
2012	0,5	2,9	6,5	
2013	0,5	2,5	5,6	
2111	0,5	3,5	8,0	
2112	0,5	2,6	6,0	
2211	0,5	2,6	5,8	
2212	0,5	2,2	5,0	
2311	0,5	1,9	4,4	
2312	0,5	1,75	4,0	
2411	0,5	1,6	3,6	
2412	0,5	1,3	3,1	
3411	0,5	1,1	2,45	3,2
3412	0,5	0,95	2,1	2,8
3413	0,5	0,8	1,75	2,5
3414	0,5	0,7	1,5	2.2
3415	0,35	0,46	1,03	1,5
3416	0,28	-	0,89	1,3

Таблиця А2.2

Specific loss in electrical steel $p_{1,0/50}$ and values of β at sheets thickness of 0, 5 mm

Steel grade	$p_{1,0/50}$, W/kg	β
2013	2,5	1,5
2211	2,6	1,5
2312	1,75	1,4
2411	1,6	1,3

Appendix 3

Table A 3.1

Fill factor for steel package

Sheet thickness, mm	Sheets insulated with	
	oxidation	varnishing
1	0,98	0,97
0,5	0,95	0,93
0,35	0,93	0,91
0,3	0,92	0,89
0,28	0,91	0,88

Appendix 4

Table A 4.1

Maximum allowable exceeding of temperature for parts of electric machines at the temperature of a gaseous-like cooling environment of 40 degrees and altitude of no more than 1000 m above sea level

Parts of electric machines	Insulation thermal class				
	A	E	B	F	H
1. Windings of AC electric machines of rated power of 5000 kVA and more or having a core length of 1 m or more	60	70	80	100	125
2. Windings: a) AC machines having rated power less than 5000 kVA with the core length less than 1 b) field windings of DC and AC machines of DC field current except the indicated in items 3…5 of this table c) armature windings connected to the commutator	55	70	75	90	115
3. Field windings of cylindrical rotor machines excited with DC current	–	–	90	110	135
4. Single row field windings with bare surfaces	65	80	90	110	135
5. Field windings of low resistance with several layers and compensating windings	60	75	80	105	125
6. Insulated windings continuously closed to themselves	60	75	80	100	125
7. Non-insulated windings continuously closed to themselves	Exceeding the temperature of these parts should not reach values that would create a danger of damaging the insulating or other adjacent materials of the elements themselves and adjacent parts				
8.Magnetic cores and other steel parts not touching insulated windings					
9. Magnetic cores and other steel parts touching insulated windings	60	75	80	100	125
10. Protected and unprotected commutators and slip rings	60	70	80	90	100

Notes: 1. For rotor bar windings of induction machines, it is allowed to exceed the temperature according to point 4 by agreement with the customer.

2. The temperature exceeding indicated in point 9 must be not greater than allowable exceed for the adjoining windings.

Appendix 5

Table A 5.1

Values of coefficients of thermal conductivity

Material	W/(°C·m)
Copper	380
Aluminum	220
Silver	420
Electrotechnical sheet steel along the layer:	
weakly alloyed	48...35
medium alloy	30...26
heavily alloyed	20...19
Electrotechnical sheet steel:	
across the layer	1,2...0,87
with paper insulation, alloyed	4,4...3,1
Lacquer fabric	0,15
Letheroid	0,23
Electrically insulating cardboard:	
dry	0,180
soaked in oil	0,250
Micanite	0,20
Asbestos	0,19
Enamel, porcelain	1,50...1,63
Glass	1,1
Wood across the grain	0,11
Getinax	0,226...0,276
Air at a pressure of 760 mm Hg. and a temperature of 40 °C	0,0266
Hydrogen at a temperature of 40 °C	0,190
Water at a temperature of 40 °C	0,633
Transformer oil at a temperature of 40 °C	0,164
Slots insulation of the armature windings of DC machines and the rotors winding of asynchronous machines:	
classes A, E	0,10
classes B, F, H	0,16
The same for the stator windings of asynchronous machines:	
classes A, E, B (uncompounded)	0,10
classes B (compounded), F, H	0,16

Appendix 6

Specific resistance of windings conductors

Table A6.1

Specific resistance of conducting materials used in windings of induction machines

Winding type	Material	Specific resistance (in Ohm·m) under temperature (°C)		
		20	75	115
Windings of copper	Copper	$0{,}01754 \cdot 10^{-6}$	$0{,}02128 \cdot 10^{-6}$	$0{,}02439 \cdot 10^{-6}$
Squirrel-cage windings	Aluminum busses	$0{,}02857 \cdot 10^{-6}$	$0{,}03571 \cdot 10^{-6}$	$0{,}03846 \cdot 10^{-6}$
	Casted aluminum	$0{,}03333 \cdot 10^{-6}$	$0{,}04167 \cdot 10^{-6}$	$0{,}04545 \cdot 10^{-6}$

Note: The casted aluminum specific resistance should be taken some greater than indicated in the Table due to arising air bulbs in the material while casting and changing the material structure at it hardening in the narrow space of slots. On these reasons the specific resistance for casted aluminum conductors of a squirrel-cage is accepted equal $\rho\theta = 0.04651 \cdot 10 - 6$ Ω·m under temperatures θ=75 and 115°C.

Appendix 7
Winding wires, strips, and busbars

Diameter and cross-section area for round conductors of ПЕТВ and ПЕТ-155 grades

Table A7.1

Rated diameter of non-insulated conductor, mm	Rated diameter of insulated conductor, mm	Cross-section area of non-insulated conductor, mm^2	Rated diameter of non-insulated conductor, mm	Rated diameter of insulated conductor, mm	Cross-section area of non-insulated conductor, mm^2	Rated diameter of insulated conductor, mm	Rated
0,08	0,10	0,00502	(0,53)	0,585	0,221		
0,09	0,11	0,00636	0,56	0,615	0,246		
0,10	0,122	0,00785	0,60	0,655	0,283		
0,112	0,134	0,00985	0,63	0,69	0,312		
0,125	0,147	0,01227	(0,67)	0,73	0,353		
0,14	0,162	0,01539	0,71	0,77	0,396		
0,15	0,18	0,01767	0,75	0,815	0,442		
0,16	0,19	0,0201	0,80	0,865	0,503		
0,17	0,20	0,0227	0,85	0,915	0,567		
0,18	0,21	0,0255	0,90	0,965	0,636		
(0,19)	0,22	0,0284	0,95	1,015	0,709		
0,20	0,23	0,0314	1,00	1,08	0,785		
(0,212)	0,242	0,0353	1,06	1,14	0,883		
0,224	0,259	0,0394	1,12	1,20	0,985		
(0,236)	0,271	0,0437	1,18	1,26	1,094		
0,25	0,285	0,0491	1,25	1,33	1,227		
(0,265)	0,300	0,0552	1,32	1,405	1,368		
0,28	0,315	0,0616	1,40	1,485	1,539		
(0,30)	0,335	0,0707	1,50	1,585	1,767		
0,315	0,350	0,0779	1,60	1,685	2,011		
0,335	0,370	0,0881	1,70	1,785	2,27		
0,355	0,390	0,0990	1,80	1,895	2,54		
0,375	0,415	0,1104	1,90	1,995	2,83		
0,40	0,44	0,1257	2,00	2,095	3,14		
0,425	0,465	0,1419	2,12	2,22	3,53		
0,45	0,49	0,1590	2,24	2,34	3,94		
(0,475)	0,515	0,1772	2,36	2,46	4,36		
0,50	0,545	0,1963	2,50	2,60	4,91		

Примітки: 1. Wires, which dimensions are given in brackets, are used in the cases of technical and economical substantiation.

2. Average values of insulated wire diameters had been found with consideration of bilateral enamel insulation thickness obtained as rounded average value of minimum and maximum thickness.

Table A7.2

Dimensions and cross-section areas of rectangular conductors

Rated dimension by greater side, mm	Rated dimension by smaller side, mm																	
	0,80	0,85	0,90	0,95	1,00	1,06	1,12	1,18	1,25	1,32	1,40	1,50	1,60	1,70	1,80	1,90	2,00	2,12
	Design conductor cross-section area mm^2																	
2,00	1,463	1,545	1,626	1,706	1,785	1,905	2,025	2,145	2,285	2,425	2,585	–	–	–	–	–	–	–
2,12	1,559	–	1,734	–	1,905	–	2,160	–	2,435	–	2,753	–	–	–	–	–	–	–
2,24	1,655	1,749	1,842	1,934	2,025	2,160	2,294	2,429	2,585	2,742	2,921	3,145	3,369	–	–	–	–	–
2,36	1,751	–	1,950	–	2,145	–	2,429	–	2,735	–	3,089	–	3,561	–	–	–	–	–
2,50	1,863	1,970	2,076	2,181	2,285	2,435	2,585	2,736	2,910	3,085	3,285	3,535	3,785	3,887	4,137	–	–	–
2,65	1,983	–	2,211	–	2,435	–	2,753	–	3,098	–	3,495		4,025	–	4,407	–	–	–
2,80	2,103	2,225	2,346	2,466	2,585	2,753	2,921	3,089	3,285	3,481	3,705	3,985	4,265	4,397	4,677	4,957	5,237	–
3,00	2,263	–	2,526	–	2,758	–	3,145	–	3,535	–	3,985	–	4,585	–	5,038	–	5,638	–
3,15	2,383	2,522	2,661	2,799	2,935	3,124	3,313	3,502	3,723	3,943	4,195	4,510	4,825	4,992	5,307	5,622	5,937	6,315
3,35	2,543	–	2,841	–	3,135	–	3,537	–	3,973	–	4,475	–	5,145	–	5,667	–	5,937	–
3,55	2,703	2,862	3,021	3,179	3,335	3,548	3,761	3,974	4,223	4,471	4,755	5,110	5,465	5,672	6,027	6,382	6,337	7,163
3,75	2,863	–	3,201	–	3,535	–	3,985	–	4,473	–	5,035	–	5,785	–	6,387	–	7,137	–
4,00	3,063	3,245	3,426	3,606	3,785	4,025	4,265	4,505	4,785	5,065	5,385	5,785	6,185	6,437	6,837	7,237	7,637	8,117
4,25	3,263	–	3,651	–	4,035	–	4,545	–	5,098	–	5,735	–	6,585	–	7,287	–	8,137	–
4,50	3,463	3,670	3,876	4,081	4,285	4,555	4,825	5,095	5,410	5,725	6,085	6,535	6,985	7,287	7,737	8,187	8,637	9,177
4,75	3,663	–	4,101	–	4,535	–	5,105	–	5,723	–	6,435	–	7,385	–	8,188	–	9,137	–
5,00	3,863	4,095	4,326	4,556	4,785	5,085	5,385	5,685	6,035	6,385	6,785	7,285	7,785	8,137	8,637	9,137	9,637	10,24
5,30	4,103	–	4,596	–	5,085	–	5,721	–	6,410	–	7,205	–	8,265	–	9,177	–	10,24	–
5,60	4,343	4,605	4,866	5,126	5,385	5,721	6,057	6,393	6,785	7,177	7,625	8,185	8,745	9,157	9,717	10,28	10,84	11,51
6,00	4,663	–	5,226	–	5,785	–	6,505	–	7,285	–	8,185	–	9,385	–	10,44	–	11,64	–
6,30	4,903	5,200	5,496	5,791	6,085	6,463	6,841	7,219	7,660	8,101	8,605	9,235	9,865	10,35	10,98	11,61	12,24	12,99
6,70	–	–	5,856	–	6,485	–	7,289	–	8,160	–	9,165	–	10,51	–	11,70	–	13,04	–
7,10	–	–	6,216	6,551	6,885	7,311	7,737	8,163	8,660	9,157	9,725	10,44	11,15	11,71	12,42	13,13	13,84	14,69
7,50	–	–	–	–	7,285	–	8,185	–	9,160	–	10,29	–	11,79	–	13,14	–	14,64	–
8,00	–	–	–	–	7,785	8,265	8,745	9,225	9,785	10,35	10,99	11,79	12,59	13,24	14,04	14,84	15,64	16,60
8,50	–	–	–	–	–	–	9,305	–	10,41	–	11,69	–	13,39	–	14,94	–	16,64	–

Table A7.2 (continuation)

Rated dimension by greater side, mm	Rated dimension by smaller side, mm																	
	0,80	0,85	0,90	0,95	1,00	1,06	1,12	1,18	1,25	1,32	1,40	1,50	1,60	1,70	1,80	1,90	2,00	2,12
	Design conductor cross-section area mm^2																	
9,00	–	–	–	–	–	–	9,865	10,41	11,04	11,67	12,39	13,29	14,19	14,94	15,84	16,74	17,64	18,72
9,50	–	–	–	–	–	–	–	–	11,66	–	13,09	–	14,99	–	16,74	–	18,64	–
10,0	–	–	–	–	–	–	–	–	12,29	12,99	13,79	14,79	15,79	16,64	17,64	18,64	19,64	20,84
10,6	–	–	–	–	–	–	–	–	–	–	14,63	–	16,75	–	18,72	–	20,84	–
11,2	–	–	–	–	–	–	–	–	–	–	15,47	16,59	17,71	18,68	19,80	20,92	22,04	23,38
11,8	–	–	–	–	–	–	–	–	–	–	–	–	18,67	–	20,88	–	23,24	–
12,5	–	–	–	–	–	–	–	–	–	–	–	–	19,79	20,89	22,14	23,39	24,64	26,14

Table A7.2 (continuation)

Rated dimension by greater side, mm, мм	Rated dimension by smaller side, mm																
	2,24	2,36	2,5	2,65	2,80	3,0	3,15	3,35	3,55	3,75	4,00	4,25	4,50	4,75	5,00	5,30	5,60
	Design conductor cross-section area mm^2																
2,00	–	–	–	–	–	–	–	–	–	–	–	–	–	–	–	–	–
2,12	–	–	–	–	–	–	–	–	–	–	–	–	–	–	–	–	–
2,24	–	–	–	–	–	–	–	–	–	–	–	–	–	–	–	–	–
2,36	–	–	–	–	–	–	–	–	–	–	–	–	–	–	–	–	–
2,50	–	–	–	–	–	–	–	–	–	–	–	–	–	–	–	–	–
2,65	–	–	–	–	–	–	–	–	–	–	–	–	–	–	–	–	–
2,80	–	–	–	–	–	–	–	–	–	–	–	–	–	–	–	–	–
3,00	–	–	–	–	–	–	–	–	–	–	–	–	–	–	–	–	–
3,15	6,693	–	–	–	–	–	–	–	–	–	–	–	–	–	–	–	–
3,35	7,141	–	–	–	–	–	–	–	–	–	–	–	–	–	–	–	–
3,55	7,589	7,829	8,326	–	–	–	–	–	–	–	–	–	–	–	–	–	–
3,75	8,037	–	8,826	–	–	–	–	–	–	–	–	–	–	–	–	–	–
4,00	8,597	8,891	9,451	10,65	10,85	–	–	–	–	–	–	–	–	–	–	–	–

Table A7.2 (continuation)

Rated dimension by greater side, mm, мм	Rated dimension by smaller side, mm, мм																
	2,24	2,36	2,5	2,65	2,80	3,0	3,15	3,35	3,55	3,75	4,00	4,25	4,50	4,75	5,00	5,30	5,60
	Design conductor cross-section area mm^2																
4,25	9,157	–	10,08	–	11,35	–	–	–	–	–	–	–	–	–	–	–	–
4,50	9,717	10,07	10,70	11,38	12,05	12,95	13,63	–	–	–	–	–	–	–	–	–	–
4,75	10,28	–	11,33	–	12,75	–	14,41	–	–	–	–	–	–	–	–	–	–
5,00	10,84	11,25	11,95	12,70	13,45	14,45	15,20	16,20	17,20	–	–	–	–	–	–	–	–
5,30	11,51	–	12,70	–	14,29	–	16,15	–	18,27	–	–	–	–	–	–	–	–
5,60	12,18	12,67	13,45	14,29	15,13	16,25	17,09	18,21	19,33	20,14	21,54	–	–	–	–	–	–
6,00	13,08	–	14,45	–	16,25	–	18,35	–	20,75	–	23,14	–	–	–	–	–	–
6,30	13,75	14,32	15,20	16,15	17,09	18,35	19,30	20,56	21,82	22,77	24,34	25,92	27,49	–	–	–	–
6,70	14,65	–	16,20	–	18,21	–	20,56	–	23,24	–	25,94	–	29,29	–	–	–	–
7,10	15,54	16,21	17,20	18,27	19,33	20,75	21,82	23,24	24,66	25,77	27,54	29,32	31,09	32,87	34,64	–	–
7,50	16,44	–	18,20	–	20,45	–	23,08	–	26,08	–	29,14	–	32,89	–	36,64	–	–
8,00	17,56	18,33	19,45	20,65	21,85	23,45	24,65	26,25	27,85	29,14	31,14	33.14	35.14	37,14	39,24	41,54	43,94
8,50	18,68	–	20,70	–	23,25	–	26,23	–	29,63	–	33,14	–	37,39	–	41,64	–	46,74
9,00	19,80	20,69	21,95	23,30	24,65	26,54	27,80	29,60	31,40	32,89	35,14	37,39	39,64	41,89	44,14	46,84	49,54
9,50	20,92	–	23,20	–	26,05	–	29,38	–	33,18	–	37,14	–	41,89	–	46,64	–	52,34
10,0	22,04	23,05	28,45	25,95	27,45	29,45	30,95	32,95	34,95	36,64	39,14	41,64	44,14	46,64	49,14	52,14	55,14
10,6	23,38	–	25,95	–	29,13	–	32,84	–	37,08	–	41,54	–	46,84	–	52,14	–	58,50
11,2	24,73	25,88	27,45	29,13	30,81	33,05	34,73	36,97	39,21	41,14	43,94	46,74	49,54	52,34	55,14	58,50	61,86
11,8	26,07	–	28,95	–	32,49	–	36,62	–	41,34	–	46,34	–	52,24	–	52,14	–	65,22
12,5	27,64	24,95	30,70	32,58	34,45	36,95	38,83	41,33	43,83	46,02	49,14	52,27	55,39	58,52	61,64	65,39	69,14

Table A7.2 (continuation)

Rated dimension by greater side, mm, мм	Rated dimension by smaller side, mm, мм												
	3,28	3,35	3,53	3,55	3,75	3,80	4,00	4,10	4,25	4,40	4,50	4,70	4,75
	Design conductor cross-section area mm^2												
10,8	–	–	–	–	–	–	–	–	–	–	–	–	–
11,2	–	36,97	–	39,21	41,14	–	43,94	–	46,74	–	49,54	–	52,34
11,6	–	–	–	–	–	–	–	–	–	–	–	–	–
11,8	–	–	–	41,34	–	–	46,34	–	–	–	52,24	–	–
12,5	–	41,33	–	43,83	46,02	–	49,14	–	52,27	–	55,39	–	58,52
13,2	–	–	–	46,31	–	–	51,94	–	–	–	58,54	–	–
13,5	–	–	–	–	–	–	–	–	–	–	–	–	–
14,0	–	46,35	–	49,15	51,95	–	55,14	–	58,64	–	62,14	–	65,64
14,5	–	–	–	–	–	–	–	–	–	–	–	–	–
15,0	–	–	–	52,70	–	–	59,14	–	–	–	66,64	–	–
15,6	–	–	–	–	–	–	–	–	–	–	–	–	–
16,0	–	53,05	–	56,25	59,14	–	63,14	–	67,14	–	71,14	–	75,14
16,8	54,62	–	58,82	–	–	63,36	–	68,02	–	73,06	–	78,10	–
18,0	58,56	–	63,06	–	–	67,92	–	72,94	–	78,34	–	83,74	–
19,5	63,48	–	68,35	–	–	73,62	–	79,09	–	84,94	–	90,79	–
20,0	–	–	–	–	–	–	79,52	–	–	–	–	–	–
22,0	71,68	–	77,18	–	–	83,12	–	89,34	–	95,94	–	102,54	–
25,0	81,52	–	87,77	–	–	94,52	99,52	101,64	–	109,14	–	116,40	–
26,3	–	–	92,36	–	–	99,46	–	106,97	–	114,86	–	122,75	–
28,0	–	–	–	–	–	105,92	111,94	113,97	–	122,34	–	130,74	–
30,0	–	–	–	–	–	113,52	119,52	122,14	–	131,14	–	140,14	–
32,0	–	–	–	–	–	–	–	130,34	–	139,94	–	149,54	–
35,0	–	–	–	–	–	–	–	–	–	153,14	–	163,64	–

Table A7.2 (continuation)

Rated dimension by greater side, mm, мм	Rated dimension by smaller side, mm,												
	5,00	5,10	5,30	5,50	5,60	6,00	6,50	7,00	8,00	9,00	10,0	11,0	12,5
	Design conductor cross-section area mm^2												
10,8	–	–	–	–	–	–	–	–	–	94,34	–	–	–
11,2	55,14	–	58,50	–	61,86	–	–	–	–	–	–	–	–
11,6	–	–	–	–	–	–	–	–	–	103,54	–	–	–
11,8	58,14	–	–	–	65,22	–	–	–	–	–	–	–	–
12,5	61,64	–	65,39	–	69,14	–	–	–	99,14	111,64	124,14	136,66	155,41
13,2	65,14	–	–	–	73,06	–	–	–	–	–	–	–	–
13,5	–	–	–	–	–	–	–	93,64	107,14	120,64	–	–	–
14,0	69,14	–	73,34	–	77,54	–	–	–	–	–	–	–	–
14,5	–	–	–	–	–	–	93,39	100,64	115,14	129,64	–	–	–
15,0	74,14	–	–	–	83,14	–	–	–	–	–	–	–	–
15,6	–	–	–	–	–	–	100,54	108,34	123,94	139,54	154,14	–	–
16,0	79,14	–	83,94	–	88,74	94,14	–	–	127,14	–	–	–	–
16,8	–	84,82	–	91,54	–	99,94	108,34	116,74	133,54	–	–	–	–
18,0	–	90,94	–	98,14	–	107,14	116,14	125,14	143,14	–	–	–	–
19,5	–	98,59	–	106,39	–	116,14	125,89	135,64	155,14	–	–	–	–
20,0	99,14	–	–	–	–	119,14	–	–	159,14	–	–	–	–
22,0	–	111,34	–	120,14	–	131,14	142,14	153,14	–	–	–	–	–
25,0	124,14	126,64	–	136,64	–	149,14	161,64	174,14	–	–	–	–	–
26,3	–	133,27	–	143,79	–	158,94	170,09	183,24	–	–	–	–	–
28,0	–	141,94	–	153,14	–	167,14	181,14	195,14	–	–	–	–	–
30,0	149,14	152,14	–	164,14	–	–	–	–	–	–	–	–	–
32,0	–	162,34	–	175,14	–	–	–	–	–	–	–	–	–

Note: Wire having dimensions located in limits between bold lines above and below (▬▬) can be produced as a winding wire of ПЕТВП і ПЕТП–155 grades with heat resistant, high strength enamel insulation, in limits between thin lines (———)- as a winding wire of ПСД і ПСДК grades with gluing and impregnation with heat-resistant or silicone varnish, in limits between dashed lines (– – – – –) – as a wire of ПСДК grade with thin alkali-free fiberglass insulation with bonded and impregnated with silicone varnish

Table A7.3

Maximum winding wires insulation thickness

Wire grade	Bilateral insulation thickness															
	At bare wire diameter *d*, mm													Rectangle wire with smaller side of the wire cross-section, mm		
	0,05… 0,09	0,10... 0,19	0,20... 0,25	0,265... 0,30	0,315... 0,355	0,375... 0,50	0,53... 0,71	0,75... 0,95	1,00... 1,40	1,50... 1,60	1,70... 2,12	2,24... 5,00	5,00... 5,20	0,85... 1,9	2,12... 3,75	4,0... 5,6
ПБД	–	–	0,19	0,22	0,22	0,22	0,22	0,22	0,27	0,27	0,27	0,33	0,33	0,27	0,23	0,44
АПБД	–	–	–	–	–	–	–	–	0,27	0,27	0,27	0,33	0,33	0,27	0,23	0,44
ПЕЛБО	–	–	0,125	0,155	0,16	0,165	0,17	0,18	0,21	0,21	0,21	–	–	–	–	–
ПЕЛШО, ПЕЛШКО	0,07	0,075	0,09	0,10	0,105	0,11	0,115	0,125	0,135	0,155	0,155	–	–	–	–	–
ПСД, ПСДК	–	–	–	–	0,23	0,23	0,25	0,25	0,27	0,27	0,27	0,33	0,33	0,27	0,33	0,40
ПСДТ	–	–	–	–	0,18	0,18	0,19	0,20	0,21	0,21	0,23	–	–	–	–	–
ПСДКТ	–	–	–	–	0,14	0,14	0,16	0,16	0,18	0,18	–	–	–	0,22	–	–
ПДА	–	–	–	–	–	–	–	–	0,30	0,30	0,30	0,35	0,35	0,40	0,40	0,40
ПЕВП, ПЕМП, ПЕВППИ, ПЕТВП, ПЕТ – 155	–	–	–	–	–	–	–	–	–	–	–	–	–	0,1– 0,12	0,15	–
ППТБО, ППЛБО	–	–	–	–	–	–	–	–	–	–	–	–	–	0,45	0,45	0,50

Table A7.4

Rated dimensions, mm, and design cross-section area, mm^2, of copper busbars

b	*a*																	
	4,0	4,5	5,0	5,5	6,0	6,5	7	8	9	10	11	12,5	14	16	18	20	25	30
16	–	–	–	–	–	–	–	–	–	–	175,1	199,1	233,1	255,1	–	–	–	–
20	–	–	–	–	–	–	–	–	–	199,1	219,1	249,1	279,1	319,1	359,1	399,1	–	–
25	–	–	–	–	–	–	–	199,1	224,1	249,1	274,1	311,6	349,1	399,1	449,1	499,1	624,1	–
30	–	–	–	–	179,1	194,1	209,1	239,1	269,1	299,1	329,1	374,1	419,1	479,1	539,1	599,1	749,1	899,1
32	–	–	–	–	191,1	207,1	–	–	–	–	–	–	–	–	–	–	–	–
35	–	–	174,1	191,6	209,1	226,6	–	279,1	–	349,1	–	436,6	–	–	–	699,1	–	–
40	159,5	179,1	199,1	219,1	239,1	259,1	279,1	319,1	359,1	399,1	439,1	499,1	559,1	639,1	719,1	799,1	999,1	1199,1
45	179,5	201,6	224,1	246,6	269,1	291,6	314,1	359,1	404,1	449,1	494,1	561,6	629,1	719,1	809,1	899,1	–	–
50	199,5	224,1	249,1	274,1	299,1	324,1	349,1	399,1	449,1	499,1	549,1	624,1	699,1	799,1	899,1	999,1	–	–
55	219,5	246,6	274,1	301,6	329,1	356,6	384,1	429,1	494,1	549,1	–	686,6	–	879,1	–	1099,1	–	–
60	239,5	269,1	299,1	329,1	359,1	389,1	439,1	479,1	539,1	599,1	–	749,1	–	959,1	–	1199,1	–	–
65	259,5	291,6	324,1	–	389,1	–	454,1	–	584,1	649,1	–	811,6	–	1039,1	–	–	–	–
70	279,5	314,1	349,1	–	–	–	–	559,1	629,1	699,1	–	874,1	–	1119,1	–	–	–	–
75	–	–	–	–	–	–	–	599,1	–	–	–	–	–	–	–	–	–	–
80	319,5	359,1	399,1	–	479,1	–	559,1	639,1	–	799,1	–	999,1	–	–	–	–	–	–
90	359,5	404,1	449,1	–	539,1	–	629,1	719,1	–	899,1	–	1124,1	–	–	–	–	–	–
100	399,5	449,1	499,1	–	599,1	–	699,1	799,1	–	999,1	–	1249,1	–	–	–	–	–	–
120	–	–	–	–	–	–	–	959,1	–	1199,1	–	–	–	–	–	–	–	–

Note: The design cross section area is determined considering corners rounding

Table A7.5

Classification, heat resistance and design data the main types of enameled copper wires

Wire brand, mm	Thermal class of insulation	Type of enamel insulation	Nominal dimensions of the current-conducting wire	Two-sided insulation thickness, mm
ПЕЛ	A	Enamel on an oil-resin basis	0,063...2,50	0,010–0,065
ПЕВ-1	A	High strength enamel on polyvinyl acetyl basis	0,063...0,05 0,063...2,50	0,01...0,02 0,20...0,085
ПЕВ-2	A	The same with thickened insulation	0,063...2,50	0,025...0,090
ПЕМ-1	A	High strength enamel based on polyvinyl acetyl (polyvinyl formalin)	0,063...2,50	0,02...0,08
ПЕМ-2	A	The same with thickened insulation	0,063...2,50	0,025...0,085
ПЕВД і ПЕВДБ	A	Polyvinyl acetal enamel with an additional thermoplastic layer based on polyvinyl acetate or polyvinyl butyral	0,063...1,00	0,033...0,085
ПЕЛР-1	A	High-strength enamel based on polyamide resol	0,1...2,50	0,02...0,08
ПЕЛР-2	A	The same with thickened insulation	0,1-2,50	0,025…0,09
ПЕВТЛ-1	E	High-strength polyurethane-based enamel	0,063...1,60	0,015...0,07
ПЕВТЛ-2	E	The same with thickened insulation	0,063...1,60	0,02...0,08
ПЕВТЛК	E	Double enamel based on polyurethane and polyamide resins	0,063...0,35	0,03...0/05
ПЕТВ-943 ПЕТВ-939	B B	High-strength polyester-based enamel (Varnish PE-943) The same (varnish PE-939)	0,063...2,50 0,063...2,50	0,025...0,09 0,025...0,09
ПЕТВД	B	High-strength enamel on a polyester basis, with an additional layer of thermoplastic resin	0,063...0,365	0,037...0,065
ПЕТ-155А	F	High-strength enamel on polyetherimide basis	0,063...2,50	0,025...0,09
ПЕТ-amid	До 200° С	High-strength polyamide-based enamel (nickel-plated copper wire)	0,10...1,32	0,025...0,06
ПЕТ-amid	Те ж	The same on bare copper wire	0,10...1,32	0,025...0,06

Table A7.6

Assortments and estimated sizes of enameled copper wires

Nominal diameter of bare wire, mm	Estimated outer diameters, mm			Nominal diameter of bare wire, mm	Estimated outer diameters, mm		
	ПЕЛ	ПЕВ-1, ПЕМ-1, ПЕЛР-1, ПЕВТЛ-1,	ПЕТ-155А, ПЕВ-2, ПЕМ-2, ПЕДР-2, ПЕВТЛ-2, ПНЕТ, ПЕТ-Iamid, ПЕТВ-939, ПЕТВ-943		ПЕЛ	ПЕВ-1, ПЕМ-1, ПЕЛР-1, ПЕВТЛ-1,	ПЕТ-155А, ПЕВ-2, ПЕМ-2, ПЕДР-2, ПЕВТЛ-2, ПНЕТ, ПЕТ-amid, ПЕТВ-939, ПЕТВ-943
0,02	0,03	0,03	–	0,425	0,460	0,455	0,465
10,025	0,035	0,035	–	0,45	0,485	0,48	0,49
0,032	0,04	0,042	–	0,475	0,510	0,505	0,515
0,04	0,05	0,052	–	0,50	0,54	0,545	0,555
0,05	0,062	0,07	–	0,53	0,57	0,575	0,585
0,06	0,072	0,083	0,087	0,56	0,60	0,605	0,615
0,07	0,082	0,093	0,097	0,60	0,64	0,645	0,655
0,08	0,092	0,103	0,107	0,63	0,67	0,675	0,685
0,09	0,102	0,113	0,117	0,67	0,71	0,715	0,730
0,10	0,115	0,123	0,127	0,71	0,76	0,755	0,770
0,112	0,135	0,143	0,147	0,75	0,80	0,80	0,815
0,125	0,140	0,148	0,153	0,85	0,90	0,90	0,915
0,132	0,147	0,155	0,159	0,90	0,95	0,95	0,965
0,14	0,155	0,163	0,167	0,95	1,00	1,00	1,015
0,15	0,168	0,177	0,180	1,00	1,06	1,07	1,08
0,16	0,178	0,187	0,190	1,06	1,12	1,13	1,14
0,17	0,188	0,197	0,200	1,12	1,18	1,19	1,20
0,18	0,198	0,207	0,210	1,18	1,24	1,25	1,16
0,19	0,208	0,217	0,220	1,25	1,31	1,32	1,33
0,20	0,222	0,227	0,230	1,32	1,38	1,39	1,40
0,212	0,234	0,239	0,242	1,40	1,465	1,47	1,48
0,224	0,246	0,251	0,254	1,50	1,565	1,57	1,58
0,236	0,258	0,266	0,271	1,60	1,665	1,67	1,68
0,25	0,272	0,28	0,285	1,70	1,765	1,77	1,78
0,265	0,291	0,295	0,30	1,80	1,865	1,875	1,88
0,28	0,306	0,31	0,315	1,90	1,965	1,975	1,98
0,30	0,326	0,33	0,335	2,00	2,065	2,075	2,08
0,315	0,345	0,345	0,350	2,12	2,185	2,205	2,21
0,335	0,365	0,365	0,370	2,24	2,305	2,325	2,33
0,355	0,385	0,385	0,395	2,36	2,425	2,445	2,45
0,375	0,405	0,405	0,415	2,50	2,565	2,585	2,59
0,40	0,435	0,43	0,44				

Table A7.7

Асортименти мідних обмотувальних проводів зі скловолокнистою ізоляцією

Name of the winding wire	Wire brand	Thermal class	Nominal dimensions of the conductor, mm	Double-sided thickness of insulation, mm	Breakdown voltage, V
Insulated with two-layer fiberglass winding with gluing and impregnation of each layer with heat-resistant varnish	ПСД	F	Round in diameter of 0,315...2,6	0,23...0,33	450...650
			Rectangular (0,9...5,6)× (2,1...12,5)	0,27...0,4 0,32...0,38	550...650
Insulated with two-layer fiberglass winding with gluing and impregnation of each layer with organosilicon varnish	ПСДК	H	The same	0,23...0,33 0,27...0,4 0,32...0,38	450...650 550...650
Wire with two-layer insulation with thinned fiberglass with gluing and impregnation of each layer with heat-resistant varnish	ПСДТ	F	Round in diameter of 0,315...2,12	0,18...0,23	350...450
Wire with two-layer thinned (three-micron) fiberglass insulation with gluing and impregnation of each layer with organosilicon varnish	ПСДКТ	H	Round in diameter of 0,315...2,12	0,14...0,22	300...450
			Rectangular (0,9...3,55× (2,12.10)	0,22 0,26...0,32	450
Wire insulated with a layer of organosilicon enamel and single-layer winding with thinned (three-micron) glass fiber with under-gluing and impregnation with organosilicon varnish.	ПЕТКСОТ	H	Round in diameter of 0,30...1,60	0,14...0,16	350
			Rectangulari (0,85...1,4)× (2,12...4,75)	0,20...0,22 0,18...0,2	350
Insulated with a layer of block polymer organosilicon enamel and single-layer winding with thinned glass fiber with gluing and impregnation with organosilicon varnish	ПНЕТКСОТ	200° C for 10,000 hours, assuming short-term heating (up to 50 h) to 300°C	Round in diameter of 0,20 i 0,315	0,12...0,14	350...400
A wire with an aluminum core, insulated with a double-layer fiberglass winding with gluing and impregnation of each layer with a heat-resistant varnish	АПСД	F	Round in diameter of 1,60...2,50	0,27	550
			Rectangular (2,12...5,6)× (4,0...14,0)	0,32...0,48	550

Table A7.8

Wire diameters for terminals of electric machines

Nominal cross-section, mm2	Nominal outer diameter, mm, of wire brands					
	ПВВТ	ПВКВ, ПВКФ for voltage, V		РКГМ, РКГМПТ	ПВФС for voltage, V	
		380	660		660	1140
0,75	2,5	2,8	3,6	3,2	3,6	4,0
1,0	2,7	2,9	3,7	3,3	3,7	4,1
1,5	3,1	3,3	4,1	3,7	4,1	4,5
2,5	3,5	4,1	4,5	4,3	4,5	4,9
4,0	4,3	4,7	5,1	5,1	5,1	5,5
6,0	4,8	5,2	5,6	5,6	5,6	6,0
10,0	6,5	7,1	7,5	7,3	7,3	7,7
16,0	-	8,5	8,9	8,7	8,7	9,2
25,0	-	10,5	10,9	10,7	10,7	11,2
35,0	-	11,9	12,3	12,1	12,1	12,5
50,0	-	14,9	15,3	15,1	15,1	15,5
70,0	-	16,5	16,9	16,7	16,7	17,1
95,0	-	18,6	19,0	18,8	18,8	19,2
120,0	-	-	21,2	20,8	20,8	21,6

Notes: 1. Limit deviation from the nominal outer diameter +10%. Minus tolerance is not normalized.
2. On the surface of wires of PVVT, PVKV, PVKF and PVFS brands, dents and indentations are not allowed, which bring the outer diameter of the wires beyond the limit deviations.

Appendix 8

Brushes for electric machines

Table Д8.1

A combination of the main recommended brush sizes

Tangential size b, mm	Axial size l, mm															Brush height h, mm
1,6	**2,0**	**2,5**														8,0
2,0		**2,5**	**3,2**													8,0
2,5			**3,2**	4,0												8,0
			3,2	**4,0**	5,0											10,0
					5,0											12,5
3,2				4,0												8,0
		2,5		**4,0**	5,0											10,0
				4,0	**5,0**	**6,3**										12,5
4,0		**2,5**	3,2		5,0											10,0
					5,0	6,3										12,5
						6,3	8,0	10								16
							8,0	**10**								20
5,0			**3,2**	4,0		6,3										12,5
						6,3	8,0	10								16
							8,0	**10**	12,5	16						20
							8,0	10	**12,5**	**16**	20					25
									12,5	16	**20**	**25**	32			32
												25	**32**			40
6,3			**3,2**	4,0												12,5
				4,0	5,0											16
							8,0	**10**	12,5							20
							8,0	10	**12,5**	**16**	20					25
								10	12,5	16	**20**	**25**	32			32
											20	25	**32**			40
											20	25	50			50
8,0				4,0	5,0											16
				4,0	**5,0**	6,3		10								20
								10	**12,5**	**16**	20					25
								10	12,5	**16**	**20**	**25**	32			32
										16	20	25	**32**			40
											20	25	32			50
													32			64
10,0					5,0	6,3										16
					5,0	**6,3**	8,0									20
						6,3	**8,0**		**12,5**	16	20					25
							8,0		12,5	**16**	**20**	25	32			32
									12,5	16	20	**25**	**32**	40		40
											20	25	32	**40**		50
											20	25	32	40		64

Table A8.1 (continuation)

Tangential size b, mm	Axial size l, mm															Brush height h, mm
16						**6,3**										20
						6,3	**8,0**	10								25
							8,0	**10**	**12,5**		**20**	25	32			32
								10	12,5		20	**25**	**32**	40		40
											20	25	32	**40**	50	50
												25	32	40	**50**	64
													32	40	50	80
20							**8,0**	10								25
							8,0	**10**	**12,5**	**16**						32
								10	12,5	16		**25**	**32**	40		40
									12,5	16		25	32	**40**	50	50
												25	32	40	**50**	64
													32	40	50	80
25							**8,0**	**10**	**12,5**	16	20					32
							8,0	10	12,5	**16**	**20**		**32**	40		40
							8,0	10	12,5	16	20		32	**40**	50	50
										16	20		32	40	**50**	64
													32	40	50	80
													32	40	50	100
32								**10**	12,5	16	20					32
								10	**12,5**	**16**	**20**	**25**		40		40
								10	12,5	16	20	25		**40**	50	50
								10	12,5	16	20	25		40	**50**	64
										16	20	25		40	50	80
											20	25		40	50	100
												25		40	50	125
40									**12,5**	**16**	20	25	32			40
									12,5	16	**20**	**25**	**32**			50
									12,5	16	20	25	32			64
										16	20	25	32		**50**	80
											20	25	32		50	100
												25	32		50	125
50											20	25				40
											20	**25**	32			50
											20	25	**32**	40		64
											20	25	32	**40**		80
											20	25	32	40		100
												25	32	40		125

Notes: 1. The best combinations of sizes are highlighted in bold.
2. Brushes with a width of 25 mm and more are divided into two.

Table A8.2

Physical and mechanical and commutating characteristics of electric machine brushes

Brush brand	The name of the brush brand group	Nominal current density, (10^4 A/m^2)	Permissible district, m/s	Specific pressure, kPa	Resistivity, μOhm·m	Hardness, 10^7 Pa	Transitional drop in voltage on a pair of brushes, V	Friction coefficient, no more	Wear in 20 hours, mm, no more	Field of application
Г3	Coal-graphite	12	60	20...25	14 ± 6	13 ± 6	1 ± 0,4	0,3	0,5	Generators and motors with easy commutation conditions and alternating current collector machines
Г21		5	30	15...100	300 ± 150	40 ± 20	4,6 ± 1,4	0,25	–	
Г33		5,5	36	29...54	300 ± 150	40 ± 23	4,7 ± 1,3	0,25	–	
Г33М		10	35	12...22	≈ 1600	40 ± 20	–	–	–	
Г34		15	25	<34	< 220	35 ± 21	2,2 ± 0,8	0,27	0,30	
611М	Graphite	12	40	20...25	–	–	2,0	–	–	Generators and motors with easy commutation conditions and slip rings
6110М		15	90	12...22	15 ± 7	1,2 ± 0,5	2,0	0,3	0,4	
ЕГ2А	Electrogra-phitized	12	50	20...25	20 ± 8	15 ± 7	1,4 ± 0,5	0,23		Generators and motors with medium and difficult commutation conditions and slip rings
ЕГ2АФ		15	90	15...21	24 ± 11	14 ± 8	1,6 ± 0,5	0,23		
ЕГ4		12	60	15...20	11 ± 5	4 ± 2	1,4 ± 0,6	0,25	0,6	
ЕГ8		11	45	20...40	43 ± 7	22 ± 13	1,4 ± 0,4	0,25	0,4	
ЕГ14		12	45	20...40	29 ± 9	19 ± 11	1,6 ± 0,5	0,25	0,4	
ЕГ17		–	–	–	12 ± 3	12 ± 3	18 ± 7	–		
ЕГ61А		13	60	–	54 ± 18	45 ± 23	2,5 ± 0,7	0,15	0,3	
ЕГ62		10	50	29...49	45 ± 25	–	2,1 ± 0,9	0,17	0,4	
ЕГ71		12	45	20...25	27 ± 8	10 ± 4	1,6 ± 0,5	0,3	0,4	
ЕГ74		15	50	17...25	55 ± 20	33 ± 17	1,8 ± 0,6	0,22	0,4	
ЕГ74АФ		15	60	15...21	29 ± 9	35 ± 15	1,5 ± 0,5	0,22	0,4	
ЕГ74ДО		12	60	17...27	55 ± 20	–	1,9 ± 0,6	0,22		
ЕГ75		13	60	34...49	50 ± 15	–	2,35 ± 0,85	0,17	0,3	

Table A8.2 (continuation)

Brush brand	The name of the brush brand group	Nominal current density, (10^4 A/m^2)	Permissible district, m/s	Specific pressure, kPa	Resistivity, μOhm·m	Hardness, 10^7 Pa	Transitional drop in voltage on a pair of brushes, V	Friction coefficient, no more	Wear in 20 hours, mm, no more	Field of application
ЕГ84	Electrogra-phitized	17	50	23...39	50 ± 20	–	2,5 ± 1,0	0,19	0,4	Generators and motors with average and difficult commutation conditions and slip rings
ЕГ 84-1		17	55	23...50	60 ± 20	–	2,7 ± 1,0	0,17	0,35	
ЕГ85		15	50	17...35	55 ± 20	34 ± 16	2,1 ± 0,5	0,2	0,4	
ЕГ86		12	45	–	27,5 ± 17,5	21 ± 14	1,75 ± 0,75	0,28	–	
ЕГ141		17	60	20...30	35 ± 15	20 ± 10	1,6 ± 0,5	0,20	0,35	
Ml	Metal-graphite	25	33	15...20	3,5 ± 1,5	16 ± 8	1,4 ± 0,4	0,25	0,18	Low-voltage generators and slip rings
М1Л		–	–	–	4 ± 2	16 ± 8	1,5 ± 0,5	0,22	0,18	
Мб		24	35	15...20	3,5 ± 2,5	17,5 ± 7,5	1,5 ± 0,5	0,2	0,35	
М20		15	45	15...20	8 ± 5	16 ± 8	1,4 ± 0,4	0,26	0,2	
МГ		30	35	18, 23	< 0,12	9 ± 5	< 0,3	0,2	0,8	
МГ4		24	30	20...25	<1,3	16 ± 6	< 1,6	0,2	0,3	
МГ4С		–	–	–	1,7 ± 1,3	–	1,1 ± 0,5	0,2	0,3	
МГС01		–	–	–	< 0,8	13 ± 7	< 3,5	0,25	0,60	
МГС0А		–	–	–	0,2 ± 0,1	29 ± 15	0,3 ± 0,2	0,24	0,60	
МГС01А		–	–	–	< 0,8	13 ± 7	< 0,5	0,25	0,60	
МГС5		24	35	20...25	8,5 ± 6,5	13 ± 7	1,3 ± 0,6	0,24	0,4	
МГС9А		–			< 10	25 ± 13	< 2,0	0,25	0,4	
МГС20		–			< 0,4	15 ± 10	0,65 ± 0,35	0,25	0,6	
МГС51		–			7,5 ± 5,5	13 ± 7	1,85 ± 0,65	0,22	0,35	

Note: 50 hours wear is given for metal-graphite brushes.

Appendix 9
Installation dimensions of alternating current electric machines

Table A9.1

Connection between rated power and installation dimensions for motors of the basic version, degree of protection IP44

Height of the axis of rotation, mm	Conventional bed length	Power, kW, at the number of poles					
		2	4	6	8	10	12
50		0,09; 0,12	0,06; 0,09	-	-	-	-
56	-	0,18; 0,25	0,12; 0,18	-	-	-	-
63	-	0,37; 0,55	0,25; 0,37	0,18; 0,25	-	-	-
71	-	0,75; 1,1	0,55; 0,75	0,37; 0,55	0,25	-	-
80	-	1,5; 2,2	1,1; 1,5	0,75; 1,0	0,37; 0,55	-	-
90	L	3,0	2,2	1,5	0,75; 1,1	-	-
100	S	4,0	3,0	-	-	-	-
	L	5,5	4,0	2,2	1,5	-	-
112	M	7,5	5,5	3,0; 4,0	2,2; 3,0	-	-
132	S	-	7,5	5,5	4,0	-	-
	M	11,0	11,0	7,5	5,5	-	-
160	S	15,0	15,0	11,0	7,5	-	-
	M	18,5	18,5	15,0	11,0	-	-
180	S	22,0	22,0	-	-	-	-
	M	30,0	30,0	18,5	15,0	-	-
200	M	37,0	37,0	22,0	18,5	-	-
	L	45,0	45,0	30,0	22,0	-	-
225	M	55,0	55,0	37,0	30,0	-	-
250	S	75,0	75,0	45,0	37,0	30,0	-
	M	90,0	90,0	55,0	45,0	37,0	-
280	S	110,0	110	75,0	55,0	37,0	-
	M	132	132	90,0	75,0	45,0	-
315	S	1610	160	110	90,0	55,0	45,0
	M	200	200	132	110	75,0	55,0
355	S	250	250	160	132	90,0	75,0
	M	315	315	200	160	110	90,0

Table A9.2

Connection between rated power and installation dimensions for motors of the basic version, degree of protection IP23

Height of the axis of rotation, mm	Conventional bed length	Power, kW, at the number of poles					
		2	4	6	8	10	12
160	S	22,0	18,5	-	-	-	-
	M	30,0	22,0	-	-	-	-
180	S	37,0	30,0	18,5	15,0	-	-
	M	45,0	37,0	22,0	18,5	-	-
200	M	55,0	45,0	30,0	22,0	-	-
	L	75,0	55,0	37,0	30,0	-	-
225	M	90,0	75,0	45,0	37,0	-	-
250	S	110	90,0	55,0	45,0	-	-
	M	132	110	75,0	55,0	-	-
280	S	160	132	90,0	75,0	45,0	-
	M	200	160	110	90,0	55,0	-
315	S	-	200	132	110	75,0	55,0
	M	250	250	160	132	90,0	75,0
335	S	315	315	200	160	110	90,0
	M	400	400	250	200	132	110

Table A9.3

Sketches of 4A series moors with various designs and the degree of protection, and the height of the axis of rotation and their main dimensions

Method of mounting	Degree of protection	Hight of axis of rotation, мм	Motor sketch	
			Side view	Front view
IM1081	IP44 IP54	50...250	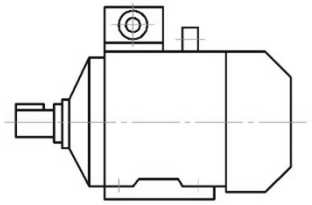	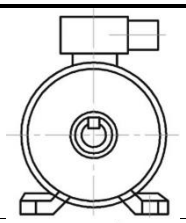
IM1001	IP44 IP54	280...355	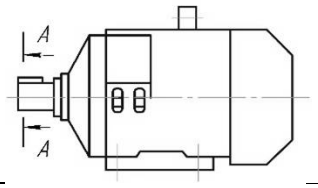	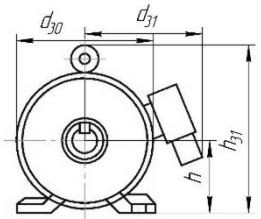
IM2081	IP44 IP54	50...250	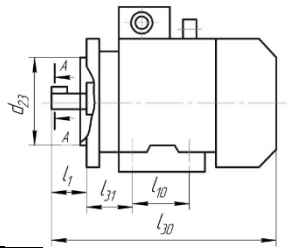	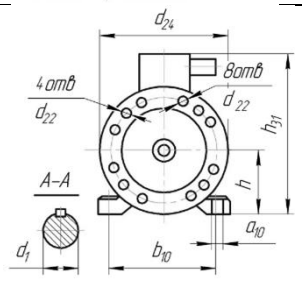
IM2001	IP44 IP54	280...355	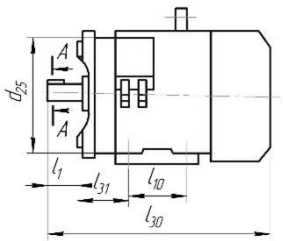	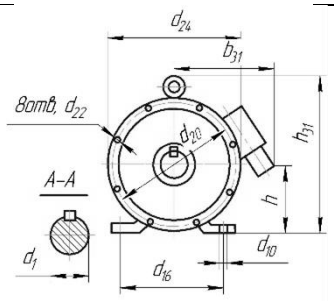
IM3081 IM3011 IM3031	IP44 IP54	50...280	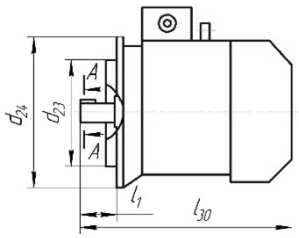	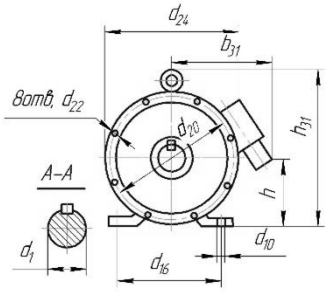
IM2181	IP44 IP54	50...90	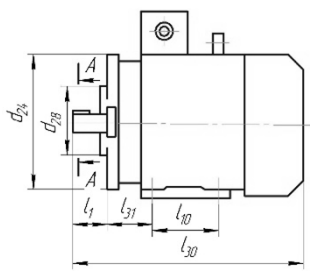	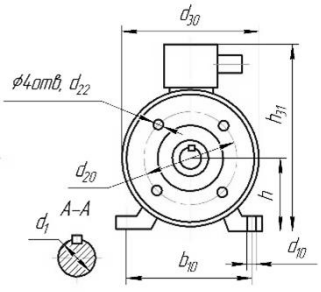

Table A9.3 (continuation)

Method of mounting	Degree of protection	Hight of axis of rotation, мм	Motor sketch	
			Side view	Front view
IM3681	IP44 IP54	50...100	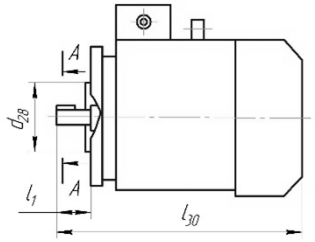	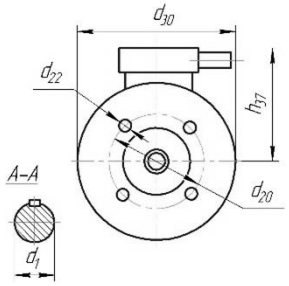
IM1001	IP23	160...250	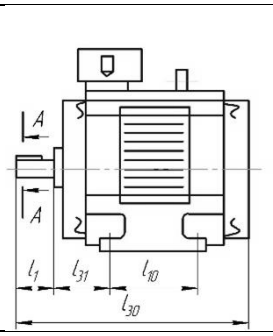	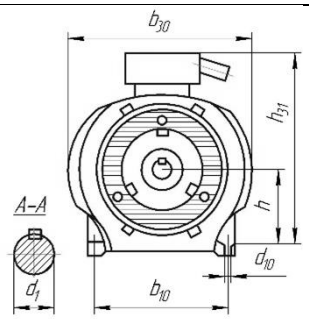
IM3681	IP23	280...355	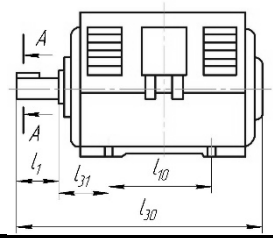	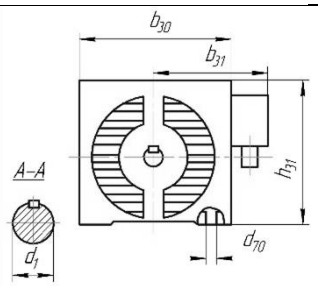

Note: For IM2081, IP44 or IP54 and 50...250 at $h \leq 180$ mm – 4 holes; at $180 < h \leq 250$ mm – 8 holes.

Appendix 10
Winding insulation of alternating current machines

Table A10.1

Insulation of single layer and two-layer stator windings of motors with axis of rotation height to 250 mm, voltage to 660 V, thermal classes D, F and H

Drawing	Winding type	Hight of axis of rotation, mm	Position	Material			Number of layers	One-sided thickness, mm
				Name, brand		Thickness, mm		
				Клас B	Клас F Клас H			
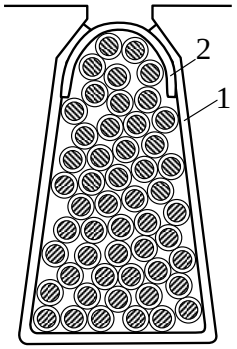	Single layer	50-80		Film fiberglass				
			1	Isolex	Imidoflex	0,2	1	0,2
			2	isolex	Imidoflex	0,3	1	0,3
	Single layer	90–132		Film fiberglass				
			1	isolex	Imidoflex	0,25	1	0,25
			2	isolex	Imidoflex	0,35	1	0,35
	Single layer a	160		Film fiberglass				
			1	isolex	Imidoflex	0,4	1	0,4
			2	isolex	Imidoflex	0,5	1	0,5
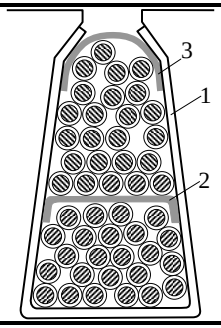	Two-layer	180–250		Film fiberglass				
			1	Isoflex	Imidoflex	0,4	1	0,4
			2	Isoflex	Imidoflex	0,4	1	0,4
			3	Isoflex	Imidoflex	0,5	1	0,5

Note: Interlayer insulation in winding end connections are made of the material specified for pos. 1 indicated at the drawings.

Table A10.2

Insulation of stator wed-in windings of induction motors having shaft axis height h≤ 280 mm, and voltage to 660 V.

Drawing	Position	Material						Number of layers	One-sided thickness, mm		
		Name, brand			Thickness, mm						
		Thermal class B	Thermal class F	Thermal class H	Thermal class B	Thermal class F	Thermal class H		Thermal class B	Thermal class F	Thermal class H
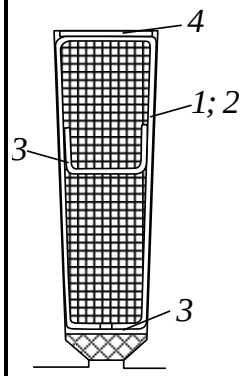	1*	Film-synth cardboard									
		ПСК-Л	ПСК-Ф	ПСК-Н	0,25	0,28	0,28	1	0,25	0,28	0,28
	2**	Electronit			0,3	0,3	0,28	1	0,3	0,3	0,28
		Total thickness of slot liner			0,55	0,58	0,56		0,55	0,58	0,56
	3	Lacquer fabric Micaplast									
		ГІТ-ЛСБ-ЛСЛ	ГІТ-ЛСП-ЛСЛ	ГІТ-ЛСК-ЛСЛ	0,55	0,55	0,55	1	0,55	0,55	0,55
	4	Film-synth cardboard									
		ПСК-Л	ПСК-Ф	ПСК-Н	0,25	0,28	0,28	1	0,25	0,28	0,28
	5	ПСК-Л	ПСК-Ф	ПСК-Н	0,25	0,28	0,28	1	0,25	0,28	0,28

Note: Interlayer insulation in winding end connections are made of mica plastic varnish fabric

* To coil sides

** To the slot

Table A10.3

Thermal class F stator winding coils sleeve insulation of alternating current machines having the rated power from 100 to 1000 kW and voltage from 3000 to 3300 V

Part of a winding	Position	Material			Number of layers		Insulation thickness, mm	
		Name	Grade	Thickness, mm	In width	By height	In width	By height
Slot 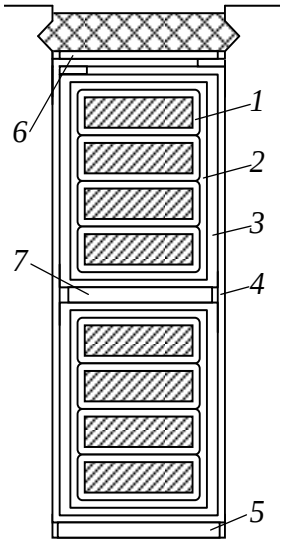	*1*	Conductor insulation	–	–	–		–	–
	2	Glass tape	ЛЕС	0,1	1 layer, scattered		0,2	0,2
	3	Glass Mikafolium	МФП-Т	0,2	0,5 turnover		2,6	2,6
		Thickness of coil insulation	–	–	–	–	2,8	2,8
		Allowable deviation	–	–	–	–	±0,4	+0,6 -1,2
	4	Fiberglass cloth	ЛСК	0,15	2	3	0,3	0,45
	5	Glass-textolite	СТЕФ	0,5	–	1	–	0,5
	6	Glass-textolite	СТЕФ	0,5	–	1	–	0,5
	7	Glass-textolite	СТЕФ	1,0	–	1	–	1,0
		Tolerance for laying	–	–	–	–	0,5	0,5
		Totally for the slot without the wedge	–	–	–	–	3,6	8,6
End winding 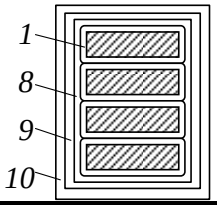	*8*	Glass tape	АЕС	0,1	1 layer, scattered		0,2	0,2
	9	Glass mica tape	ЛФЕ-ТТ	0,13	5 layers, half overlap		2,6	2,6
	10	Glass tape	ЛЕС	0,1	1 layer, half overlap		0,4	0,4
		Swelling due to soaking	–	–	–	–	0,5	0,5
		Coil insulation thickness	–	–	–	–	3,7	3,7
		Allowable deviation	–	–	–	–	±0,5	±1,0
Terminal leads		Glass mica tape	ЛФЕ-ТТ	0,13	4 layers, half overlap		–	–
		Glass tape	ЛЕС	0,1	1 layer, half overlap		–	–

Table A10.4

Thermal class B stator winding coils thermosetting insulation of alternating current machines having rated power from 100 to 1000 kW and voltage of 6600 V

Part of a winding	Position	Insulation destination	Material			Число шарів	Bilateral thickness, mm, at number of conductors														
			Найменування	Марка	Товщина мм		In width		By height												
							1	2	2	3	4	5	6	7	8	9	10	11	12	13	14	15
Пазова 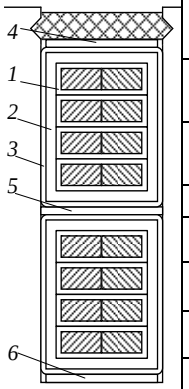	*1*	Turn	Own insulation of ПЕТВСД conductor	–	0,5 on two sides	–	0,5	1,0	1,0	1,5	2,0	2,5	3,0	3,5	4,0	4,5	5,0	5,5	6,0	6,5	7,0	7,5
	2	Encapsulated	Glass mica cloth	–	0,17	–	4,0		4,0												
			Conductor insulation swelling	–	–	–	0,05	0,10	0,10	0,15	0,20	0,25	0,30	0,35	0,40	0,45	0,50	0,55	0,60	0,65	0,70	0,75
	3	Covering	Glass tape	ЛЕС	0,1	1 layer, tight	0,2		0,2												
		Total insulation per coil					4,75	5,30	5,30	5,85	6,40	6,95	7,50	8,05	8,10	9,15	9,70	10,25	10,8	11,35	11,90	12,45
	4	Interlayer	Glass textolite	СТ	0,5	1	–		0,5												
	5	Interlayer	Glass textolite	СТ	1	2	–		2,0												
	6	Interlayer	Glass textolite	СТ	0,5	1	–		0,5												
		Laying gap		–	–	–	0,2		–												
		Total insulation in a slot					4,95	5,5	13,6	14,7	15,8	16,9	18,0	19,1	20,2	21,3	22,4	23,5	24,6	25,7	26,8	27,9
Лобова 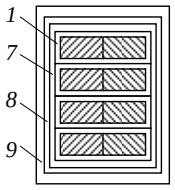	*1*	Turn	Own insulation of ПЕТВСД conductor		0,5 on two sides	–	0,5	1,0	1,0	1,5	2,0	2,5	3,0	3,5	4,0	4,5	5,0	5,5	6,0	6,5	7,0	7,5
		Insulation swelling		–	–	–	0,05	0,10	0,10	0,15	0,20	0,25	0,30	0,35	0,40	0,45	0,50	0,55	0,60	0,65	0,70	0,75
	7	Encapsulated	Mica plastic tape	СЛФЧ	0,13	3 layers, overlap	1,56		1,56												
	8	Encapsulated	Glass exponite tape	ЛСЕЛ	0,17	3 layers, overlap	2,04		2,04												
	9	Covering	Glass tape	ЛЕС	0,1	3 layers, overlap	0,4		0,4												
		Insulation swelling		–	–	–	1,0		1,0												
		Total insulation in a coil					5,55	6,10	6,10	6,65	7,20	7,75	8,30	8,85	9,40	9,95	10,50	11,05	11,60	12,15	12,7	13,25

Table A10.5

Continuous class B insulation of the coils of the alternating current machines stator windings up to 10,000 V

Part of a winding	Position	Material		Number of layers	Insulation thickness	
		Name	Thickness, mm	Not less than	In width	By thickness
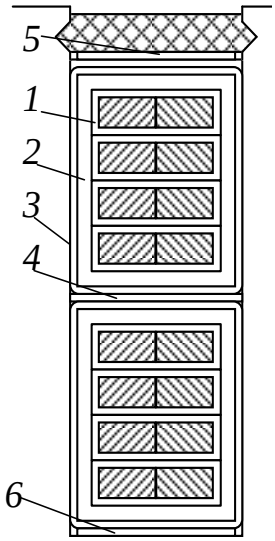 Slot insulation		*Turn insulation*				
	1	Insulation of conductor	–			
	2	*Coil insulation*				
		Fiberglass tape ЛС:	0,13			
		at U =10,5 kV		9 half overlap	6,0	6,0
		U =6,6 kV		6 half overlap	4,5	4,5
		$U \le 660$ V		half overlap	2,0	2,0
		Glass tape ЛЕС	0,1	1 tight	0,2	0,2
		Coil side insulation thickness				
		at U =10,5 kV			6,2	6,2
		U = 6,6 kV			4,7	4,7
		$U \le 660$ V			2,2	2,2
		Interlayer insulation				
		Glass textolite CT-1	1	2	2	2
		Glass textolite CT-1	0,5	2	1	1
		Total insulation thickness per slot				
		at U =10,5 kV			6,2	15,4
		U = 6,6 kV			4,7	12,4
		$U \le 660$ V			2,2	7,4
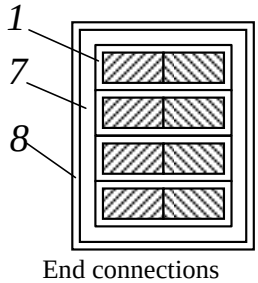 End connections insulation	1	Turn insulation	–			
	7	Fiberglass tape ЛС:	0,13			
		at U =10,5 kV		9 half overlap	6,0	6,0
		U = 6,6 kV		6 half overlap	4,5	4,5
		$U \le 660$ V		3 half overlap	2,0	2,0
	8	Glass tape ЛЕС (covering)	0,1	1 tight	0,2	0,2
		Discontinuities and unevenness	–	–	1,0	1,0
		Total slot side insulation thickness				
		at U =10,5 kV			7,2	7,2
		U = 6,6 kV			5,7	5,7
		$U \le 660$ V			3,2	3,2

Table A10.6

Sleeve insulation (solid sleeve) of the alternating current machines stator windingswith voltage of up to 660 V , the insulation thermal class B of normal and reinforced moisture-resistant performance

Class B of normal and reinforced moisture-resistant performance								
Part of the winding insulation	Позиція	Material			Number of layers		Thickness of insulation, mm	
		Name	Brand	Thickness, mm	In width	By height	In width	By height
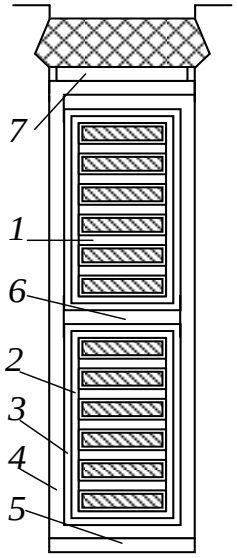 Slot insulation	1	Turn insulation[1]						
	2	Glass tape	ЛЕС	0,1	1 layer, scattered		0,2	0,2
	3	Micafolius	МФГ	0,2	3,5 turnover		1,4	1,4
		Double-sided insulation thickness of the slot part of the coil					1,6	1,6
	4	Electronite		0,2	2	3	0,4	0,6
	5	Electronite		0,5	–	1	–	0,5
	6	Varnish impregnated glass-mikanite	ГФГС-ЛСБ	0,5	–	1	–	0,5
	7	Textolite	В					
		Tolerance for laying		0,5	–	1	0,3	0,5
		Totally per slot (without the wedge and turn insulation)				–	2,3	5,8
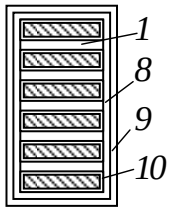 Insulation of end connections	8	Mica tape	ЛФЧ-II	0,17	2 layers half overlap		1,4	1,4
	9	Glass tape	ЛЕС	0,10	1 layer half overlap		0,4	0,4
	10	Glass tape	ЛЕС	0,10	1 layer scattered		0,2	0,2
		Swelling due to soaking					0,5	0,5
		Double-sided insulation thickness of the coil end connections					2,5	2,5

Table A10.7

Continuous thermos-reactive insulation of alternating current machine stator windings at voltage up to 660 V, thermal classes B and F

Part of winding	Позиція	Insulation destination	Material: Name	Material: Brand	Thickness	Number of layers	Double-sided thickness, mm, at number of conductors: In width 1	In width 2	By height 2	By height 3	By height 4	By height 5	By height 6
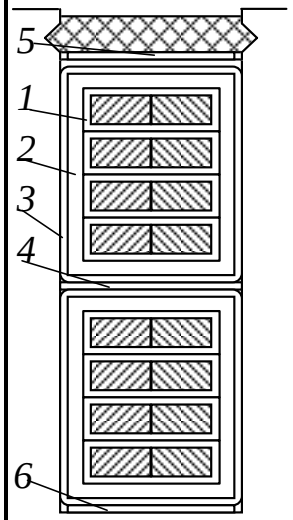 slot	1	Turn	Glass tape (impregnated with varnish ПЕ 933)	ЛЕС	0,1	1 layer half overlapped	0,45	0,45	0,9	1,35	1.8	2,25	2,7
			Swelling due to coating with varnish				0,05	0,1	0,1	0,15	0,20	0,25	0,3
	2	Coil	Glass-mica tape	ЛСП-7	0,13	4 layers half overlapped	2,08	2,08	2,08	2,08	2,08	2,08	2,08
	3	Covering	Glass tape (soaked with varnish ПЕ-933)	ЛЕС		1 layer half overlapped	0,45	0,45	0,45	0,45	0,45	0,45	0,45
			Total insulation in coil				3,03	3,08	3,53	4,03	4,53	5,03	5,53
	4	Interlayer	Glass-mica insulation	СТЕФ-1	0,5	1	–	–	0,5	0,5	0,5	0,5	0,5
	5	Interlayer	Glass-mica insulation	СТЕФ-1	1,0	1	–	–	1,0	1,0	1,0	1,0	1,0 0
	6	Interlayer	Glass-mica insulation	СТЕФ-1	0,5	1	–	–	0,5	0,5	0,5	0,5	5
			Tolerance for laying				0,2	0,2	–	–	–	–	–
			Total insulation in a slot				3,23	3.28	9,06	10,06	11,06	12,06	13,06
Glass tape (soaked with varnish ПЕ-933)	1	Turn	Glass tape (soaked with varnish ПЕ-933)	ЛЕС	0,1	1 layer half overlapped	0,45	0,45	0,9	1,35	1,8	2,25	2,7
			Swelling				0,05	0,1	0,1	0,15	0,2	0,15	0,3
	7	Coil	Glass-mica tape	ПЕ-934-ТП	0,13	3 layers half overlapped	1,56	1,56	1,56	1,56	1,56	1,56	1,56
	8	Interlayer	Glass tape (soaked with varnish ПЕ-933)	ЛЕС	0,2	2 layers right up close	0,9	0,9	0,9	0,9	0,9	0,9	0,9
			Total insulation in the end connections				2,96	3,01	3,46	3,96	4,46	4,96	5,46

Notes 1. PSD or PETVSD wires are used for the manufacture of coils.

2. Do not apply turn insulation (position 1) when using PETVSD wires.

Table A10.8

Insulation of alternating current machine stator windings at semi-open rectangular slots under the voltage of up to 660 V and insulation classes B, F, H

Part of the winding			Position	Material: Name, brand: Class B	Class F	Class H	Thickness, mm	Number of layers	Double-sided thickness: In width	By height
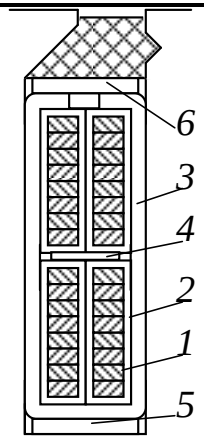 Slot part			1	Enveloping coating			0,05	1	0,2	0,2
			2	Bakelite telephone paper	Lacquered phenylene paper		0,09	1,5 turnover	0,6	0,6
			3	Lacquer fabric-mica plastic: ГІТ-ЛСБ-ЛСЛ	ГИП-ЛСП-ЛСЛ	ГИК-ЛСК-ЛСЛ	0,55	1	1,1	1,1
			4	Glass textolite: СТ	СТЕФ	СТК	1.0	1	–	1.0
			5	СТ	СТЕФ	СТК	0,5	1	–	0,5
			6	СТ	СТЕФ	СТК	0,5	1	–	0,5
				Tolerance for laying					0,3	0,6
				Total insulation thickness in the slot (without turn insulation and the wedge)					2.2	4.5
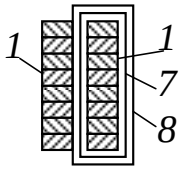 End connection's part	Half-coil groups	Edge located		Fastening bandage made of LES glass tape 20 mm wide in two places			0,1	2,5 turnover	0,5	0,5
			1	Enveloping coating			0,05	1	0,1	0,1
			7	Fiberglass fabric: ЛСБ-105/120	ЛСП-130/155	ЛСК-155/180	0,15	1 half overlapped	0,6	0,6
			8	Glass tape ЛЕС			0,1	1 half overlapped	0,4	0,4
				Total insulation thickness of a half-coil (without turn insulation)					1,6	1,6
		Located in the middle		Fastening bandage made of LES glass tape 20 mm wide in three places			0,1	2,5 turnover	0,5	0,5
			1	Enveloping coating			0,05	1	0,1	0,1
				Total insulation thickness of a half-coil (without turn insulation)					0,6	0,6

Table A10.9

Insulation of phase winding coils of slip-ring induction motors with rated power up to 100 kW (class B insulation)

Part of the winding		Position	Material			Number of layers		Double-sided insulation thickness	
			Name	Brand	Thickness, mm	In width	By height	In width	By height
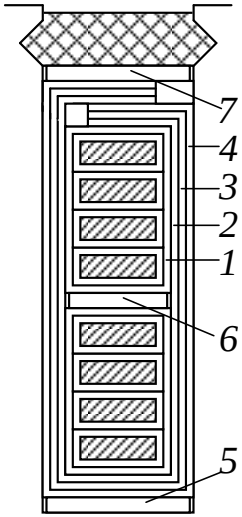 Пазова			Swelling due to coating with varnish					0,1	0,1
		1	Glass tape	ЛЕС	0,1	1 layer scattered		0,2	0,2
			Totally per a coil		–	–	–	0,3	0,3
		2	Fiberglass cloth	ЛСБ	0,2	2	3	0,4	0,6
		3	Flexible micanite	ГФС	0,2	2	3	0,4	0,6
		4	Fiberglass cloth	ЛСБ	0,2	2	3	0,4	0,6
		5	Fiberglass cloth	СТ	0,5	–	1	–	0,5
		6	Fiberglass cloth	СТ	0,5	–	1	–	0,5
		7	Fiberglass cloth	СТ	0,5	–	1	–	0,5
			Tolerance for laying					0,5	0,8
			Totally per slot without the wedge					2,0	4,7
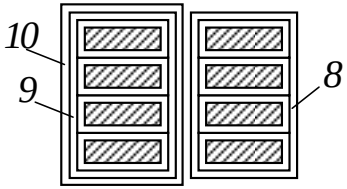 End connections	Coils in the middle of a coil group	8	Glass tape	ЛЕС	0,2	1 half overlapped		0,8	0,8
	Edge coils of a coil group	9	Fiberglass cloth	ЛСБ	0,2	1 half overlapped		0,8	0,8
		10	Glass tape	ЛЕС	0,2	1 half overlapped		0,8	0,8
			Thickness of edge coils insulation					1,6	1,6

Table A10.10

Insulation of bar windings of phase rotors of induction motors with a height of the axis of rotation h≥ 280 мм

Part of the winding	Position	Material					Voltage to 750 V				Voltage to 1200 V			
		Name, brand			Thickness, mm		Number of layers		Double-sided insulation thickness		Number of layers		Double-sided insulation thickness	
		Class B	Class F	Class H	Class B	Classes F and H	Class B	Classes F and H	In width	By height	Class B	Classes F and H	In width	By height
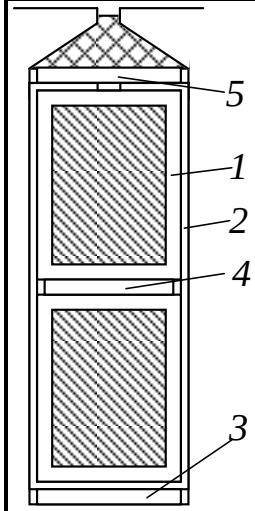 Slot	1	Mica plastofolium ИФГ-Б	Synthofolium F	Synthofolium H	0,15	0,16	4,5* turnover	3,5 turnover	1,1	2,2	9,5* turnover	7,5 turnover	2,4	4,8
	2	Fiberglass fabric: ЛСБ-105/120	ЛСП-130/155	ЛСК-155/180	0,15		1		0,3	0,3	1	1	0,3	0,3
	3	СТ	СТЕФ	СТК	0,5		1			0,5	1	1	–	0,5
	4	СТ	СТЕФ	СТК	0,5		1			0,5	1	1	–	0,5
	5	СТ	СТЕФ	СТК	0,5		1			0,5	1	1	–	0,5
		Tolerance for laying							0,3	0,5			0,3	0,5
		Total insulation thickness in the slot (without turn insulation and the wedge)							1,7	4,0			3,0	6,6
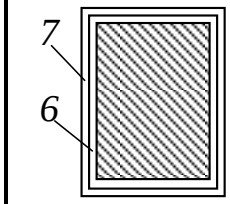 End connection	6	Glass-mica tape ПЕ-934-ТП	Polyimide film ПМ 0,05× 3=0,15 mm		0,15		1 half overlapped		0,6	0,6	2 half overlapped		1,2	1,2
	7	Glass tape ЛЕС			0,1		1 half overlapped		0,4	0,4	2 half overlapped		0,6	0,6
		Total bar insulation thickness in the end connection part							1,0	1,0			1,8	1,8

* Taking into account shrinkage by 15-20%.

Appendix 11

Greek alphabet

Letter Upper, lower	Name	Pronounced	When speaking, sounds like
Α, α	alpha	AHL-fah	ah
Β, β	vita	VEE-tah	the letter **v**
Γ, γ	gamma	GHAH-mah	the letter **y** when it comes before e, u, i; otherwise like a soft gargle **gh**
Δ, δ	thelta	THEL-tah	hard **th** as in "there"
Ε, ε	epsilon	EHP-see-lon	eh
Ζ, ζ	zita	ZEE-tah	the letter **z**
Η, η	ita	EE-tah	ee
Θ, θ	thita	THEE-tah	soft **th** as in "through"
Ι, ι	iota	YO-tah	ee
Κ, κ	kappa	KAH-pah	the letter **k**
Λ, λ	lamtha	LAHM-thah	the letter **l**
Μ, μ	mu	mee	the letter **m**
Ν, ν	nu	nee	the letter **n**
Ξ, ξ	xee	ksee	the letter **x**
Ο, ο	omikron	OH-mee-kron	oh
Π, π	pi	pee	the letter **p**
Ρ, ρ	ro	roh, roe	a rolled **r**
Σ, σ, ς	sigma	SEEGH-mah	the letter **s**
Τ, τ	tau	tahf	the letter **t**
Υ, υ	upsilon	EWP-see-lon	ee
Φ, φ	phi	fee	the letter **f**
Χ, χ	chi	hee	a light gargly **ch** as in "challah"
Ψ, ψ	psi	psee	**ps** as in "chips"
Ω, ω	omega	oh-MEH-ghah	somewhere between "awe" and "oh"

Appendix 12

Latin alphabet

Letter	Name		Name pronunciation			
	Modern English	Latin	Modern English	Latin	Old French	Middle English
A	*a*	*ā*	/ˈeɪ/, /ˈæ/[nb 1]	/aː/	/aː/	/aː/
B	*bee*	*bē*	/ˈbiː/	/beː/	/beː/	/beː/
C	*cee*	*cē*	/ˈsiː/	/keː/	/tʃeː/ > /tseː/ > /seː/	/seː/
D	*dee*	*dē*	/ˈdiː/	/deː/	/deː/	/deː/
E	*e*	*ē*	/ˈiː/	/eː/	/eː/	/eː/
F	*ef*, *eff* *eff* as a verb	*ef*	/ˈɛf/	/ɛf/	/ɛf/	/ɛf/
G	*gee*	*gē*	/ˈdʒiː/	/geː/	/dʒeː/	/dʒeː/
H	*aitch* *haitch*[nb 2]	*hā*	/ˈeɪtʃ/ /ˈheɪtʃ/	/haː/ > /ˈaha/ > /ˈakːa/	/ˈaːtʃə/	/aːtʃ/
I	*i*	*ī*	/ˈaɪ/	/iː/	/iː/	/iː/
J	*jay* *jy*[nb 4]	–	/ˈdʒeɪ/ /ˈdʒaɪ/	–	–	[nb 3]
K	*kay*	*kā*	/ˈkeɪ/	/kaː/	/kaː/	/kaː/
L	*el*, *ell*[nb 5]	*el*	/ˈɛl/	/ɛl/	/ɛl/	/ɛl/
M	*em*	*em*	/ˈɛm/	/ɛm/	/ɛm/	/ɛm/
N	*en*	*en*	/ˈɛn/	/ɛn/	/ɛn/	/ɛn/
O	*o*	*ō*	/ˈoʊ/	/oː/	/oː/	/oː/
P	*pee*	*pē*	/ˈpiː/	/peː/	/peː/	/peː/
Q	*cue*, *kew*, *kue*, *que*[nb 6]	*qū*	/ˈkjuː/	/kuː/	/kyː/	/kiw/
R	*ar* *or*[nb 7]	*er*	/ˈɑːr/ /ˈɔːr/	/ɛr/	/ɛr/	/ɛr/ > /ar/
S	*ess* *es-* in compounds[nb 8]	*es*	/ˈɛs/	/ɛs/	/ɛs/	/ɛs/
T	*tee*	*tē*	/ˈtiː/	/teː/	/teː/	/teː/
U	*u*	*ū*	/ˈjuː/	/uː/	/yː/	/iw/
V	*vee*	–	/ˈviː/	–	–	–
W	*double-u*	–	/ˈdʌbəl.juː/[nb 9]	–	–	–
X	*ex*	*ex* *ix*	/ˈɛks/	/ɛks/ /ɪks/	/iks/	/ɛks/
Y	*wy*, *wye*, *why*[nb 10]	*hȳ* *ī graeca*	/ˈwaɪ/	/hyː/ /iː/ /iː ˈgraɪka/	*ui*, *gui* ? /iː grɛːk/	/wiː/
Z	*zed*[nb 11] *zee*[nb 12]	*zēta*	/ˈzɛd/ /ˈziː/	/ˈzeːta/	/ˈzɛːdə/	/zɛd/

Appendix 13

International System of Units

Coherent system of units based on the International System of Quantities (ISQ), their names and symbols, including a series of prefixes and their names and symbols, together with rules for their use, adopted by the General Conference on Weights and Measures (CGPM)

Note 1 to entry: The SI is founded on the seven base quantities of the ISQ and the names and symbols of the corresponding base units that are contained in the following table:

Base quantity	**Base unit**	
Name	**Name**	**Symbol**
length	metre	m
mass	kilogram	kg
time, duration	second	s
electric current	ampere	A
thermodynamic temperature	kelvin	K
amount of substance	mole	mol
luminous intensity	candela	cd

Note 2 to entry: The base units and the coherent derived units of the SI form a coherent set, designated the "set of coherent SI units".

Note 3 to entry: For a full description and explanation of the International System of Units, see the current edition of the SI brochure published by the International Bureau of Weights and Measures (BIPM) and available on the BIPM website.

Note 4 to entry: In quantity calculus, the quantity "number of entities" is often considered to be a base quantity, with the base unit one, symbol 1.

The SI prefixes for multiples and submultiples of units

Unit prefix used together with a SI unit to form decimal multiples or submultiples of this unit.

Note 1 – The list of approved SI prefixes is given in the following table:

Multiples			Submultiples		
Factor	Prefix		Factor	Prefix	
	Name	Symbol		Name	Symbol
10^{1}	deca	da	10^{-1}	deci	d
10^{2}	hecto	h	10^{-2}	centi	c
10^{3}	kilo	k	10^{-3}	milli	m
10^{6}	mega	M	10^{-6}	micro	µ
10^{9}	giga	G	10^{-9}	nano	n
10^{12}	tera	T	10^{-12}	pico	p
10^{15}	peta	P	10^{-15}	femto	f
10^{18}	exa	E	10^{-18}	atto	a
10^{21}	zetta	Z	10^{-21}	zepto	z
10^{24}	yotta	Y	10^{-24}	yocto	y

Note 2 – When the prefixes are used, the prefix name and the unit name are combined to form a single word, and similarly the prefix symbol and the unit symbol are written without any space to form a single symbol, which may itself be raised to any power. For example, we may write: kilometre, km; microvolt, µV; femtosecond, fs; 50 V/cm = 50 V $(10^{-2}\ \mathrm{m})^{-1}$ = 5000 V/m.

Note 3 – As an exception, multiples and submultiples of the kilogram are written by combining a prefix with the gram, such we write: milligram, mg, not microkilogram, µkg.

REFERENCES

1. Проєктування електричних машин : навч. посіб. / Д.В. Ципленков, О.Б Іванов, О.В. Бобров, В.В. Кузнецов, В.В. Артемчук, М.О. Баб'як ; Нац. техн. ун-т «Дніпровська політехніка». – Д. : НТУ «ДП», 2020. – 408 с.

2. Oleksii B. Ivanov, Fedir P. Shkrabets, Jan Zawilak. Electrical generators driven by renewable energy systems. - Poland, Wroclaw, Wroclaw University of Technology, 2011. – 170 p.

3. Півняк Г.Г., Довгань В.П., Шкрабець Ф.П. Електричні машини: Навч. посібник. – Д.: Національний гірничий університет, 2003. – 327 с.

4. Осташевський М.О. Електричні машини і трансформатори: навч. посібник / М.О. Осташевський, О.Ю. Юр’єва; за ред. д-ра техн. наук, професора В.І.Мілих. – Київ: Каравела, 2018. – 452 с.

5. Андрієнко В.М. Електричні машини: навч. посіб. для студ. вищ. навч. закл., які навч. за напрямом підгот. «Електротехніка та електротехнології» / В.М. Андрієнко, В.П. Куєвда. – К.: НУХТ, 2010. – 366 с.

6. Бєлікова Л.Я. Електричні машини: навч. посіб. для студ. вищ. навч. закл. / Л.Я. Бєлікова, В.П. Шевченко. – Одеса: Наука і техніка, 2012. – 478 с.

7. Загірняк М.В. Електричні машини: підручник \ М.В. Загірняк, Б.І. Невзлін. - Київ: Знання, 2009. – 399 с.

8. Електричні машини: підручник / Б.Т. Кононов, Г.І. Лагутін, О.Б. Котов та ін.; за заг. ред. Б.Т. Кононова. – Харків: ХУПС, 2015. – 493 с.

9. Яцун М.А. Електричні машини: навч. посіб. для студ. Базового напряму «Електромеханіка» / М.А. Яцун – 2-ге вид., стер. – Львів: Вид-во Нац. ун-ту «Львівська політехніка», 2004. – 440 с.